HELSINKI INSTITUTE OF PHYSICS INTERNAL REPORT SERIES

HIP-2025-04

Early Universe Cosmology with Sphalerons and Modifications of General Relativity

Jaakko Annala

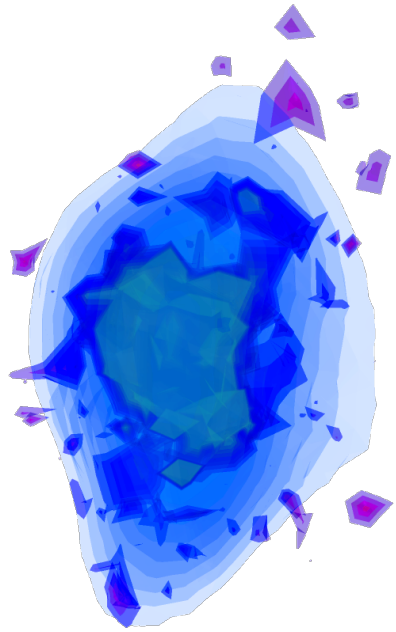

Helsinki Institute of Physics
University of Helsinki
Finland

DOCTORAL DISSERTATION

To be presented for public discussion with the permission of the Faculty of Science of the University of Helsinki, in Auditorium E204, Physicum building, on the 1st of August, 2025 at 12 o'clock.

Helsinki 2025

ISBN 978-952-84-0008-0 (paper)
ISBN 978-952-84-0009-7 (pdf)
ISSN 1455-0563 (print)
ISSN 2814-9459 (online)
http://ethesis.helsinki.fi
Unigrafia

Helsinki 2025

“ *»Time is money», people are used to saying and modern man simply has no time to think about its nature. Nevertheless, through the centuries man has been fascinated by the riddle and mystery of time.*”

— Pauli Annala, *Transparency of Time*

J. Annala: Early Universe Cosmology with Sphalerons and
Modifications of General Relativity,
University of Helsinki, 2025, 94 pages,
Helsinki Institute of Physics, Internal Report Series, HIP-2025-04,
ISBN 978-952-84-0008-0 (paper), ISBN 978-952-84-0009-7 (pdf)
ISSN 1455-0563 (print), ISSN 2814-9459 (online).

Abstract

One of the major long-standing problems in physics is how the observed matter versus antimatter asymmetry in our universe was generated, and a second one is the question what is the fundamental nature of gravity. This thesis is divided into two main topics: in part I we discuss electroweak matter and in part II we discuss modifications of gravity.

A crucial ingredient needed in any attempt of explaining the asymmetry between matter and antimatter is the violation of baryon number. There are processes present in the electroweak sector of the Standard Model able to change the baryon number called sphalerons. The fact that there could have been (hyper)magnetic fields present in the early universe around the electroweak scale motivates us to study how the sphalerons are affected by an external (hyper)magnetic field. In the first part of this thesis we first review the theoretical framework, introduce the semi-classical sphaleron solution and discuss the sphalerons magnetic dipole moment. We then review the thermal field theory and lattice field theory methods that we used to study the sphaleron. We finally discuss the results of our study where we computed the changes to the rate of sphaleron transitions from an external (hyper)magnetic field. In addition to the effects from the sphalerons dipole moment the external magnetic field changes the electroweak transition which changes the behavior of the rate of sphaleron transitions through the history of the early universe.

One well motivated modification of General Relativity is to consider higher order curvature terms. There are different ways of formulating General Relativity and when introducing modifications different formulations generally lead to very different theories. The higher order terms can in general lead to new degrees of freedom which may lead to pathologies bringing the physicality of these theories into question. In this thesis we consider higher order curvature terms in the Palatini formulation where the metric and the connection are taken to be independent degrees of freedom. In the second part of this thesis we first review the Palatini formulation. We then present our results on studying the possible new perturbative degrees of freedom in non-degenerate theories depending on the curvature via first contractions of the Riemann tensor. We then proceed by studying how higher order curvature terms can change the inflationary observables in a theory that depends on the curvature only via the symmetric part of the Ricci tensor where no new degrees of freedom appear. We begin this by first briefly introducing the inflationary paradigm and finally presenting how the inflationary observables change from the higher order curvature terms.

Acknowledgements

I am deeply grateful to my supervisors Syksy Räsänen and Kari Rummukainen for all the invaluable guidance and support they have provided me before and during my doctoral studies. I am also very grateful for Mark Hindmarsh for helping me in the early stages of my doctoral studies.

I am grateful for the fellow students and postdocs that make the working environment at the campus pleasant and engaging. A special thanks also for the computational field theory group for providing a welcoming and friendly working group to be part of.

I have had access to great computational resources to carry out my research, which were provided by CSC – IT Center for Science, Finland, and the Finnish Computing Competence Infrastructure (FCCI). I am grateful for the financial support during my doctoral studies from the Vilho, Yrjö and Kalle Väisälä Foundation of the Finnish Academy of Science and Letters.

I want to thank Tomi Koivisto and Guy Moore for being my pre-examiners and Javier Rubio for agreeing to be my opponent.

Finally, I want to thank my family and loved ones. Pauli, Eeva, thank you for always being there and supporting me in my endeavours. Heikki, Vuokko, I am lucky to have grown up alongside such curious and creative minds which has certainly contributed to my own motivation to learn new things. Anni, I am eternally thankful for being here with me. Without all of you this journey would not have been possible.

Included publications

The thesis is based on the following publications, listed in reverse chronological order, [1–3]:

I Electroweak sphaleron in a magnetic field
J. Annala and K. Rummukainen,
Phys. Rev. D 107 (2023) 073006

II Stability of non-degenerate Ricci-type Palatini theories
J. Annala and S. Räsänen,
JCAP 04 (2023) 014 [Erratum: JCAP 08, E02 (2023), JCAP 05, E01 (2025)]

III Inflation with $R_{(\alpha\beta)}$ terms in the Palatini formulation
J. Annala and S. Räsänen,
JCAP 09 (2021) 032

The authors are listed alphabetically according to particle physics convention.

The author's contributions

In paper I the author extended existing simulation code and performed all the simulations and data analysis. The author also performed the semianalytical computations and drafted the initial version of the paper. In papers II and III, the author performed most the analytical calculations and wrote the first drafts of the papers. In the paper III, the author performed the numerical computations.

Contents

Introduction

Early universe cosmology is an important field that can guide our fundamental theories beyond our two standard pillars of modern physics: The Standard Model of particle physics that describes the visible matter content of our universe and General Relativity that describes the force of gravity and the cosmic evolution of spacetime.

This thesis is divided into two main parts: part I where we discuss electroweak matter in the early universe and part II where we discuss modifications of gravity in the context of cosmic inflation.

The Higgs boson was discovered at the LHC in 2012 [4, 5] completing the Standard Model and, since, no new fundamental physics beyond it have been discovered at particle colliders. Early universe cosmology provides an additional avenue of testing our theories in extreme conditions. Furthermore, the technological advances that enabled direct detection of gravitational waves in 2015 [6] opened an additional avenue of probing the early universe to even earlier times than what can be probed by observing electromagnetic radiation. Notably, upcoming space-based gravitational wave experiments may be able to probe the electroweak scale of the early universe [7–10].

Even though the Standard Model is very successful, there are multiple mysteries that have not been explained in the frames of the Standard Model and thus physics beyond it is expected. The mysteries include e.g. dark matter, dark energy and, in particular what we discuss in this thesis, is the observed matter-antimatter asymmetry of the universe. A scenario where the matter-antimatter asymmetry is generated is called baryogenesis. Any viable baryogenesis scenario must have a way of producing an asymmetry of the baryon number. In the Standard Model electroweak sector there is such mechanism: the sphaleron. This is the main focus of the part I of this thesis. The properties of the sphaleron are important to assess the viability of baryogenesis scenarios. A property that we studied in more detail in our work is the magnetic dipole moment of the sphaleron.

We have observed large-scale extra-galactic magnetic fields, which could have a primordial origin [11, 12]. The origin of these fields could span back to the era before

the electroweak phase transition corresponding to hypermagnetic fields before and turning into the magnetic fields after the transition. Thus, in this thesis when we talk about magnetic fields we mean the hypermagnetic fields before the transition that transform to the true electromagnetic magnetic fields after the transition. There are constraints that can be put on the magnitude of these fields depending on when the fields were generated [13–15]. As the magnetic fields scale in an expanding universe naively as $B \sim a^{-2}$, where a is the scale factor, the field magnitudes could have been large in the past.

Thus, if there were magnetic fields around in the early universe these could have affected the sphalerons lowering their energy. This can finally affect the amount of baryon number change taking place affecting viability of baryogenesis scenarios. Magnetic fields can also on themselves lead to baryon number change, see e.g. [16–22], however, we do not focus on this aspect here.

Additionally, presence of magnetic fields around the electroweak phase transition can affect the form of the transition [23], which also affects the amount of baryon number change over the history of the universe.

In our work we investigated the effects of external magnetic fields on the sphalerons and the form of the phase transition.

General Relativity is the standard theory of gravitation and, like the previously discussed Standard Model, it has seen remarkable success in predicting and explaining phenomena we observe in our universe. The lack of theory of quantum gravity and General Relativity being non-renormalizable from the effective field theory perspective suggests that General Relativity cannot be the full story [24]. Moreover, it has not yet been ruled out completely that dark matter and dark energy could be explained by modified gravity. Thus, we are motivated to study modifications of General Relativity. There are numerous ways to modify gravity that have been proposed, see e.g. [25, 26].

The paradigm of cosmic inflation, discussed in section 6.1, gives an effective setting of investigating the effects of different modifications of gravity. In the minimal model with General Relativity and the Standard Model the only new dimension four operator is the non-minimal coupling between the Higgs field and gravity giving rise to the Higgs inflation [27, 28]. Even in this minimal modification of gravity the question of what are the most fundamental degrees of gravity becomes interesting.

General relativity can be formulated by starting with different fundamental degrees of freedom leading to equivalent dynamics. Metric formulation is the canonical formulation where gravity is completely described by the metric tensor. In our work we focus on the Palatini formulation, introduced in section 4, where in addition to

the metric the connection is taken as an independent degree of freedom.[1] The different formulations give equivalent dynamics for the Einstein–Hilbert action. However, when the gravity sector is modified the different formulations can lead to very different dynamics. For example, the introduction of non-minimal coupling in Higgs inflation results into different inflationary predictions for the metric and Palatini formulations [30].

A natural modification of General Relativity is the inclusion of higher order Riemann tensor terms, i.e. higher order curvature terms, into the action. These can be motivated from effective field theory perspective, ultraviolet completion of the theory or quantum corrections. These terms lead to very different theories depending on the formulation of gravity used.

Due to the structure of the Riemann tensor in the metric formulation these terms generally lead to equations of motion with derivatives of higher order than two which lead to Ostrogradski instabilities. In general these instabilities make it difficult to have physically consistent theory. These problems have been studied more extensively in the metric formulation of gravity and more is known on how to construct a physically viable theory in the metric formulation. By the Lovelock's theorem [31] it is known that in four spacetime dimensions the only local action that yields a set of second order field equations is the Einstein–Hilbert action leading to the Einstein field equations.

The extra degrees of freedom originating from higher order derivatives may not always lead to instabilities if the assumptions of the Ostrogradski theorem are evaded. Indeed, in the metric formulation, without matter fields, the most general healthy theory depends only on the Ricci scalar. For example, in the $f(R)$ gravity one finds an extra healthy scalar field [32]. Including matter fields, more complicated actions that lead to healthy theories are possible. For example, including scalar fields lead to healthy theories, such as the Horndeski and beyond Horndeski theories, see e.g. [33].

In the Palatini formulation the types of actions that lead to healthy theories are less well known. In first sight the situation might seem better since Ostrogradski instabilities are avoided due to the equations of motion being second order. However, instabilities turn out to appear in general from the higher order terms. In our paper [2] we extend previous work on the subject by considering the stability of theories constructed from the first contractions of the Riemann tensor.

As mentioned earlier, the period of cosmic inflation provides a setting where effects of the higher order curvature terms between formulations can be compared in light of to cosmic microwave background (CMB) observables. Thus, in principle,

[1] Other formulations include for example the teleparallel formulation where the metric curvature vanishes and gravity is described purely by torsion and/or non-metricity, see e.g. the review [29].

with CMB observations we may probe the structure of gravity getting insight into its fundamental degrees of freedom. In our paper [3] we studied how the inflationary observables are changed in a theory with arbitrary functional dependence on the symmetric part of the Ricci tensor. In this case there are no new degrees of freedom, as seen in section 5.1, which makes the analysis more tractable.

Part I is organized as follows. In chapter 1 we first discuss properties of non-Abelian gauge theories and their nontrivial vacuum structure. We then briefly describe the electroweak sector of the Standard Model before describing the sphaleron configuration. We then discuss the chiral anomaly and baryogenesis focusing on the role of the sphaleron. In chapter 2 we briefly review the tools used to construct an effective theory that we used to study the sphalerons in dynamical lattice simulations. Finally, in chapter 3 we introduce the lattice methods used and discuss effects of an external magnetic field on the electroweak transition and the sphaleron.

The part II is organized as follows. First in chapter 4 we review the Palatini formulation and introduce the relevant geometrical quantities. In chapter 5 we discuss the stability of higher order curvature Palatini theories. In chapter 6 we first give a brief introduction to inflation and then discuss how the higher order curvature terms affect inflationary observables.

Notation and conventions

- To make comparisons with existing literature easier in part I we use the mostly minus metric signature $\mathrm{diag}(+1,-1,-1,-1)$ and in part II we use the mostly plus metric signature $\mathrm{diag}(-1,+1,+1,+1)$.
- We use natural units where $\hbar = c = k_B = 1$. Additionally, we set the Planck mass to unity $M_{\mathrm{pl}} \equiv 1/\sqrt{8\pi G_N} = 1$.
- In part I, repeated downstairs Lorentz indices are understood to be summed over using the Euclidean metric.
- The (anti)symmetrization of indices is defined to include the factor of a half: i.e. $T_{[\alpha\beta]} = \frac{1}{2}(T_{\alpha\beta} - T_{\beta\alpha})$, and $T_{(\alpha\beta)} = \frac{1}{2}(T_{\alpha\beta} + T_{\beta\alpha})$.

Part I

Matter

"*For whatever is must also be something.*"
— Lucretius, *De rerum natura*

Chapter 1

Electroweak Sphaleron

Let us first briefly review non-Abelian gauge theories, which is where the baryon number violation and sphalerons originate in the Standard Model.

1.1 Yang–Mills gauge theory

Yang–Mills theory is based on a gauge group G which is a compact Lie group that has a corresponding Lie-algebra. The relevant gauge group for the non-trivial vacuum structure of the electroweak sector is $G = \mathrm{SU}(2)$. The gauge field $A_\mu(x)$ is a $\mathfrak{su}(2)$ Lie algebra valued vector field. Choosing a set of (Hermitian) generators T^a that satisfy $[T^a, T^b] = i\epsilon_{abc}T^c$ and are normalized as $\mathrm{Tr}\, T^a T^b = \frac{1}{2}\delta^{ab}$ we can express the gauge field as $A_\mu(x) = A^a_\mu(x)T^a$.

The Lagrangian for the pure Yang–Mills gauge theory is

$$\mathcal{L}_{\mathrm{YM}} = -\frac{1}{2}\mathrm{Tr}\, F_{\mu\nu}F^{\mu\nu} \ , \tag{1.1}$$

where

$$F_{\mu\nu} = \partial_\mu A_\nu - \partial_\mu A_\nu - ig[A_\mu, A_\nu] \ , \tag{1.2}$$

is the field strength (curvature) of A_μ and g is the gauge coupling. The theory has a gauge symmetry: it is invariant under local SU(2) gauge transformations $\Omega(x) \in \mathrm{SU}(2)$. The gauge field transforms as

$$A_\mu(x) \to \Omega(x)A_\mu(x)\Omega^{-1}(x) + \frac{i}{g}\Omega(x)\partial_\mu\Omega^{-1}(x). \tag{1.3}$$

Gauge symmetry is understood as a mathematical redundancy in our theoretical description and is not a real symmetry of nature. All physical quantities are gauge invariant. This is made apparent by Elitzur's theorem [34], which states that any expectation value of a gauge dependent local operator vanishes.

Gauge theory has a geometrical interpretation that is useful for studying the global topological structure of the theory and when constructing the theory on a discrete lattice, both of which we get to discuss in this thesis. This is the notion of gauge theory being a theory of a connection A_μ living on a principal-G fiber bundle and matter fields living on its associated vector bundle [35, 36]. Principal-G fiber bundle is a fiber bundle where the fibers are identical to the structure group G, see e.g. [36, Ch. 9-10].

Consider a field ϕ that transforms non-trivially under a representation of $G = \mathrm{SU}(2)$, i.e. it has some internal SU(2) degrees of freedom. At each spacetime point there is a set of possible values ϕ can take that form a SU(2) valued vector space, these are the *fibers* of the bundle. Gauge symmetry implies that on each fiber the basis can be chosen locally which makes the comparison of ϕ in two different points meaningless. The connection A_μ relates two infinitesimally close points to each other allowing us to make these comparisons. Just like in General Relativity the connection allows to relate tensors in different points. Thus, the gauge field (or connection) tells how the SU(2) degrees of freedom evolve when moving along a curve C from x to y through a parallel transport

$$\phi(y) = U(x, y; C)\phi(x) \ , \tag{1.4}$$

where $U(x, y; C)$ is the Wilson line given by

$$U(x, y, C) = \mathcal{P} \exp\left[i \int_C \mathrm{d}x^\mu A_\mu \right] \ . \tag{1.5}$$

Here $\mathcal{P}$ is the *path ordering* operator which means that when expanding the exponential the gauge fields $A_\mu(x[\tau])$ are ordered from left to right in the order they appear as the path $C[\tau]$ is traversed. The Wilson lines turn out to be the natural variables to choose when considering lattice gauge theories that we will discuss in chapter 3.1.

The Wilson line can be seen to transform under a gauge transformation Ω as $U(x, y; C) \to \Omega(x)U(x, y; C)\Omega^\dagger(y)$. From this we can note that if we consider a closed loop C and take the trace we obtain a gauge invariant quantity: the Wilson loop

$$W_C = \mathrm{Tr}\, \mathcal{P} \exp\left[i \oint_C \mathrm{d}x^\mu A_\mu \right] \ . \tag{1.6}$$

The Wilson loop thus describes the way the internal degrees of freedom change when going around a closed loop (i.e. holonomy). One may guess that, in analogy to General Relativity, infinitesimally this has something to do with the field strength (curvature) of the gauge field (connection), as we will see later.

In a perturbative setting a local description of the gauge field A_μ is usually

sufficient. However, there can be interesting global non-trivial topological structure that a local description is unable to capture.

We will not attempt a proper introduction to bundles here, see e.g. [36, 37]. To illustrate the structure: a principal-G bundle is a smooth manifold E that has fibers $F \cong G$. The bundle can be locally described on open sets $\mathcal{O}_a \subset M$ of the base manifold M (here M is the spacetime manifold) by *local trivializations* $E \cong \mathcal{O}_a \times G$. So, there are *local sections* of E given by maps $\sigma_{(a)} : \mathcal{O}_a \to \mathcal{O}_a \times G$. In other words, the bundle looks locally like the direct product space of the gauge group and the spacetime manifold.

There is a formal globally defined connection form $\mathcal{A}_\mu$ on E that defines the familiar local description of the gauge field on a chart $\mathcal{O}_a$ via a pullback defined with the local section $A_\mu^{(a)} = \sigma_{(a)}^* \mathcal{A}_\mu$. Where $A_\mu^{(a)}$ is now a local description on an open set $\mathcal{O}_a$. Now, (as in General Relativity) we have a patchwork of local descriptions, an atlas of charts $\mathcal{O}_a \subset M$ that cover M, which have to be consistently glued together. This is accomplished with *transition functions* $\mathrm{t}_{ab} : \mathcal{O}_a \cap \mathcal{O}_b \to G$, which describe the global structure of the manifold locally by relating different charts to each other on their overlaps. These relate two descriptions $A_\mu^{(a)}$ and $A_\mu^{(b)}$ on the overlap $\mathcal{O}_a \cap \mathcal{O}_b$ as

$$A_\mu^{(b)} = \mathrm{t}_{ab}^{-1} A_\mu^{(a)} \mathrm{t}_{ab} + \mathrm{t}_{ab}^{-1} \partial_\mu \mathrm{t}_{ab} \ , \tag{1.7}$$

where $\mathrm{t}_{ab}^{-1} = \mathrm{t}_{ba}$. These do change under local gauge transformations $\Omega_a : \mathcal{O}_a \to G$ as $\mathrm{t}_{ab} \to \Omega_a^{-1} \mathrm{t}_{ab} \Omega_b$. Thus, we can see that the relation between two local descriptions (1.7) is left invariant under a gauge transformation. So, the transition functions describe the global structure of the bundle. These come into play when we look at the global structure of gauge theories in the next section.

1.2 Vacuum structure of Yang–Mills gauge theories

Let us now discuss the non-trivial vacuum structure of Yang–Mills fields in the semi-classical approximation, for a full non-perturbative picture see e.g. [38].

To discuss the vacuum structure let us inspect the Euclidean path integral and finite action field configurations. We can move to Euclidean space by performing a Wick rotation to imaginary time $t \to it$. To keep the gauge field action real and to preserve the structure of gauge covariant derivative the time component of the gauge field is transformed as $A_0 \to iA_0$. The Euclidean Lagrangian is then

$$\mathcal{L}_E = -\mathcal{L}_{\mathrm{YM}}(t \to it) = +\frac{1}{2} \mathrm{Tr}\, F_{\mu\nu} F_{\mu\nu} \ , \tag{1.8}$$

where repeated indices are understood to be contracted with the Euclidean metric

$\delta_{\mu\nu}$. The Euclidean path integral then reads

$$Z = \int \mathcal{D}A_\mu \exp\left[-\int \mathrm{d}^4x \mathcal{L}_E\right] \ . \tag{1.9}$$

Field configurations with infinite action would give zero contributions in the path integral and semiclassical computation would not yield anything. For finite action configurations we see from the action that this implies that the field strength must vanish $F_{\mu\nu} \to 0$ faster than $|x|^{-2}$ as $|x| \to \infty$, where $x \in \mathbb{R}^4$. Thus, the gauge field must fall off as $|x|^{-2}$. This means that the gauge field approaches a "pure gauge" configuration at infinity

$$A_\mu \xrightarrow{|x|\to\infty} \frac{i}{g}\Omega_\infty \partial_\mu \Omega_\infty^{-1} \ , \tag{1.10}$$

where $\Omega_\infty : S^3 \to \mathrm{SU}(2)$ is a gauge transform necessarily depending only on the angular variables of the boundary at infinity. Requiring finite action field configurations gives us the one-point (conformal) compactification of Euclidean space $\mathbb{R}^4 \to S^4$ [37, Ch. 6][39]. So, the gauge transformations are functions from a 4-sphere to the gauge group $\Omega : S^4 \to \mathrm{SU}(2)$. This is a crucial step to take to get anything non-trivial since all principal bundles over $\mathbb{R}^4$ are trivial [37, Ch. 4]. Trivial here means that the bundle is globally a direct product space of the base space and the fibers $\mathbb{R}^4 \times \mathrm{SU}(2)$, which means the topology is trivial. In other words, there exists a local description of the gauge field that can be trivially extended everywhere.

Considering the compactified space S^4 allows for principal bundles with non-trivial topology. The principal SU(2) bundles over S^4 are characterized topologically by the homotopy classes of the transition function of the bundle. Principal SU(2) bundle over S^4 can be covered by two local descriptions: "north" U_N and "south" U_S hemispheres of the S^4 glued together by one S^3 "equatorial" transition function $\mathrm{t} : S^3 \to \mathrm{SU}(2)$ defined on the intersection of the two local descriptions ($U_S \cap U_N \cong S^3$), see e.g. [36, Ch. 10].

Before explaining how these maps are classified, let us move to using a seemingly one local description of the bundle often used in physics. Let the "south" hemisphere U_S be the one which surrounds the point at infinity and choose its local description for the gauge field to be $A_\mu^{(S)} = 0$. Then the transition function relates the two descriptions as $A_\mu^{(N)} = \mathrm{t}^{-1}A_\mu^{(S)}\mathrm{t} + \mathrm{t}^{-1}\partial_\mu \mathrm{t} = \mathrm{t}^{-1}\partial_\mu \mathrm{t}$. Thus, the gauge field at the boundary in (1.10) can be identified as the transition function. Thus, one can obtain the same classification by looking at the seemingly one local description without the notions of bundles. However, without the global description the requirement of $A_\mu^{(S)} = 0$, i.e. $A_\mu \xrightarrow{|x|\to\infty} 0$ seems arbitrary, which can now be seen as the condition that it is a proper gauge transformation on the bundle. See, also [39].

Let us now see how the transition functions or the gauge transforms at infinity

are classified. First note that any SU(2) element can be parametrized as

$$\Omega = d\mathbb{1} + c_a\sigma^a \in \mathrm{SU}(2) \iff c_1^2 + c_2^2 + c_3^2 + d^2 = 1 \ , \tag{1.11}$$

where σ^a are the Pauli matrices. Thus, the SU(2) group manifold is homotopic to a 3-sphere,

$$\mathrm{SU}(2) \cong S^3 \ . \tag{1.12}$$

So, the gauge transform at infinity is a map $\Omega_\infty : S^3 \to S^3$. These maps fall into different homotopy classes.[2] They are in different homotopy classes described by the third homotopy group $\pi_3(S^3) \cong \mathbb{Z}$.[3]

To get an idea of the structure of these maps lets look at an analogy that is simpler to picture [40, Ch. 7]: maps from a circle to another $S^1 \to S^1$. We can implement these as an imaginary number of unit modulus. We can define a set of standard maps over the circle $\left\{s(\theta, n) = e^{in\theta} | n \in \mathbb{Z},\ \theta \in [0, 2\pi]\right\}$. We see that for $n = 0$ we have the trivial mapping, for $n = 1$ we have a map that "winds" around the circle once in positive direction, $n = 2$ twice and so on. One can show that maps differing by how many times they wind around the circle and in what direction, however complicated, cannot be continuously deformed to one another. Thus, the maps form $S^1 \to S^1$ are classified by how many times they wind around the circle. This is called the "winding number" or the degree of a map in general. So, we have $\pi_1(S^1) \cong \mathbb{Z}$, see figure 1.1 for illustration. The winding number in this simple case can be computed from

$$n = \frac{i}{2\pi} \int_{S^1} \mathrm{d}\theta \ s \frac{\mathrm{d}s^{-1}}{\mathrm{d}\theta} \ , \tag{1.13}$$

which gives an integer winding number of any general continuous map $s : S^1 \to S^1$.

One can extend the previous illustration for maps from surfaces of spheres to itself $S^2 \to S^2$ and again find $\pi_2(S^2) \cong \mathbb{Z}$. Thus, it is not too surprising that for a hypersphere the answer turns out to also be $\pi_3(S^3) \cong \mathbb{Z}$, see e.g. [41, Ch. 4] for proofs.

Thus, we have seen that in the Yang–Mills theory for SU(2) the gauge fields are separated into infinite number of topologically distinct sectors classified by the homotopy group of transition functions (or the gauge transforms at infinity) $\pi_3(S^3) \cong \mathbb{Z}$. We find that there are infinite number of classically equivalent but topologically distinct vacua labeled by a winding number (degree of the map). For the maps

[2] Two functions $f, g : X \to Y$ are said to be homotopic if there exists a continuous function $h : X \times [0, 1] \to Y$ such that $h(x, 0) = f(x)$ and $h(x, 1) = g(x)$ for all $x \in X$. Meaning that there is a continuous deformation h from f to g.

[3] The n-th homotopy group $\pi_n(X)$ is the group formed by equivalence classes of continuous functions $f : S^n \to X$, where two functions are in the same equivalence class if they are homotopic. The group multiplication is intuitively the notion of gluing together the paths traced by the functions.

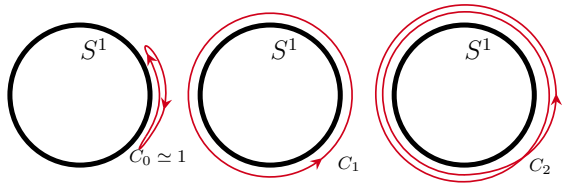

Figure 1.1. Illustrative picture of maps on a circle S^1 with different winding numbers. A map that does not go around the circle is continuously deformable to the trivial map $C_0 \cong 1$. A map C_1 going around the circle once cannot be continuously deformed into the trivial map nor the map C_2 going around the circle twice. Maps can be also distinguished by the direction which they wind the circle. The different maps are classified by how many times they go around the circle $\pi_1(S^1) \cong \mathbb{Z}$.

$\Omega : S^3 \to \mathrm{SU}(2)$ the winding number, also called the Chern-Simons number, is given by (in analogy to (1.13))

$$Q = \frac{1}{24\pi^2} \int_{S^3} \mathrm{d}S^3_\alpha \epsilon_{\alpha\beta\gamma\delta} \mathrm{Tr}\, \Omega\partial_\beta\Omega^{-1}\Omega\partial_\gamma\Omega^{-1}\Omega\partial_\delta\Omega^{-1} \ , \tag{1.14}$$

where $\mathrm{d}S^3_\alpha$ is the normal surface element. For vacuum configurations this is an integer. For excited configurations Q can differ from an integer and is often called the topological charge. This can be seen to be the integral of the "volume" element of SU(2). The integrand is sometimes called the Wess-Zumino term. For detailed discussion why this gives the degree of the map, see [40, Ch. 7]. There is an useful form for the winding number as an integral of the field strength over the bulk

$$Q = \frac{g^2}{16\pi^2} \int \mathrm{d}^4x \ \mathrm{Tr}\, F_{\mu\nu} {}^\star F_{\mu\nu} \ , \tag{1.15}$$

where ${}^\star F_{\mu\nu} = \frac{1}{2}\epsilon_{\mu\nu\alpha\beta} F_{\alpha\beta}$ is the Hodge dual of the field strength (often called the dual field strength). To see that (1.14) and (1.15) are equivalent note that the above integrand can be written as a total derivative $\partial_\mu K_\mu = \mathrm{Tr}\, F_{\mu\nu} {}^\star F_{\mu\nu}$ where

$$K_\mu \equiv 2\epsilon_{\mu\alpha\beta\gamma} \mathrm{Tr} \left[A_\alpha \partial_\beta A_\gamma - \frac{2i}{3} g A_\alpha A_\beta A_\gamma \right] \ . \tag{1.16}$$

Now by Stokes' theorem the integral (1.15) can be transformed into a surface integral

$$\int \mathrm{d}^4x \ \mathrm{Tr}\, F_{\mu\nu} {}^\star F_{\mu\nu} = \int \mathrm{d}S^3_\mu \lim_{|x|\to\infty} K_\mu \ . \tag{1.17}$$

For finite configurations the field strength $F_{\mu\nu}$ must vanish faster than $|x|^{-2}$ meaning that the gauge field must vanish faster than $|x|^{-1}$ up to a pure gauge part. This

implies the first term in K_μ vanishes at the boundary. Now since, the gauge fields approach pure gauge configurations at infinity (1.10) we get that K_μ as $|x| \to \infty$ equals the integrand in (1.14). Thus, (1.15) and (1.14) are equivalent.

The evolution of the topological charge, here also called the Chern-Simons number N_{CS}^W of the SU(2) field is given by

$$\Delta N_{CS}^W \equiv N_{CS}^W(t) - N_{CS}^W(0) = \frac{g^2}{16\pi^2} \int_0^t \mathrm{d}t \int \mathrm{d}^3x \ \mathrm{Tr}\, F_{\mu\nu}{}^\star F^{\mu\nu} \ . \tag{1.18}$$

Let us also define here the corresponding Chern-Simons number for the Abelian U(1) field

$$\Delta N_{CS}^Y \equiv N_{CS}^Y(t) - N_{CS}^Y(0) = \frac{g'^2}{16\pi^2} \int_0^t \mathrm{d}t \int \mathrm{d}^3x \ B_{\mu\nu}{}^\star B^{\mu\nu} \ , \tag{1.19}$$

which in vacuum is trivial since the U(1) bundle over S^4 is trivial, i.e. the U(1) has trivial topology. However, this can change if we are not in vacuum, in particular if we consider external hypermagnetic fields.

In the pure SU(2) Yang–Mills theory the topologically distinct vacua are connected by Euclidean finite action solutions of the classical equations of motion called the *Belavin–Polyakov–Schwarz–Tyupkin* (BPST) *instantons* [42]. In Minkowski signature these can be interpreted as describing the quantum tunneling between the different vacua. A general bound for the action in Euclidean space can be obtained from the fact that

$$\int \mathrm{d}^4x \ \mathrm{Tr}\, [F_{\mu\nu} \pm {}^\star F_{\mu\nu}]^2 \geq 0 \ , \tag{1.20}$$

leading to

$$S_E = \int \mathrm{d}^4x \ \frac{1}{2} \mathrm{Tr}\, F_{\mu\nu} F_{\mu\nu} \geq \frac{1}{2} \left| \int \mathrm{d}^4x \ \mathrm{Tr}\, F_{\mu\nu}{}^\star F_{\mu\nu} \right| = \frac{8\pi^2}{g^2} |Q| \ , \tag{1.21}$$

which is known as the Bogomol'nyi bound. From the Bianchi identity $D_\mu {}^\star F_{\mu\nu} = 0$ it follows that the instanton solutions are self dual $F_{\mu\nu} = \pm {}^\star F_{\mu\nu}$ for which this bound is saturated. Thus, for example the action for the unit instanton with winding number $Q = 1$ is $S_E = 8\pi^2/g^2$.

In the electroweak theory scaling argument known as the Derrick's theorem excludes the existence of the BPST instantons, see e.g. [43, Ch. 4]. In the electroweak theory it is possible to get from one vacuum to another through another type of configuration: the sphaleron. Before describing the sphaleron configuration let us briefly review the electroweak sector of the Standard Model.

1.3 Electroweak Theory

The Standard Model of particle physics is a non-Abelian chiral gauge theory with the gauge group given by $\mathrm{SU}(3) \times \mathrm{SU}(2)_L \times \mathrm{U}(1)_Y$. The SU(3) describes the Quantum Chromodynamics (QCD) which is the theory of the strong nuclear force. The fields charged under $\mathrm{SU}(2)_L \times \mathrm{U}(1)_Y$ describe the electroweak sector. Only the left-handed fermions transform non-trivially under the $\mathrm{SU}(2)_L$ and left and right-handed fermions couple differently to the hypercharge $\mathrm{U}(1)_Y$, meaning that the theory is chiral. An important part of the electroweak sector is the Higgs field ϕ which is in the fundamental representation of $\mathrm{SU}(2)_L$ and is charged under the hypercharge $\mathrm{U}(1)_Y$ with a charge of $\frac{1}{2}$. At zero temperature the Higgs mechanism gives rise to tree-level masses for the fermions and $\mathrm{SU}(2)_L$ gauge bosons which results into the seemingly separate weak nuclear and electromagnetic forces.

At high temperatures the QCD and fermionic contributions can be taken into account perturbatively which we discuss in chapter 2. The relevant part of the electroweak Lagrangian for our discussion here is

$$\mathcal{L}_{\mathrm{EW}} = -\frac{1}{2}\mathrm{Tr}\, F_{\mu\nu}F^{\mu\nu} - \frac{1}{4}B_{\mu\nu}B^{\mu\nu} + (D_\mu\phi)^\dagger(D^\mu\phi) + m^2\phi^\dagger\phi - \lambda(\phi^\dagger\phi)^2 \ , \qquad (1.22)$$

where ϕ is the Higgs doublet and the covariant derivative is $D_\mu = \partial_\mu - igA_\mu - i\frac{g'}{2}B_\mu$. The g is the $\mathrm{SU}(2)_L$ and g' is the $\mathrm{U}(1)_Y$ gauge coupling. The field strengths of the gauge fields are

$$\begin{aligned} F_{\mu\nu} &= \partial_\mu A_\nu - \partial_\mu A_\nu - ig[A_\mu, A_\nu] \ , \ \text{for } \mathrm{SU}(2)_L \\ B_{\mu\nu} &= \partial_\mu B_\nu - \partial_\mu B_\nu \ , \qquad\qquad\qquad \text{for } \mathrm{U}(1)_Y \ . \end{aligned} \qquad (1.23)$$

With an appropriate gauge choice we may choose the Higgs potential to be minimized by $\phi = \frac{1}{\sqrt{2}}\left(\begin{smallmatrix} 0 \\ v \end{smallmatrix}\right)$ with a non-zero Higgs vacuum expectation value $v > 0$. With this the usual picture of a "spontaneous symmetry breaking" is recovered. To be exact the gauge freedom is removed by the gauge fixing. Gauge symmetries cannot be broken as stated by the Elitzur's theorem [34].[4] Nevertheless, in this perturbative picture one finds mass terms for the $W^\pm$ and Z bosons while the photon given by

$$a_\mu = \sin\theta_W A^3_\mu + \cos\theta_W B_\mu \ , \qquad (1.24)$$

remains massless, where θ_W is the *weak mixing angle* given by $\tan\theta_W = \frac{g'}{g}$. See e.g. [45] for more detailed introduction. The electroweak symmetry group $G = \mathrm{SU}(2)_L \times \mathrm{U}(1)_Y$ is reduced to the electromagnetic symmetry group $H = \mathrm{U}(1)_{\mathrm{em}}$.

[4] For a non-perturbative description of the Higgs mechanism see e.g. [38, 44].

Thus, the vacuum manifold after symmetry breaking can be identified as the coset space [46, Ch. 2][5]

$$V_0 \cong G/H = \mathrm{SU}(2)_L \times \mathrm{U}(1)_Y / \mathrm{U}(1)_{\mathrm{em}} \cong SU(2) \ , \tag{1.25}$$

which will be relevant when we discuss the sphaleron configuration.

In the cosmic past, our universe was in a dense hot thermal state. Taking into account thermal corrections to the Higgs potential, at a sufficiently large temperatures these corrections dominate making the minimum of the effective potential shift to the origin, making the Higgs mechanism inactive and restoring the electroweak symmetry. Depending on the details of the physics that governs the energy scales at the electroweak scale $T_{\mathrm{EW}} \sim 100$ GeV this transition could have been a first order phase transition happening at some critical temperature T_c.

In the Standard Model, however, the transition is a smooth crossover, due to the mass of the Higgs boson being sufficiently large [47–51]. The transition would be of first order for Higgs masses below $m_H \lesssim 72$ GeV. From lattice simulations the crossover transition in the Standard Model is found to happen over a quite narrow region of width ~ 5 GeV at a pseudocritical temperature $T_c = 159.5 \pm 1.5$ GeV [52]. So, in the Standard Model the phases below and above the crossover are in fact connected analytically and the same thermodynamical phase. There are still qualitative differences and thus being above or below the crossover is an useful notion. We nevertheless choose to use the common nomenclature of "broken phase" below the crossover and "symmetric phase" above it. Perhaps better labels would be the Higgs phase at $T < T_c$ and confining phase at $T > T_c$.

1.4 The sphaleron configuration

The electroweak *sphaleron*[6] can be thought as the minimum energy unstable saddle-point configuration sitting on top of an energy barrier between two topologically distinct vacua. It is a static unstable finite energy solution of the classical field equations. The solution was first found in [54] and its connection to the topology of SU(2) gauge fields was first found in [53, 55].

The vacuum structure of the electroweak sector is analogous to the pure SU(2) Yang–Mills theory discussed previously. Now, however, the Higgs field in the broken phase gives a scale for the energy barrier between the topologically distinct vacua giving rise to the sphaleron configuration. In temporal gauge $A_0 = 0$ (and finite configurations with $\lim_{|x|\to\infty} \Omega \to 1$) the sphaleron can be seen as the configuration

[5] For a group G and its subgroup H the coset space is defined as $G/H = \{gH \mid g \in G\}$ where $gH = \{gh \mid h \in H\}$.

[6] From Greek word σφαλερός (sphaleros) meaning "ready to fall", coined in [53].

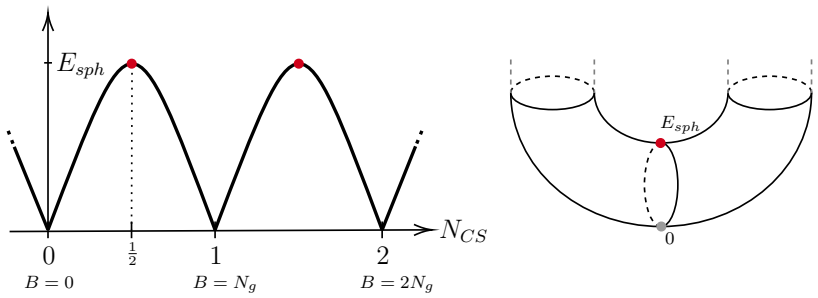

Figure 1.2. Schematic picture of the electroweak sphaleron and vacuum structure. **(Left)** In the temporal gauge the sphaleron is seen as the configuration on top of an energy barrier separating two topologically distinct vacua. The height of the barrier is the sphaleron energy $E_{sph} \simeq 9.0$ TeV. **(Right)** In the radial gauge it can be seen to be a non-contractible loop in field configuration space that connects the vacuum to itself. The surface of a torus illustrates the field configuration space with possible non-contractible loops.

on top of an energy barrier separating two neighboring topologically distinct vacua, see figure 1.2 (left). In other gauges the picture can be different. For example, in the radial gauge with $A_r = 0$ and $A_0 = 0$, there is only one vacuum and sphaleron is a non-contractible loop in field configuration space, see figure 1.2 (right). The field configuration space has non-contractible loops that connect the vacuum to itself, see e.g. [56, Ch. 13] [55] [57] [58]. The radial gauge is where the configuration is often constructed.

With Higgs field in the unitary gauge the static field configuration energy functional (action) is

$$E_0 = \int \mathrm{d}^3x \left[\frac{1}{2} \mathrm{Tr}\, F_{ij} F_{ij} + \frac{1}{4} B_{ij} B_{ij} + (D_i \phi)^\dagger (D_i \phi) + \frac{\lambda}{4} \left(\phi^\dagger \phi - v^2 \right)^2 \right] . \tag{1.26}$$

The topology of the space of finite static field configurations is described by the asymptotics of the fields at spatial infinity. These are functions from the asymptotic boundary of $\mathbb{R}^3$ to the vacuum manifold V_0: $\mathrm{Maps}(S^2 \to V_0)$. As we saw previously in the broken phase the vacuum manifold is given by $V_0 \simeq \mathrm{SU}(2)$, see (1.25). So, this space has non-contractible loops[7]

$$\pi_1(\mathrm{Maps}(S^2 \to \mathrm{SU}(2))) \cong \pi_3(\mathrm{SU}(2)) \cong \pi_3(S^3) \cong \mathbb{Z} . \tag{1.27}$$

The non-trivial topology is again inherited from an SU(2) group.

Let us now describe the sphaleron configuration with U(1) included using a spher-

[7]This follows from the composition of homotopy groups $\pi_n(\mathrm{Maps}(S^m \to Y)) = \pi_{n+m}(Y)$ for $n \geq 1$ [43, Ch. 3].

ically symmetric ansatz for simplicity (see any of [43, 53, 56, 59] for the construction without U(1) fields $\theta_W = 0$). With U(1) and $\theta_W \neq 0$ the sphaleron is only axially symmetric [60, 61]. However, with zero or small external (hyper)magnetic fields the angular dependence is found to be mild. In this case the sphaleron solution, to a good approximation, can be found with a spherically symmetric ansatz. One starts by specifying the form of the asymptotic fields that have a winding number one

$$\phi_\infty(\theta,\varphi;\mu) = \begin{bmatrix}\phi^0_\infty \\ \phi^1_\infty\end{bmatrix} = \begin{bmatrix}\sin\mu\sin\theta e^{i\varphi} \\ e^{-i\mu}(\cos\mu + i\sin\mu\cos\theta)\end{bmatrix} \ , \ \Omega_\infty = \begin{bmatrix}(\phi^1_\infty)^* & \phi^0_\infty \\ -(\phi^0_\infty)^* & \phi^1_\infty\end{bmatrix} \ , \tag{1.28}$$

where $\mu \in [0,\pi]$ is the non-contractible loop parameter, φ and θ are the angular coordinates, and $\Omega_\infty \in \mathrm{SU}(2)$. The values $\mu = 0, \pi$ correspond to the vacuum and half-way between $\mu = \pi/2$ corresponds to the sphaleron solution. To extend the solution on the boundary (at $\mu = \pi/2$) to the bulk one introduces the ansatz which, with the Higgs field in unitary gauge, is given by [62]:

$$\begin{aligned} gA^a_i\sigma^a \mathrm{d}x^i &= [1-f(\xi)]\left[F_1\sigma^1 + F_2\sigma^2\right] + [1-f_3(\xi)]\,F_3\sigma^3 \ , \\ g' B_i \mathrm{d}x^i &= [1-f_0(\xi)]\,F_3 \ , \\ \phi &= \frac{v}{\sqrt{2}}\begin{bmatrix}0 \\ h(\xi)\end{bmatrix} \ , \end{aligned} \tag{1.29}$$

where $\xi = gvr$ is a dimensionless radial coordinate, v is the Higgs vacuum expectation value, σ^a are the Pauli matrices and F_a are given by

$$\begin{aligned} F_1 &= -2\sin\varphi \mathrm{d}\theta - \sin 2\theta\cos\varphi \mathrm{d}\varphi, \\ F_2 &= -2\cos\varphi \mathrm{d}\theta + \sin 2\theta\sin\varphi \mathrm{d}\varphi, \\ F_3 &= 2\sin^2\theta \mathrm{d}\varphi. \end{aligned} \tag{1.30}$$

To smoothly connect the ansatz to the boundary (1.28) (and to avoid singularities at the origin) the functions have to satisfy the boundary conditions

$$\begin{aligned} f, h \to 1 \ , \quad f_3, f_0 \to 1 \ , \quad \text{when } \xi \to \infty \ , \\ f, h, f_3 \to 0 \ , \qquad f_0 \to 1 \ , \quad \text{when } \xi \to 0 \ . \end{aligned} \tag{1.31}$$

Substituting the ansatz (1.29) into (1.26) the energy becomes

$$\begin{aligned} E_0 = \frac{4\pi v}{g}\int_0^\infty \mathrm{d}\xi \Bigg[& \frac{8}{3}f'^2 + \frac{4}{3}f_3'^2 + \frac{1}{2}\xi^2 h'^2 + \frac{4g^2}{3g'^2}f_0'^2 \\ & + \frac{8}{3\xi^2}\left\{ 2f_3^2(1-f)^2 + [f(2-f)-f_3]^2 + \frac{g^2}{g'^2}(1-f_0)^2 \right\} \\ & + \frac{h^2}{3}\left\{ (f_0-f_3)^2 + 2(1-f)^2 \right\} + \frac{\lambda}{4g^2}\xi^2(h^2-1)^2 \Bigg] . \end{aligned} \tag{1.32}$$

Extremising the above energy one gets the equations for the ansatz functions

$$\begin{aligned} & h'' + \frac{2}{\xi}h' - \frac{2h}{3\xi^2}\left[2(1-f)^2 + (f_0-f_3)^2\right] - \frac{\lambda}{g^2}(h^2-1)h = 0, \\ & f'' + \frac{1-f}{\xi^2}\left[2f(f-2) + 2f_3 + 2f_3^2\right] + \frac{1}{4}(1-f)h^2 = 0, \\ & f_0'' + \frac{2(1-f_0)}{\xi^2} - \frac{g'^2}{4g^2}(f_0-f_3)h^2 = 0, \\ & f_3'' - \frac{2}{\xi^2}\left[3f_3 + f(f-2)(1+2f_3)\right] - \frac{h^2}{4}(f_3-f_0) = 0, \end{aligned} \tag{1.33}$$

where $'$ denotes derivatives with respect to ξ. Solving these with the boundary conditions (1.31) one obtains the sphaleron configuration. The forms of the numerical solutions can be seen in figure 1.3 as the blue curves with $g_0 = f_0$ and $g_3 = f_3$. The spherical ansatz with $\theta_W = 0$ can be recovered by taking $f_0 \to 1$ and $f_3 \to f$.

After finding the sphaleron configuration its energy can be computed. In the Standard Model the energy of the electroweak sphaleron is found to be $E_{\mathrm{sph}} \simeq 9.11$ TeV [63]. The U(1) fields affect the sphaleron energy only by less than 1% [60]. The solution can be shown to have one unstable mode [43, 64, 65], i.e. the sphaleron is unstable.[8] Furthermore, using the ansatz described above the sphaleron configuration can be found to have a half integer Chern-Simons number (or topological charge) $N_{CS} = n + \frac{1}{2}$, $n \in \mathbb{Z}$ [53] (see also [66, Appendix A]).

1.4.1 Magnetic dipole moment

When the U(1) is included the sphaleron can be seen to have a magnetic dipole moment. From the ansatz we find that the electromagetic field is

$$a_i \mathrm{d}x^i = (\sin\theta_W A_i^3 + \cos\theta_W B_i)\mathrm{d}x^i = (1 - \sin^2\theta_W f_3 - \cos^2\theta_W f_0)F_3 \ , \tag{1.34}$$

[8] If the Higgs self coupling would be large ($\lambda > 18.1$), there would be instead a configuration called the deformed sphaleron or bisphaleron [64, 65].

which has the asymptotic behavior of a pure magnetic dipole [62]

$$a_i \mathrm{d}x^i \simeq \frac{\mu_{\mathrm{dip}}}{\xi} \sin^2\theta \mathrm{d}\varphi \ . \tag{1.35}$$

Taking the effects of U(1) to be small to first order the magnetic dipole moment is [53]

$$\mu_{\mathrm{dip}} \simeq \frac{2\pi g'}{3g^3 v} \int_0^\infty \mathrm{d}\xi h^2 \left[1 - f_3(\xi)\right] \ . \tag{1.36}$$

The magnetic dipole moment can be seen to originate from a monopole-antimonopole pair connected by a tube of Z boson flux (Z-string) [67].

Due to the dipole moment the energy of the sphaleron can be lowered if there is an external magnetic field. To first order it gets lowered by a simple dipole interaction term $\Delta E = E^{(1)}_{\mathrm{dip}} - E_0$ with $E^{(1)}_{\mathrm{dip}} = \mu_{\mathrm{dip}} B_c^{\mathrm{4d}}$ where B_c^{4d} is the magnitude of the external magnetic field [68]. The external magnetic field is relatively straight forward to add into the computation of the sphaleron configuration. Following [68] we can add a dipole interaction term into the energy functional $E = E_0 - E_{\mathrm{dip}}$ with

$$E_{\mathrm{dip}} = \int \mathrm{d}^3x \frac{1}{2} B_{ij} B^c_{ij} = \int_0^\infty \mathrm{d}\xi \frac{8\pi}{3gg'v} \left[-2\xi f_0' + 2(1 - f_0)\right] B_c^{4d} \ , \tag{1.37}$$

where $B^c_{ij} = \partial_i B^c_j - \partial_j B^c_i$ and the external field pointed to z direction is given by $B^c_i = -\frac{1}{2}\epsilon_{3ij} B^{\mathrm{4d}} x_j$. The field equations (1.33) are not modified by the added term. Only the boundary conditions at infinity need to be modified as

$$f, h \to 1, \quad f_3, f_0 \to 1 - \frac{\sin 2\theta_W \xi^2}{8gv^2} B_c^{\mathrm{4d}}, \quad \text{when } \xi \to \infty \ . \tag{1.38}$$

For solving the equations it is convenient to introduce the following field redefinitions

$$g_i(\xi) = f_i(\xi) + \sin 2\theta_W \frac{\xi^2}{2gv^2}, \tag{1.39}$$

for $i = 0, 3$, so that the boundary conditions for the new functions at infinity are $g_i \to 1$ when $\xi \to \infty$. In [1] we solved (1.33) with different magnitudes for the external field B_c^{4d} to compare the semiclassical computation with our lattice results that we discuss later in section 3.5. See figure 1.3 for examples of the numerical solutions with and without an external magnetic field.

This spherical ansatz is valid only for small magnetic fields. For larger external fields the sphaleron configuration gets more and more elongated [69]. At a critical value $B_{c1} = m_W^2/(g \sin\theta_W)$ the situation is complicated due to the appearance of

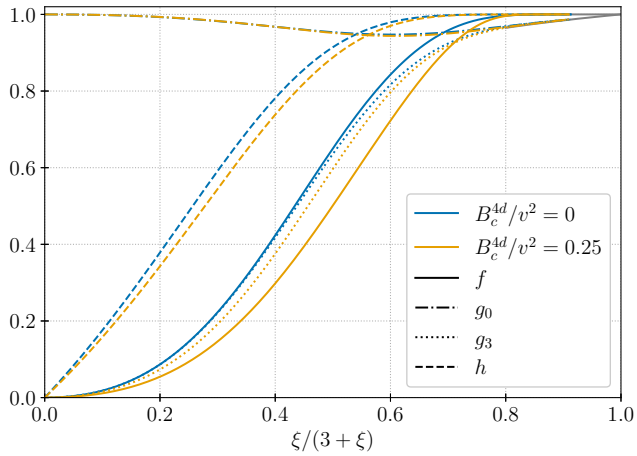

Figure 1.3. Numerical solutions for the spherically symmetric sphaleron ansatz (1.33). Blue curves correspond to zero and yellow curves to non-zero external magnetic field. Figure from [1]. Computing the energy from the two configurations at zero temperature translate to 9.0 TeV for zero magnetic field and 6.7 TeV for the non-zero magnetic field.

the Ambjorn-Olesen phase [70, 71]. A homogeneous magnetic field no longer is the favored ground state. Instead, it becomes a non-trivial structure of vortices [72] at least at zero temperature [23]. At a second critical value $B_{c2} = m_H^2/(g \sin\theta_W)$ the electroweak symmetry is restored and the sphaleron solution ceases to exist, i.e. the energy barrier goes to zero. The sphaleron energy initially decreases linearly for $B_c^{4\mathrm{d}} < B_{c1}$ and then more steeply when approaching the first critical value. After reaching the non-trivial phase the sphaleron energy decreases more slowly with increasing magnetic field compared to the normal phase [69].

Next we will discuss how the sphaleron is connected to baryon number violation in the Standard Model via the chiral anomaly.

1.5 Chiral Anomaly

In quantum field theories an anomaly is a symmetry of the classical theory that is not preserved at the quantum level. In the path integral formulation, it is a symmetry of the action but not of the path integral measure (attributed to Fujikawa [73]). In a gauge theory with massless fermions the axial current is not conserved in the quantum theory. This is the *chiral anomaly*, also called the *Adler–Bell–Jackiw* (ABJ) *anomaly* [74, 75].

The relevant part of the action for massless Dirac fermions ψ coupled to SU(2)

and U(1) gauge fields is

$$S_f = \int \mathrm{d}^4x \; i\bar{\psi}\not{D}\psi \; , \tag{1.40}$$

where γ^μ are the gamma matrices, $\bar{\psi} \equiv \psi^\dagger\gamma^0$, and $\not{D} \equiv \gamma^\mu D_\mu$. The covariant derivative is $D_\mu = \partial_\mu - ig\delta_L A_\mu + ig'YB_\mu$ where Y is the hypercharge, and $\delta_L = 1$ for left-handed and $\delta_L = 0$ for right-handed fermions. The gamma matrices satisfy the Clifford algebra $\{\gamma^\mu, \gamma^\nu\} = 2\eta^{\mu\nu}$ and the fifth gamma matrix is $\gamma^5 = -i\gamma^0\gamma^1\gamma^2\gamma^3$. Chiral left and right-handed spinors can be defined using projection operators as $\psi_L = \frac{1}{2}(1-\gamma^5)\psi$ and $\psi_R = \frac{1}{2}(1+\gamma^5)\psi$.

The action (1.40) is invariant under the global chiral transformations

$$\psi \to e^{i\alpha\gamma^5}\psi \; , \quad \bar{\psi} \to \bar{\psi}e^{i\alpha\gamma^5} \; . \tag{1.41}$$

In the classical theory with Noether's theorem one obtains the conserved axial vector current

$$J_A^\mu = \bar{\psi}\gamma^\mu\gamma^5\psi \; , \tag{1.42}$$

which classically satisfies $\partial_\mu J_A^\mu = 0$. The time component of the chiral current gives the difference between left and right-handed spinors $J_A^0 = \psi_L^\dagger\psi_L - \psi_R^\dagger\psi_R$. So, classically the ratio of left and right-handed particle number densities is conserved.

This will no longer be the case in the quantum theory. Likewise when deriving the classical Noether current, we promote the global chiral transformation to a local one, i.e. $\alpha \to \alpha(x)$ in (1.41). The Jacobian of this transformation turns out to be given by

$$\begin{aligned}\int \mathcal{D}\psi\mathcal{D}\bar{\psi} \to \int \mathcal{D}\psi\mathcal{D}\bar{\psi} \exp\Bigg[&-\frac{ig^2\delta_L}{16\pi^2}\int \mathrm{d}^4x\alpha(x)\epsilon^{\alpha\beta\gamma\delta}\mathrm{Tr}\, F_{\alpha\beta}F_{\gamma\delta} \\ &-\frac{ig'^2Y^2}{16\pi^2}\int \mathrm{d}^4x\alpha(x)\epsilon^{\alpha\beta\gamma\delta}B_{\alpha\beta}B_{\gamma\delta}\Bigg] \; ,\end{aligned} \tag{1.43}$$

see e.g. [76]. Thus, one finds that the full path integral changes as

$$\begin{aligned}Z &= \int \mathcal{D}\Psi\mathcal{D}\psi\mathcal{D}\bar{\psi} \exp\Big[i\left(S_{\mathrm{EW}}[\Psi] + S_f\right)\Big] \\ &\to \int \mathcal{D}\Psi\mathcal{D}\psi\mathcal{D}\bar{\psi} \exp\Bigg[i\left(S_{\mathrm{EW}}[\Psi] + S_f\right) \\ &\quad + i\int \mathrm{d}^4x\alpha(x)\left(\partial_\mu J_A^\mu - \frac{ig^2\delta_L}{8\pi^2}\mathrm{Tr}\, F_{\mu\nu}{}^\star F^{\mu\nu} - \frac{ig'^2Y^2}{8\pi^2}B_{\mu\nu}{}^\star B^{\mu\nu}\right)\Bigg] \; ,\end{aligned} \tag{1.44}$$

here Ψ denotes collectively the rest of the fields in the theory. Now, since the path integral is an integral over all possible field configurations, i.e. the end result does

not depend on the fields, the result must be invariant under any change of variables. In other words, redefining the fields we integrate over should not change the physics. Thus, the terms on the last line of (1.44) must vanish for all functions $\alpha(x)$. Note that the first term on its own would indeed give us just the classical conservation of the current. However, now we have the extra terms from the Jacobian of the path integral measure. So, we get the anomalous axial current

$$\partial_\mu J_A^\mu = \frac{g^2\delta_L}{8\pi^2}\mathrm{Tr}\, F_{\mu\nu}{}^\star F^{\mu\nu} + \frac{g'^2 Y^2}{8\pi^2} B_{\mu\nu}{}^\star B_{\mu\nu} \ . \tag{1.45}$$

Baryon number is defined as $B = \frac{1}{3}(n_q - n_{\bar{q}})$ where n_q is the number of quarks and $n_{\bar{q}}$ the number of anti quarks. Furthermore, lepton number is defined as $L = n_\ell - n_{\bar{\ell}}$ where n_ℓ is the number of leptons and $n_{\bar{\ell}}$ the number of anti-leptons. Baryon and lepton numbers are both classically conserved quantities meaning that both have a corresponding global symmetry of the Standard Model Lagrangian, i.e. the Lagrangian is invariant under $\psi \to e^{iB\alpha}\psi$ and $\psi \to e^{iL\alpha}\psi$.

Due to the chiral anomaly the baryon and lepton numbers are not conserved in the electroweak sector of the Standard Model. This was first seen by 't Hooft [77]. For the left-handed quarks ψ_L the baryon number current can be written as $\frac{1}{3}(\bar{\psi}_L\gamma^\mu\psi_L) = \frac{1}{3}(\bar{\psi}\gamma^\mu\psi - \frac{1}{2}\bar{\psi}\gamma^\mu\gamma^5\psi) = \frac{1}{3}(J_V^\mu - \frac{1}{2}J_A^\mu)$ and for the right-handed quarks ψ_R it can be written as $\frac{1}{3}(\bar{\psi}_R\gamma^\mu\psi_R) = \frac{1}{3}(J_V^\mu + \frac{1}{2}J_A^\mu)$. The lepton number for the left- and right-handed leptons can be written in the same way but without the overall factor of $\frac{1}{3}$. Thus, the baryon and lepton numbers are not conserved if the left and right-handed fermions couple differently to the gauge fields, i.e. if the theory is chiral. In the electroweak sector of the Standard Model both the SU(2) and the hypercharge U(1) have different coupling to left and right-handed fermions.

Furthermore, if there are N_g generations of fermions we get exactly the same anomalous contribution for each generation. In the Standard Model we have $N_g = 3$. The quark baryon number of $\frac{1}{3}$ is compensated by the sum over quark colors and thus baryon and lepton numbers have the same anomaly. In total for the sum of all generations the baryon and lepton currents give

$$\partial_\mu J_B^\mu = \partial_\mu J_L^\mu = N_g\left[\frac{g^2}{16\pi^2}\mathrm{Tr}\, F_{\mu\nu}{}^\star F^{\mu\nu} - \frac{g'^2}{16\pi^2} B_{\mu\nu}{}^\star B^{\mu\nu}\right] \ . \tag{1.46}$$

Since, the baryon and lepton numbers have the same anomaly the difference between them $B - L$ is still a conserved quantity, while B, L or the sum $B + L$ are not. The change of baryon number is then

$$\partial_0 B = \int \mathrm{d}^3x \partial_0 J_B^0 = N_g \int \mathrm{d}^3x \left[\frac{g^2}{16\pi^2}\mathrm{Tr}\, F_{\mu\nu}{}^\star F^{\mu\nu} - \frac{g'^2}{16\pi^2} B_{\mu\nu}{}^\star B^{\mu\nu}\right] \ . \tag{1.47}$$

So, in some finite time period we see that the baryon and lepton numbers change by[9]

$$\int_0^t \partial_0 B = \Delta B = \Delta L = N_g \left[N_{CS}(t) - N_{CS}(0)\right] \equiv N_g \Delta N_{CS}(t) \ , \tag{1.48}$$

where we combine (1.18) and (1.19) into the "full" Chern-Simons number

$$\Delta N_{\rm CS} \equiv \Delta N_{\rm CS}^W - \Delta N_{\rm CS}^Y \ . \tag{1.49}$$

The U(1) field is often not considered here since it cannot induce a permanent change of baryon number in the vacuum due to its trivial topology, unlike the SU(2) fields. However, when not in vacuum, e.g. when there is an external magnetic field, the U(1) field can change the baryon number.

1.6 Sphaleron rate

We have seen that the sphaleron sources baryon number violation. In the context of baryogenesis, which we will discuss in the next section, it is important to know what is the rate of baryon number violating processes throughout the cosmic history of our universe.

The probability of the baryon number violation via the anomalous processes is described by the Chern-Simons number diffusion constant known as the *sphaleron rate*:

$$\Gamma \equiv \lim_{t,V\to\infty} \frac{\langle \Delta N_{CS}(t)^2 \rangle}{Vt} \ . \tag{1.50}$$

At zero temperature it is not possible to get over the energy barrier classically through the sphaleron and thus the rate is given by tunneling processes. As discussed previously, the electroweak theory does not have a true instanton solution. There are instead constrained instantons which turn out to give a similar exponential suppression for the rate [81–85]:[10]

$$\Gamma_0 \sim e^{-16\pi^2/g^2} \sim 10^{-161}, \quad \text{at} \quad T = 0 \ . \tag{1.51}$$

Thus, at zero temperature the rate is unobservably small. At higher temperatures, however, one can get over the energy barrier via the sphaleron by thermal activation. At temperatures below the electroweak transition the rate is given by the sphalerons

[9] Yukawa interactions ($y\bar{\psi}_L \phi \psi_R$ that give rise to the fermion masses through the Higgs mechanism) do not change this conclusion, see e.g. [56, Ch. 17.3] [78–80].

[10] The instanton bound (1.21) in the electroweak theory becomes a strict lower bound $S_E > 8\pi^2/g^2|Q|$, see e.g. [56, Ch. 13].

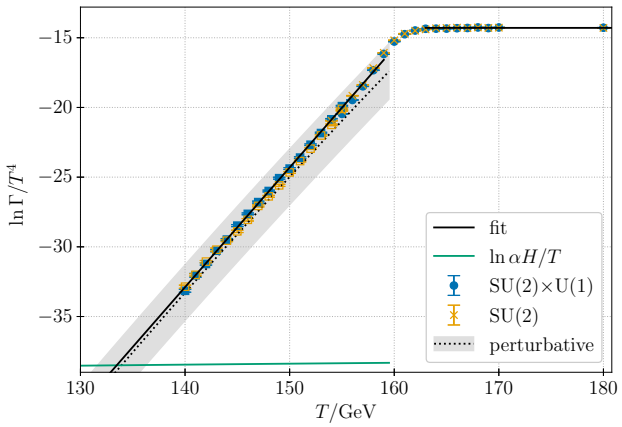

Figure 1.4. The sphaleron rate with (blue) and without (yellow) U(1) included. The green approximately horizontal line $\ln \alpha H/T$ is the effective Hubble rate as a function of temperature. From [1].

and can be shown to be suppressed by the sphaleron energy [83, 86, 87]

$$\Gamma_{\text{brk}} \sim (g^2T)^4 e^{-E_{\text{sph}}/T}, \quad \text{at} \quad T < T_c \ , \tag{1.52}$$

where T_c is the (pseudo)critical temperature where the electroweak transition takes place. Above the critical temperature where the Higgs vacuum expectation value vanishes, the sphaleron solution no longer exists. There are, however, still field configurations that change the Chern-Simons number N_{CS}. These are no longer suppressed since the energy barrier, sphaleron energy, has vanished. In the symmetric phase the rate is still customarily called the *hot sphaleron rate* (or just sphaleron rate). In the symmetric phase the rate behaves as [88–93]:

$$\Gamma_{\text{sym}} \sim \ln(1/g)\, g^{10}T^4, \quad \text{at} \quad T > T_c \ , \tag{1.53}$$

On dimensional grounds the rate would go as $\Gamma \sim (g^2T)^4$ [94]. Taking into account dynamics of the soft modes (discussed in the section 2.1) one arrives at $\Gamma \sim g^2(g^2T)^4$ [88]. Furthermore, noting that also the semi-hard modes affect the soft modes (see section 2.2) one obtains the behavior $\Gamma \sim \ln(1/g)g^2(g^2T)^4$ [95].

The sphaleron rate has been computed successfully on the lattice with methods that we will describe shortly. Most recently for the Standard Model it was computed in [96]. The previous computations have neglected the U(1) field since it is shown to have a negligible effect on the sphaleron and the form of the phase transition. Since, in [1] we were interested in performing the simulations in a (hyper)magnetic field we

had the U(1) field included. Thus, we also got to check the difference between the sphaleron rate with and without the U(1) field. The effect is indeed negligible, see figure 1.4. In the symmetric phase with U(1) field included we found

$$\Gamma_{\text{sym}}/T^4 = (6.23 \pm 0.05) \times 10^{-7} \simeq (13.9 \pm 0.1)\alpha_W^5 \ , \tag{1.54}$$

with $\alpha_W \simeq 0.03389$ and the value without U(1) field was well within the statistical errors. In the broken phase the rate is indeed exponentially suppressed and we found

$$\ln(\Gamma_{\text{brk}}/T^4) = (0.86 \pm 0.01)T/\text{GeV} - (153.1 \pm 0.9) \ , \tag{1.55}$$

with U(1) field included and again the result without U(1) field was well within the statistical errors. Both the broken and symmetric phase values are slightly different from what was previously found in [96] using the same methods. This is due to us using an updated value for the top quark mass and using all the available $\mathcal{O}(a)$ improvements in the computation of the lattice parameters. The computation of these lattice parameters are discussed in section 2.1.

The behavior of the sphaleron rate is important for many baryogenesis scenarios which is what we discuss next.

1.7 Baryogenesis

We only observe matter in large densities in our universe. The existence of large densities of antimatter in our observable universe is highly constrained by observations, such as the diffuse γ-ray background, see [97] and references therein. There is thus an observed baryonic matter-antimatter asymmetry.

The baryon asymmetry of our universe can be quantified by the ratio between the number density of baryons n_B to number density of photons n_γ. This is because the annihilation of matter and antimatter result into mostly photons and the fact that we do not observe antimatter in large quantities. This ratio can be obtained from CMB observations [98]:[11]

$$\frac{n_B - \bar{n}_B}{n_B + \bar{n}_B} \simeq \frac{n_B}{n_\gamma} = (6.12 \pm 0.04) \times 10^{-10} \ , \tag{1.56}$$

where $\bar{n}_B$ is the number density of anti-baryons.

[11] The ratio can also be observed from Big Bang nucleosynthesis giving a number compatible with the CMB observations [99]. Furthermore, often used in the literature is the baryon-to-entropy ratio $\frac{n_B}{s} = (0.87 \pm 0.006) \times 10^{-10}$, where s is the entropy density. At present times these are related by $\frac{n_B}{n_\gamma} \approx 7.04 \frac{n_B}{s}$, see e.g. [100, Ch. 4].

Now if in the very early universe there was a period of cosmic inflation any initial baryon asymmetry would be diluted away (see section 6.1 for brief introduction of inflation). Thus, there must be some dynamical *baryogenesis* process that happened after inflation where the observed baryon asymmetry was generated. Any such baryogenesis scenario must satisfy the following necessary (but not sufficient) conditions formulated by Sakharov [101]:

1. *Violation of baryon number* $\Delta B \neq 0$. — If baryon number is conserved one cannot evolve from initial state with $B = 0$ to a state with $B \neq 0$.

2. *Violation of charge (C) and charge-parity (CP) symmetries.* — If these symmetries hold any process generating baryon asymmetry would have an opposite conjugate process generating an equal but opposite asymmetry. These would cancel each other out.

3. *Deviation from thermal equilibrium.* — Assuming charge-parity-time reversal (CPT) symmetry, in thermal equilibrium the thermal average of baryon number vanishes and there can be no total baryon number change.

There are many different proposals realising baryogenesis in different ways. In many of them, e.g. electroweak baryogenesis and leptogenesis [102], the sphaleron processes play a central role. In leptogenesis scenarios there is some mechanism generating lepton number asymmetry which is then converted to baryon asymmetry by the sphaleron processes. Furthermore, the electroweak sphalerons are still crucial to take into account in theories generating the asymmetry before the electroweak transition to make sure the asymmetry is not washed out.

In electroweak baryogenesis scenarios the generation of baryon asymmetry happens at the electroweak phase transition. In the Standard Model there is C violation in the chiral electroweak sector and CP violation appears in the Yukawa interactions. Furthermore, as we have seen there is baryon number violation. However, as discussed previously, in the Standard Model the electroweak transition is a smooth crossover that happens without departure from thermal equilibrium. In addition, the CP violation present in the Standard Model is not enough [103–105]. So, electroweak baryogenesis requires physics beyond the Standard Model. Many extensions of the Standard Model lead to the electroweak transition to be a first order phase transition. Thus, leading to non-equilibrium dynamics.

As an example, at a slight deviation from thermodynamic equilibrium the baryon and lepton number change from an initial value B_0 can be related to the sphaleron

rate Γ by [106]:

$$\dot{B}(t) \simeq -\frac{13N_g^3}{4}\frac{\Gamma}{T^3}\left(B(t) - B_0\right) \ , \quad \dot{L}_i(t) = \frac{\dot{B}(t)}{N_g} \ , \tag{1.57}$$

where L_i is the lepton number of generation i.

A possible picture of the electroweak baryogenesis is as follows. Assuming a first order transition, bubbles of the broken phase start nucleating and expanding filling up all space. The expanding bubble walls bias antimatter to the outside symmetric phase, due to CP violation, producing an asymmetry of antimatter and excess matter inside the bubbles. The asymmetry outside is equilibrated and washed away due to the sphaleron processes being active in the outside symmetric phase. In contrast, inside the bubbles the sphaleron rate starts to get suppressed. Here the suppression of the sphaleron rate has to be strong enough not to also wash a way the asymmetry inside the bubble. This translates to the requirement of the phase transition being strong enough.

The sphaleron rate freezes out essentially when it becomes comparable to the Hubble rate, i.e. only a few sphaleron transitions take place in a Hubble volume and time, see e.g. [106]. In the Standard Model case this freeze-out temperature can be seen in the figure 1.4 as the intersection of the sphaleron rate and the horizontal green solid line. In the Standard Model the freeze-out happens $\sim$ 30 GeV below the pseudocritical temperature. In [1] we found the freeze-out temperature to be 133.5 ± 0.97 GeV.

Chapter 2

The Standard Model at finite temperature

2.1 Thermal field theory and Dimensional Reduction

The state of matter, in the hot and dense early universe, can be described by quantum field theory at finite temperature. This is called *thermal field theory*[12], where thermal fluctuations of the fields rising from interactions with the thermal medium are taken into account. The system is described by its ensemble averages or correlation functions. The correlation function of an operator $\mathcal{O}$ in a heat bath of temperature T is given by

$$\langle \mathcal{O} \rangle = \frac{1}{Z} \mathrm{Tr}\, \mathcal{O} e^{-\beta H} \ , \tag{2.1}$$

where H is the Hamiltonian operator for the system, $\beta = 1/T$ and

$$Z = \mathrm{Tr}\, e^{-\beta H} \ , \tag{2.2}$$

is the canonical partition function.

The Boltzmann weight $e^{-\beta H}$ has taken the role of the density operator. It can also be seen to be analogous to a quantum mechanical time-evolution operator with imaginary time. A time evolution operator with time independent Hamiltonian $e^{-iH(t-t_0)}$ can be analytically continued to imaginary time (via a Wick rotation) $t \to i\tau$ which then becomes $e^{-(\tau-\tau_0)H} \equiv e^{-\beta H}$. Following this analogy gives specific boundary conditions in the imaginary time. These can be seen from the *Kubo–Martin–Schwinger relation* which can be found by looking at a two-point correlator

[12] See e.g. [107] for an proper introduction.

of an operator $\mathcal{O}$:

$$\begin{aligned}\langle\mathcal{O}(t,x)\mathcal{O}(t_0,y)\rangle &= \frac{1}{Z}\mathrm{Tr}\,\left[\mathcal{O}(t,x)\mathcal{O}(t_0,y)e^{-\beta H}\right]\\ &= \frac{1}{Z}\mathrm{Tr}\,\left[\mathcal{O}(t,x)e^{-\beta H}e^{i(-i\beta H)}\mathcal{O}(t_0,y)e^{-i(-i\beta H)}\right]\\ &= \frac{1}{Z}\mathrm{Tr}\,\left[\mathcal{O}(t,x)e^{-\beta H}\mathcal{O}(t_0-i\beta,y)\right]\\ &= \langle\mathcal{O}(t_0-i\beta,y)\mathcal{O}(t,x)\rangle\ . \end{aligned} \tag{2.3}$$

We see that for a bosonic field that satisfies canonical commutation relations, this implies that in thermal equilibrium the fields are periodic in the imaginary time with the period $1/T$. Fermionic fields can be seen to be anti-periodic in the imaginary time. At equilibrium, thermal field theory can be thus seen as an Euclidean field theory with the imaginary time direction compactified to a circle with circumference $1/T$. This is called the imaginary time formalism.

There is a rather simple recipe of obtaining the partition function from a Lagrangian $\mathcal{L}$ given in Minkowski space. As we did in the previous chapter, we first do a Wick rotation to imaginary time $\mathcal{L}_E = -\mathcal{L}(t \to -i\tau)$. Again, if gauge fields are present the time components of gauge fields are transformed as $A_0 \to iA_0$ to preserve the structure of covariant derivatives. Now, however, the time is taken to be periodic $\tau \in [0,\beta]$ and fields are taken to satisfy boundary conditions: periodic for bosonic fields and anti-periodic for fermionic fields. The canonical partition function (2.2) (generating functional) can now be written in a path integral form

$$Z = \int\limits_{\Psi(\beta,x)=(\pm)\Psi(0,x)} \mathcal{D}\Psi(\tau,x)\exp\left[-\int_0^\beta \mathrm{d}\tau\int \mathrm{d}^3x\mathcal{L}_E(\Psi)\right]\ , \tag{2.4}$$

in analogy to zero-temperature, see e.g. [107] for a derivation. So, (2.1) can be written in a path integral form

$$\langle\mathcal{O}\rangle = \frac{\int\mathcal{D}\Psi\mathcal{O}e^{-S[\Psi]}}{\int\mathcal{D}\Psi e^{-S[\Psi]}}\ . \tag{2.5}$$

The structure of the fields in momentum space is interesting. Due to the (anti)periodic boundary conditions the Fourier modes of the compactified imaginary time direction is discrete. The Fourier transform to momentum space of a field becomes

$$\Psi(x,\tau) = T\sum_{n\in\mathbb{Z}}\int\frac{\mathrm{d}^3p}{(2\pi)^3}\Psi(\omega_n,p)e^{i\omega_n\tau - ix_ip_i}\ , \tag{2.6}$$

where ω_n are called the *Matsubara frequencies*. For a bosonic field $\omega_n = 2\pi nT$ and for a fermionic field $\omega_n = (2n+1)\pi T$, required by the boundary conditions ($e^{i\omega_n\beta} = 1$

for bosonic and $e^{i\omega_n\beta} = -1$ for fermionic).

The field modes with Matsubara frequency with $n = 0$ (called the zero modes) carry no momentum in the imaginary time direction. Thus, their dynamics is effectively three dimensional. All the modes with non-zero Matsubara frequencies have momenta larger than the zero modes. The non-zero modes have a thermal mass of order $\gtrsim \pi T$, which includes all the fermionic modes due to the boundary conditions. The *superheavy* scale πT is parametrically larger than the *heavy* scale for the zero modes which is gT (here g is a placeholder for a generic small coupling constant).

One can thus construct an effective theory for the light modes by "integrating" out all the non-zero modes. This results into a purely bosonic theory where also all the temporal bosonic modes $2\pi nT$ are integrated out. The effective theory is thus 3-dimensional, it has gone through *dimensional reduction*. Intuitively, the effective theory describes length scales longer than the extent of the compact imaginary time direction $1/T$ and thus they do not resolve the time direction.

After integrating out the superheavy scale the theory has temporal gauge field modes A_0 that are adjoint scalars. These live at the heavy scale gT which can be further integrated out to obtain an effective theory at a *light* scale g^2T. So, we have a hierarchy of scales

$$\pi T \gg gT \gg g^2T/\pi \ . \tag{2.7}$$

In contrast to the temporal gauge fields, the spatial gauge fields A_i can be found to be perturbatively massless with no available perturbative parameter. Thus, the spatial gauge fields turn out to be nonperturbative in nature. This is known as the Linde problem [108, 109].

The effective 3-dimensional theory at the light scale g^2T reads

$$\mathcal{L}_{\text{3d}} = \frac{1}{2}\text{Tr}\, F_{ij}F_{ij} + \frac{1}{4}B_{ij}B_{ij} + (D_i\phi)^\dagger(D_i\phi) + m_3^2\phi^\dagger\phi + \lambda_3(\phi^\dagger\phi)^2 \ , \tag{2.8}$$

where

$$\begin{aligned} F_{ij} &= \partial_i A_j - \partial_j A_i - g_3[A_i, A_j] \ , \\ B_{ij} &= \partial_i B_j - \partial_j B_i \ , \\ D_i &= \partial_i + ig_3 A_i + ig_3' B_i/2 \ . \end{aligned} \tag{2.9}$$

In practice, the construction of the effective theory is accomplished by perturbatively matching correlators between the 3d and 4d theory. This process is now largely automated thanks to the `DRalgo` package [110]. The dimensionful 3d parameters (g_3, g_3', λ_3, m_3^2) are mapped to the 4d Standard Model parameters (α_S, G_F, m_H,

m_W, m_Z, m_t)[13] in which the effects of SU(3) strong interactions and fermions are captured perturbatively, see [111–115] for explicit construction of the effective theory and the mapping of parameters.

We can choose the SU(2) gauge coupling g_3^2 to give the scale. Then the effective theory has three dimensionless parameters

$$x(T) \equiv \frac{\lambda_3}{g_3^2}, \quad y(T) \equiv \frac{m_3^2}{g_3^2}, \quad z(T) \equiv \frac{g_3'^2}{g_3^2} \ . \tag{2.10}$$

The y parameter varies significantly with temperature and can be used as the effective temperature parameter for the system. While the x and z parameters vary only slightly. From perturbation theory it is expected that the electroweak transition happens around $y = 0$, which using the Standard Model parameters corresponds to $T = 162.9$ GeV. As stated earlier the pseudocritical temperature has been found to be $T_c \simeq 159.5$ GeV [52]. The Standard Model is quite deep in the crossover region. In terms of the dimensionless parameters the end point of the first order phase transition is at $x \simeq 0.1$ [116] while the Standard Model corresponds to a value $x \simeq 0.3$.

This effective theory is quite powerful at describing the thermodynamical properties of a theory and can be efficiently studied on the lattice. Additional power comes from the fact that many theories beyond the Standard Model can be mapped to the same effective theory with different mappings to the parameters x, y and z. For the Standard Model case the accuracy of the 3d effective theory is estimated to be $\sim 1\%$ [111, 112, 117–119], see also [120]. However, the theory does not capture dynamical processes such as the sphaleron rate.

2.2 Effective dynamical description of soft modes

It is possible to study the sphaleron rate using the effective theory (2.8) with classical equations of motion [87, 88, 95, 121, 122], which should be a good approximation for the full quantum evolution due to the high occupation numbers. However, the classical field dynamics suffer from ultraviolet divergences and the continuum limit on the lattice does not exist [88]. The classical evolution can be improved by taking into account hard thermal loop effects [93, 123, 124], however, the continuum limit on the lattice still does not exist.

However, there exists another effective description for the evolution that does have a well-defined continuum limit on the lattice. As first shown in [89], in SU(2)

[13] The top quark Yukawa coupling is parametrically much larger than the rest and gives the dominant contribution. Thus, the rest of the quark masses are often approximated to have negligible masses.

gauge theory the dynamics of the soft modes, that are relevant for sphaleron transitions, can be shown to be fully overdamped leading to time evolution described by Langevin equation to leading logarithmic accuracy $1/\log(1/g)$. It can be also shown that the Higgs field evolves parametrically much faster than the SU(2) gauge field [125, 126]. The case for the Abelian U(1) field is less clear. However, in the broken phase the soft modes of the U(1) field evolve faster than the SU(2) field. Since the U(1) gauge coupling is much smaller than the SU(2) coupling the U(1) modes with wavelength $\lambda \sim 1/(g^2 T)$ behave as nondamped and weakly coupled modes with timescale $\tau \simeq \lambda$ in contrast to the SU(2) modes which evolve with timescale $\sim \lambda^2$. It would be interesting to study further how to describe the full quantum evolution of the U(1) field correctly, however, for our purposes of investigating the sphaleron rate this description should be sufficient.

The Langevin evolution for the soft modes is given by [89, 90, 127–129] ($A_0 = 0$):

$$\sigma_{\rm el}(D_0 A_i)^a = -\frac{\partial H}{\partial A_i^a} + \xi_i^a \ , \tag{2.11}$$

$$\sigma_{\rm el}(D_0 B_i) = -\eta_B \frac{\partial H}{\partial B_i} + \xi_B^i \ , \tag{2.12}$$

$$\sigma_{\rm el}(D_0 \phi) = -\eta_\phi \frac{\partial H}{\partial \phi^\dagger} + \xi_\phi \ , \tag{2.13}$$

where $H = S_{\rm 3d}/T$, and $S_{\rm 3d}$ is given by (2.8). The stochastic force terms ξ_i^a, ξ_B^i and ξ_ϕ are Gaussian that satisfy

$$\langle \xi_i^a(t,x)\xi_j^b(t',y)\rangle = 2\sigma_{\rm el} T \delta_{ij}\delta^{ab}\delta^3(x-y)\delta(t-t') \ , \tag{2.14}$$

$$\langle \xi_B^i(t,x)\xi_B^j(t',y)\rangle = 2\eta_B\sigma_{\rm el} T \delta^{ij}\delta^3(x-y)\delta(t-t') \ , \tag{2.15}$$

$$\langle \xi_\phi(t,x)\xi_\phi^\dagger(t',y)\rangle = 2\eta_\phi\sigma_{\rm el} T \delta^3(x-y)\delta(t-t') \ . \tag{2.16}$$

Here $\sigma_{\rm el}$ is the SU(2) non-Abelian *color conductivity* given by [129]:

$$\begin{aligned} \sigma_{\rm el} &= \frac{m_D^2}{3\gamma}, \\ \gamma &= \frac{2g^2 T}{4\pi}\left[\ln\frac{m_D}{\gamma} + 3.041... + \mathcal{O}\left(\tfrac{1}{\ln(1/g)}\right)\right] \ , \end{aligned} \tag{2.17}$$

where m_D is the Debye mass which in the Standard Model is $m_D^2 = (11/6)g^2T^2$ (the numeric value is $\sigma_{\rm el} \simeq 0.91895...$). Finally, the ratios of evolution rates $\eta_\phi \sim 1/g^2 \gg 1$ and $\eta_B \sim 1/g^2 \gg 1$, reflecting the fact that the SU(2) evolution is much slower. The Langevin-type evolution can be shown to have a well-defined continuum limit on the lattice.

Chapter 3

Sphaleron rate on the lattice

The sphaleron is inherently nonperturbative and the nonperturbative nature of high-temperature infrared gauge theories requires the use of nonperturbative methods. Let us first briefly describe the lattice methods we used in our work.

3.1 Lattice field theory

As we saw in the previous chapter the fermionic fields can be taken into account perturbatively, so we do not need to worry about the complications arising from introducing fermions on a lattice.

The purely bosonic effective theory is relatively straight forward to formulate on a lattice. The fields will live on an Euclidean lattice with a homogeneous lattice spacing a: $M = \{x \mid x = \sum_{i=1}^{d} a n_i \hat{i},\ n_i \in \mathbb{Z}\}$, where $\hat{i}$ is the unit vector into direction i and d is the dimension of the lattice. The lattice spacing introduces an ultraviolet cut-off. It is clear that the theory cannot probe distances smaller than a, meaning it cannot probe energy scales larger that $1/a$. Further restricting our theory to live in a finite volume ($0 < n_i < L_i$ for some integers L_i) it becomes possible to study the theory using computational methods. The lattice discretisation allows us to give precise meaning for the path integrals of the form (2.4) that we wish to evaluate. The path integral measure becomes a bunch of ordinary Riemann integrals, e.g. for a scalar field $\int \mathcal{D}\phi = \int \Pi_{x \in M} \mathrm{d}\phi(x)$.

For a scalar field discretising a continuum theory goes as one might expect. The partial derivatives can be replaced by finite differences $\partial_i \phi(x) = [\phi(x + i) - \phi(x)]/a$ and integrals become sums $\int \mathrm{d}^d x \to a^d \sum_{x \in M}$, where we have adopted the shorthand notation where $\phi(x + a\hat{i}) \equiv \phi(x + i)$.

Trying to implement a gauge field in similar manner leads to difficulties retaining gauge invariance. The view of gauge fields as connections on a principal bundle gives the correct idea what gauge fields are doing, as we discussed in section 1.1.

They implement the parallel transport between points. So instead of trying to put the gauge field $A_\mu(x)$ on the lattice one instead takes the smallest possible parallel transporters, the Wilson lines (1.5),

$$U_i^{(x)} = U(x, x+i) = e^{iagA_i(x)} \ , \tag{3.1}$$

to be the degrees of freedom for the gauge field. The parallel transporters $U_i^{(x)}$ are called the gauge *link* variables. They live between the lattice points x and $x+i$ and are elements of the gauge group, for the current discussion $U_i^{(x)} \in \mathrm{SU}(2)$. It is now a bit more tricky to see what is the correct discretised action that leads to the desired gauge field action in the continuum limit. As we eluded in section 1.1, the Wilson loop has something to do with the field strength. Indeed, we can construct the smallest possible Wilson loop on the lattice, the *plaquette*:

$$P_{ij}^{(x)} = U_i^{(x)} U_j^{(x+i)} U_i^{\dagger(x+j)} U_j^{\dagger(x)} \quad \sim \tag{3.2}$$

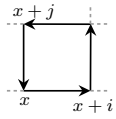

where in the pictorial representation the arrows depict the links connecting the lattice points. This can be shown[14] to be $P_{ij}^{(x)} = \exp[iga^2 F_{ij}(x) + \mathcal{O}(a^4)]$ as $a \to 0$. Furthermore, with the plaquette we can construct the Wilson gauge action [130]

$$S = \beta_G \sum_{x, i<j} \left[1 - \frac{1}{2} \mathrm{Tr}\, P_{ij}^{(x)} \right] \overset{a \to 0}{=} \int \mathrm{d}^d x \frac{1}{2} \mathrm{Tr}\, F_{ij} F_{ij} + \mathcal{O}(a^2) \ , \tag{3.3}$$

where $\beta_G = 4/(g^2 a^{4-d})$ and it can be seen to approach the correct action in continuum. This action is not unique and one may find actions with smaller than the $\mathcal{O}(a^2)$ discretisation errors, e.g. by following the Symanzik improvement program [131].

Now, we can define the path integral over the links. For that we need to define integration over the group valued variables, i.e. we need an integration measure over the group manifold. This is given by the gauge invariant measure of the links $\mathrm{d}U_i^{(x)}$ called the Haar measure, see e.g. [132, Ch. 15] for explicit construction. This is the unique measure that is invariant under left and right action of the group meaning that for $\Omega \in \mathrm{SU}(2)$: $\int \mathrm{d}U f(U) = \int \mathrm{d}U f(U\Omega) = \int \mathrm{d}U f(\Omega U)$, where $f(U)$ is some functional of the links. This makes the Elitzur's theorem quite transparent, since this implies that $\int \mathrm{d}U U = 0$ and in general the integral over $\mathrm{d}U$ gives a non-zero value only when $f(U)$ is invariant under the gauge group. Meaning that any expectation value given by a path integral of the form (2.5) of an operator that is not gauge invariant necessarily vanishes, $\langle \mathcal{O} \rangle = 0$.

[14] Using e.g. the Baker-Campbell-Hausdorff formula and (3.1).

The integrations are done over the compact group manifolds and are thus well-defined without taking care of gauge orbits by gauge fixing. (For the abelian U(1) group also a non-compact description is possible which is what we used in our work.)

We can now write down the lattice discretisation of the effective 3d action. First noting that by using the gauge links the discretised covariant derivative can be written as $\Delta_i\phi(x) = [U_i^{(x)}\phi(x+i) - \phi(x)]/a$. With this the scalar kinetic term reads

$$a^d \sum_{x,i} \left[\Delta_i\phi(x)\right]^\dagger \left[\Delta_i\phi(x)\right] \stackrel{a\to 0}{=} \int \mathrm{d}^d x (D_i\phi)^\dagger (D_i\phi) + \mathcal{O}(a^2) \ . \tag{3.4}$$

For the lattice formulation it is convenient to write the Higgs field in a matrix form

$$\Phi(x) = \frac{1}{g_3^2} \begin{bmatrix} \phi_2^* & \phi_1 \\ -\phi_1^* & \phi_2 \end{bmatrix} \ , \tag{3.5}$$

which transforms under $\mathrm{SU}(2) \times \mathrm{U}(1)$ as $\Phi(x) \to \Omega(x)\Phi(x)\exp[-i\theta(x)\sigma_3]$, where σ_3 is the third Pauli matrix and $\Omega \in \mathrm{SU}(2)$. Finally, the effective 3d continuum action (2.8) on the lattice reads:

$$\begin{aligned} S = {} & \beta_G \sum_{x,i<j} \left[1 - \frac{1}{2}\mathrm{Tr}\, P_{ij}^{(x)}\right] + \beta_Y \sum_{x,i<j} \frac{1}{2}\alpha_{ij}^2 \\ & - \beta_H \sum_{x,i} \frac{1}{2}\mathrm{Tr}\, \Phi^\dagger(x) U_i^{(x)} \Phi(x+i) \exp\left[-i\alpha_i(x)\sigma_3\right] \\ & + \beta_2 \sum_x \frac{1}{2}\mathrm{Tr}\, \Phi^\dagger(x)\Phi(x) + \beta_4 \sum_x \left[\frac{1}{2}\mathrm{Tr}\, \Phi^\dagger(x)\Phi(x)\right]^2 , \end{aligned} \tag{3.6}$$

where

$$\alpha_{ij}(x) = \alpha_i(x) + \alpha_j(x+i) - \alpha_i(x+j) - \alpha_j(x). \tag{3.7}$$

Here $\alpha_i(x)$ are non-compact U(1) link variables, and α_{ij} is its corresponding plaquette.

The lattice parameters have to be related to the 3d continuum parameters which is accomplished by matching physical quantities in the continuum renormalization and lattice perturbation theory schemes. Due to the super-renormalizability of the 3d theory these relations are exact at 2 loops. The relations have been computed in [133]. In addition, we use the partial $\mathcal{O}(a)$ improvements of these relations computed in [134, 135]. The relations used can be found in the notation of (3.6) in [1]. As an example the lattice observable $\frac{1}{2}\langle\Phi^\dagger\Phi\rangle$ is related to the $\overline{\mathrm{MS}}$ renormalized 3d

continuum Higgs condensate $\langle\phi^\dagger\phi\rangle$ as

$$\langle\phi^\dagger\phi\rangle/g_3^2 = Z_g Z_m \left[\tfrac{1}{2}\langle\Phi^\dagger\Phi\rangle - \frac{\Sigma\beta_G}{8\pi} - \frac{3+\bar{z}}{16\pi^2}\log(3\beta_G/2) + 0.66779...\right] , \tag{3.8}$$

see [134, 135] and [1, Appendix A] for the definitions of Z_g, Z_m, Σ and $\bar{z}$. Furthermore, the physical Standard Model Higgs expectation value v in unitary gauge is related to the 3d condensate as $v^2/T^2 = 2\langle\phi^\dagger\phi\rangle/T$.

To evaluate an expectation value of the form (2.5), there will be an unfeasible amount of integrals to evaluate for any reasonably sized lattice (number of lattice points times the number of degrees of freedom). This is where the Monte Carlo integration methods become very useful for computing these correlation functions on a computer. We will not go into the details of reviewing these methods here, see e.g. [132, Ch. 16].

Lastly, the Langevin-type evolution described in section 2.2 is straight forward to implement on the lattice. However, a computationally more efficient way is to use a heat bath update [136–138], that can be shown to be equivalent to the Langevin evolution (2.11) [91]. The Langevin time can be related to performing n full random order heat bath update sweeps as $\Delta t = \frac{1}{4}\sigma_{\rm el}a^2 n$ [91, 126]. To satisfy the ratio between evolution rates of the Langevin equations (as described in section 2.2) the Higgs and U(1) fields are updated more frequently as the SU(2) gauge fields, in a similar ratio as found to be sufficient in [116].

3.2 Hypermagnetic field on the lattice

Let us briefly state how the external hypermagnetic field is implemented on the lattice. Having a flux of hypermagnetic field Φ_B that is perpendicular to the x_3-direction, $g_3'\Phi_B = \int \mathrm{d}x_2\mathrm{d}x_1 B_{12}$, can be implemented on the lattice by changing the periodic boundary conditions of the U(1) links α_i. To maintain translational invariance and periodic boundary conditions the total flux is required to have quantized values $g_3'\Phi_B/(4\pi) = n_b$, where $n_b \in \mathbb{N}$ [23]. We implement this by changing the boundary conditions of one link in the x_1x_2-plane:

$$\alpha_1(n_1, 0, n_3) - \alpha_1(n_1, L_2, n_3) = 2\pi n_b \delta_{n_1,1} , \tag{3.9}$$

for each $n_3 \in [0, L_3)$ in a lattice with volume $L_1L_2L_3$. The dimensionless parameter that describes the average hypermagnetic flux density is defined as

$$b \equiv \frac{g_3' B_Y^{\rm 3d}}{g_3^4} = \frac{4\pi n_b}{L_1 L_2}\left(\frac{1}{g_3^2 a}\right) , \tag{3.10}$$

where $B_Y^{3\mathrm{d}} \equiv \Phi_B/(L_1 L_2)$ is the 3-dimensional flux density which relates to the 4-dimensional one as $B_Y^{3\mathrm{d}} = B_Y^{4\mathrm{d}}/\sqrt{T} + \mathcal{O}(g'^2)$. The dimensionless parameter then relates to the 4-dimensional flux as

$$B_Y^{4\mathrm{d}} = \frac{g'}{g^4} b T^2 + \mathcal{O}(g'^3) \approx 1.93 b T^2 + \mathcal{O}(g'^3) \ . \tag{3.11}$$

The external hypermagnetic field affects the higher dimensional operators in the effective 3-dimensional theory. To maintain the validity of the 3-dimensional effective theory the external field cannot be too large and we require $b \ll 2\pi^2$ [23].

3.3 Topology on the lattice

To study the sphaleron rate on the lattice we want to measure the evolution of the topological Chern-Simons number while evolving the system with the described effective theory. Naively, we can discretise (1.18) by

$$\begin{aligned} \delta N_{CS}^W(t) &= \frac{1}{8\pi^2} \delta t \sum_x E_i^a(x) B_i^a(x) \\ &\overset{a\to 0}{=} \frac{g^2}{16\pi^2} \int_0^t \mathrm{d}t \int \mathrm{d}^3x \ \mathrm{Tr}\, F_{\mu\nu} {}^\star F_{\mu\nu} + \mathcal{O}(a^2) \ , \end{aligned} \tag{3.12}$$

where $E_i^a(x) = \frac{1}{2}\mathrm{Tr}\,[i\sigma^a U_i^{\dagger(x+\delta t)} U_i^{\dagger(x)}]$ is the lattice SU(2) electric field with $U_i^{\dagger(x+\delta t)}$ being the link evolved forward in time for δt. The $B_i^a(x)$ is the SU(2) magnetic field at the links given by $B_i^a(x) = \frac{1}{2}\mathrm{Tr}\, i\sigma^a \epsilon_{ijk}[Q_{jk}(x) + U_i^{(x)} Q_{jk}^{(x+i)} U_i^{\dagger(x)}]$, where $Q_{ij}^{(x)}$ is the symmetrised plaquette, often called the *clover*:

$$Q_{ij}^{(x)} \equiv \frac{1}{4}\left[P_{ij}^{(x)} + P_{j,-i}^{(x)} + P_{-i,-j}^{(x)} + P_{-j,i}^{(x)}\right] \quad \sim \quad$$

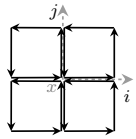

. (3.13)

However, unlike in the continuum, this discretisation is not a total derivative on the lattice and turns out to contain ultraviolet noise [121, 139, 140]. This leads to Chern-Simons number diffusion that is not related to the sphaleron transitions. We do use an improved definition for the clover that has smaller discretisation errors of

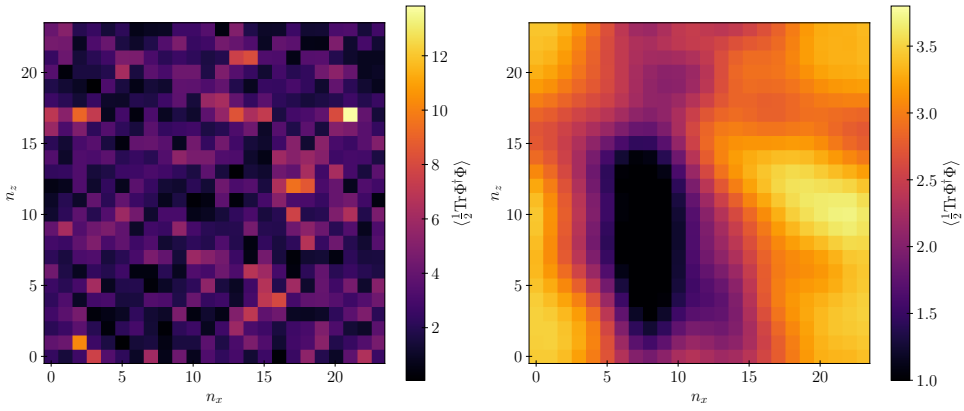

Figure 3.1. One spatial $xz-$slice of the Higgs field condensate $\frac{1}{2}\langle\Phi^\dagger\Phi\rangle$ in a lattice of volume $V = 24^3a^3$, lattice spacing $\beta_g = 12$, temperature $T = 145.0$ GeV, and an external hypermagnetic field $b = 0.589$. This is at a sphaleron configuration with $N_{CS} = \frac{1}{2}$ (same configuration as in figure 3.2 right). **(Left)** Raw lattice Higgs field configuration. **(Right)** Higgs field cooled using gradient flow with flow time $\tau = 3$.

order $\mathcal{O}(a^4)$, which is given pictorially by [141–143]:

$$Q_{ij}^{\mathrm{imp}}(x) = \frac{5}{3}\times$$ 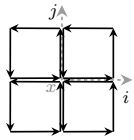 $$-\frac{1}{6}\times$$ 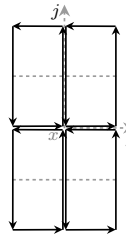 $$-\frac{1}{6}\times$$ 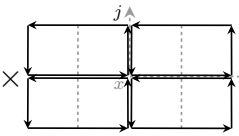 . (3.14)

The problem of ultraviolet noise persists. This problem can be fixed by first cooling the fields with gradient flow, getting rid of some of the ultraviolet modes, and then using the cooled fields to compute (3.13). This works since the lattice discretisation does recover the continuum definition for smooth fields. Furthermore, the sphaleron configuration is large in the lattice units (for reasonably fine lattices), of the order $\sim 1/(g^2T)$.[15] Similarly, the hot sphalerons that change the Chern-Simons number are dominated by the same length scale [92, 144].

This leads us to the calibrated cooling method [87, 122], see also [93, 145] for more detailed explanation. In essence, when computing the change δN_{CS} we first

[15]From the semiclassical configuration described in section 1.4 one can see that the size of the sphaleron is of order $\sim 1/(gv)$, which translates to $\sim 1/(g^2T)$ in the 3d-theory at finite temperature.

gradient flow the fields by a set amount of fictitious cooling time τ:

$$\frac{\partial U_i^{(x)}}{\partial \tau} = -i\frac{1}{2}\sigma^a U_i^{(x)} \frac{\partial S_{3\mathrm{d}}}{\partial \theta^a(x)} \ , \tag{3.15}$$

$$\frac{\partial \alpha_i(x)}{\partial \tau} = -\frac{\partial S_{3\mathrm{d}}}{\partial \alpha_i(x)} \ , \tag{3.16}$$

$$\frac{\partial \Phi(x)}{\partial \tau} = -\frac{\partial S_{3\mathrm{d}}}{\partial \phi(x)} \ , \tag{3.17}$$

where we have parametrized $U_i^{(x)} = \exp[i\frac{1}{2}\theta_i^a(x)\sigma^a]$. This removes ultraviolet fluctuations smoothing the fields by a radius $r = \sqrt{6\tau}a$ [146]. Compared to the case described in the literature, we gradient flow all the fields, since we also need to measure the U(1) Chern-Simons number N_{CS}^Y (1.19) in the "broken phase", which we can define on the lattice in complete analogy to N_{CS}^W as defined above.

In figure 3.1 we have shown an example configuration at $N_{CS} = \frac{1}{2}$ of the Higgs field condensate without gradient flow where no structure is seen (left) and smoothed configuration where the sphaleron configuration can be seen by eye (right). See also figure 3.2.

If we naively integrate N_{CS} in time all the errors will accumulate. This can be fixed by "calibrating" the N_{CS} value by periodically cooling the configuration all the way to the vacuum and correcting deviations from integer values between two vacua. This removes the accumulation of errors. This process turns out to be the most expensive part of performing the simulations on the lattice. This can be sped up by blocking the lattice to smaller lattice extent, making the lattice coarser, while performing the cooling down to vacuum. Here the improved definition (3.14) allows for more aggressive blocking while retaining acceptable accuracy.

With these methods it is possible to measure the sphaleron rate at a temperature where the exponential suppression is not yet too large. We can generate a long time trajectory of the N_{CS} and compute the diffusion constant from it, e.g. with the cosine transform method described in [140].

The exponential suppression kicks in rapidly in the "broken phase". In normal simulations the $N_{CS} = N_{CS}^W - N_{CS}^Y$ freezes down and seeing even one sphaleron transition in a reasonable simulation time becomes unpractical, see e.g. figure 3.4. This is where we need to use a multicanonical method.

3.4 Multicanonical method

Since the multicanonical method used is standard, we do not give a detailed explanation here, see e.g. [147, 148] for introduction.

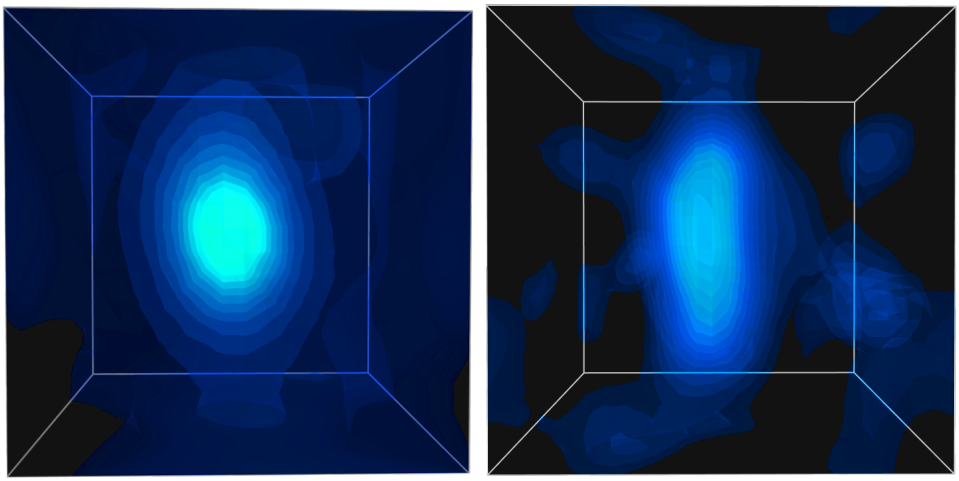

Figure 3.2. Two sphaleron configurations in a magnetic field from dynamical simulations, at $N_{CS} = \frac{1}{2}$. Plotted is the Higgs condensates isosurfaces from cooled configurations. The more bright the color the closer it is to the "broken phase" value of the condensate. The configuration is seen to get more elongated with increased magnetic field as expected. **(Left)** $T = 145$ GeV, $b = 0.392$. **(Right)** $T = 150$ GeV, $b = 0.589$.

The method used is identical to what was developed for measuring the sphaleron rate without U(1) [87], see also [116, 126, 145] for more detailed description. The only difference is in what we choose as the order parameter. In the broken phase the SU(2) and U(1) fields mix due to the Higgs and the correct order parameter that gives an integer in the vacuum and gets suppressed in the broken phase turns out to be $N_{CS} = N_{CS}^W - N_{CS}^Y$, see figure 3.4.

The computation consists of a statistical and dynamical part. First a multicanonical sampling method is used to measure the probabilistic suppression of getting to the sphaleron configuration at $N_{CS} = \frac{1}{2}$. This is given by the N_{CS} distribution between two integer vacua $P(N_{CS})$. In the dynamical part the rate of moving over the potential barrier from one vacuum to another is measured. This is given by measuring $|\delta N_{CS}/\delta t|$ from dynamical simulations at the point where the configuration crosses the sphaleron barrier at $N_{CS} = \frac{1}{2}$. The noisy nature of the dissipative Langevin update can result into multiple crossings of the barrier without resulting into a real vacuum transition. This is compensated by a "dynamical prefactor" given by $\mathrm{d} = \sum_{\mathrm{traj}} \delta_{\mathrm{tunnel}}/(N_{\mathrm{cross}} N_{\mathrm{traj}})$ where the sum is over the sample of simulated trajectories. Here $\delta_{\mathrm{tunnel}} = 1$ if the trajectory goes from one vacuum to another $\Delta N_{CS} = \pm 1$, and its $\delta_{\mathrm{tunnel}} = 0$ if it does not. Finally, N_{cross} is the number of times the trajectory crosses the barrier $N_{CS} = \frac{1}{2}$ and N_{traj} is the number of trajectories in

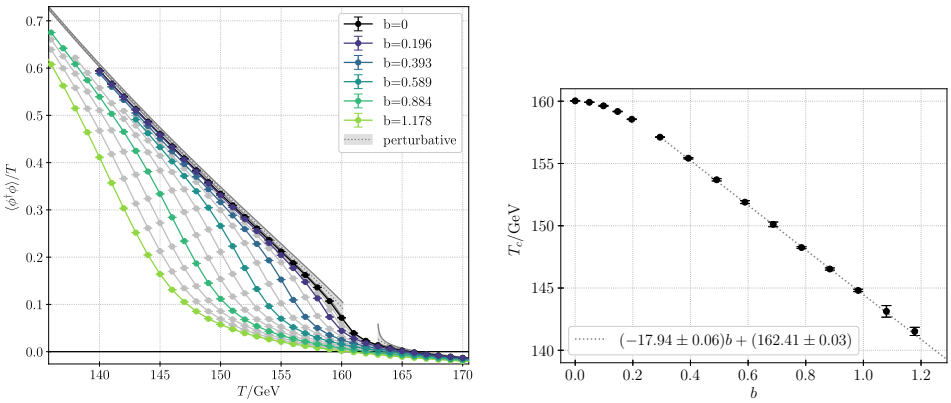

Figure 3.3. **(Left)** Regularized Higgs condensate with different magnitudes of the external magnetic field. The condensate becomes negative in the symmetric phase due to additive renormalization factor, see (3.8). **(Right)** Pseudocritical temperature (defined as the peak of the susceptibility of the Higgs condensate) as a function of the magnitude of the magnetic field. From [1].

the sample. The sphaleron rate is then given by

$$\Gamma = \underbrace{\frac{P(|N_{\mathrm{CS}} - \frac{1}{2}| < \frac{\epsilon}{2})}{\epsilon V}}_{\text{statistical}} \underbrace{\left\langle \left| \frac{\delta N_{\mathrm{CS}}}{\delta t} \right| \right\rangle \mathrm{d}}_{\text{dynamical}} , \tag{3.18}$$

where $\epsilon \ll 1$ and $\langle \delta N_{\mathrm{CS}}/\delta t \rangle$ is the expectation value computed from the same sample as the dynamical prefactor d.

3.5 Electroweak Sphaleron in a magnetic field

In [1] we computed the rate of baryon number changing processes, the sphaleron rate, with the earlier described methods in an external (hyper)magnetic field with different magnitudes over the electroweak crossover. To our knowledge this was the first nonperturbative study determining the sphaleron rate with the U(1) field included.

The electroweak crossover is affected by the external magnetic field. The crossover temperature is shifted to smaller temperatures with increased magnitude for the magnetic field. The pseudocritical temperature briefly decreases quadratically and then reaches a linear regime lasting up to field magnitudes $B_Y^{4\mathrm{d}} \simeq 2.3T^2$ as seen in figure 3.3 (right). The crossover transition region also gets broader, see figure 3.3 (left). With a large magnetic field $B_Y^{4\mathrm{d}} \simeq 2.0T^2$ there is a noticeable shift of the pseudocritical temperature from 160 GeV down to 145 GeV. For large magnetic field values

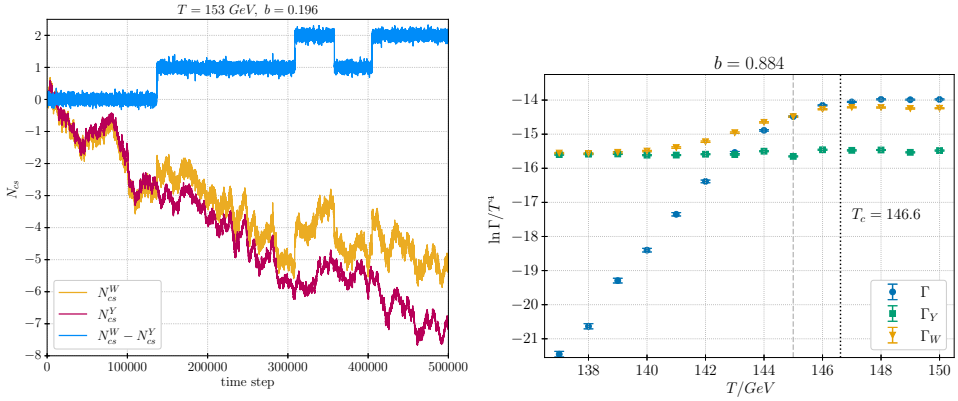

Figure 3.4. **(Left)** A realtime N_{CS} trajectory in the Higgs phase with temperature $T = 153$ GeV and external magnetic field $b = 0.196$ using the Langevin type evolution. The SU(2) N_{CS}^W (yellow), U(1) N_{CS}^Y (red) shown separately and the full N_{CS} that sources the baryon number violation (blue). **(Right)** How the SU(2) (yellow) and U(1) (green) diffusion rates behave separately over the electroweak transition. The physical difference of the two (blue) is seen to get suppressed. From [1].

this has the most noticeable effect on the sphaleron rate since it shifts the onset of the exponential suppression.

Separately the U(1) rate can be seen to stay constant over the crossover while the SU(2) rate is constant in the symmetric phase decreasing around the crossover until reaching another constant in the broken phase, see figure 3.4 (right). The Chern–Simons number diffusion (sphaleron) rate that sources the baryon number violation $\Delta N_{\mathrm{CS}}^W - \Delta N_{\mathrm{CS}}^Y$ is what gets suppressed, see figure 3.4.

In the symmetric phase the SU(2) rate is approximately unaffected by the presence of an external magnetic field, see figure 3.5 (right). The full rate in the symmetric phase increases with increased $B_Y^{4\mathrm{d}}$ with the expected behavior $\sim (B_Y^{4\mathrm{d}})^2$ from the increased U(1) rate. In the broken phase for small external field values the slope of the suppression of the rate is compatible with the $b = 0$ slope, as seen in figure 3.5 (left). For larger field values we do not have enough data to say this with confidence, however, the slope is still comparable.

To isolate the effect of the sphaleron dipole moment interacting with the external field we can look at the data with a fixed Higgs condensate, see figure 3.6. We can observe that for small field values the rate increases quadratically b^2 until around $b \simeq 0.2$ it reaches a linear regime. The linear regime ends when the magnetic field gets strong enough to "restore" the electroweak symmetry, where the symmetric rate is reached. For small field values there is no significant change to the Higgs condensate and thus the dominant effect is from the sphaleron dipole moment.

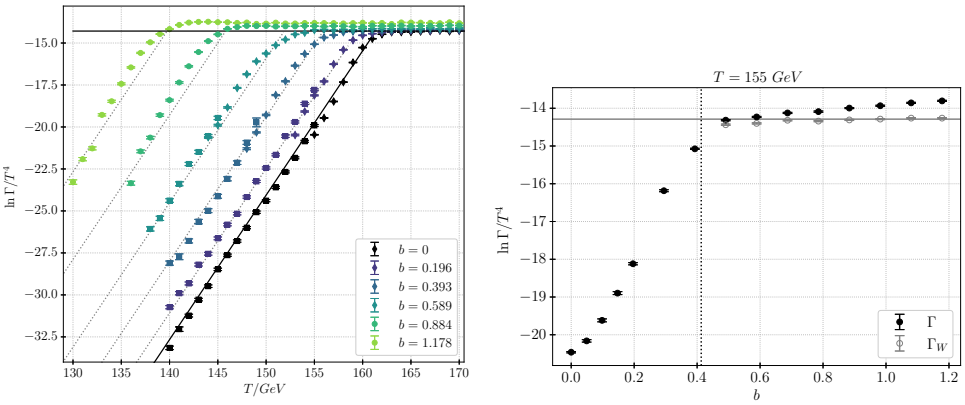

Figure 3.5. **(Left)** The full sphaleron rate as a function of temperature for different magnitudes of the external magnetic field. The black solid line is the broken phase fit for the zero magnetic field case. The gray dashed lines are the $b = 0$ fit shifted according to the shift of the pseudo critical temperature. The black horizontal line is $b = 0$ symmetric rate fit. **(Right)** How the sphaleron rate changes with magnetic field at a fixed temperature $T =$ 155 GeV. Vertical dotted line is the value of b at which the fixed temperature corresponds to the pseudocritical temperature. Horizontal line is again the symmetric rate $b = 0$ fit. The gray data points are the pure SU(2) rate, shown in the symmetric phase. From [1].

In the right plot of figure 3.6 we compare our lattice results to a semiclassical result using the spherical ansatz and simple dipole approximation described in the section 1.4. Computing the change to the sphaleron rate in the semi-classical approximation we assume that the change of the sphaleron energy is due to a simple dipole interaction of the form $\Delta E = -\vec{\mu}_{\text{sph}} \cdot \vec{B}_c^{4d}$ and further assume that the change to the rate is only due to this energy difference. If we then average over spatial orientations of the sphalerons dipole we obtain the estimate $\Delta \ln \Gamma/T^4 \simeq \ln [\sinh(\Delta E/T)/(\Delta E/T)]$. We can see, in figure 3.6 (right), that the spherical approximation quickly becomes invalid, as expected from the sphaleron configuration getting more and more elongated, see figure 3.2. The behavior of the semianalytical estimate and the lattice are similar and of the same order of magnitude for small field values. We only have a few data points from the lattice in the small field regime due to the unfortunate restriction of quantized magnitudes for the magnetic field and computational costs getting too high for larger lattices where smaller field values would be possible.

The results reviewed here are obtained from one lattice spacing $g_3^2 = 1/2$ and two different volumes $V = 16a^3$ and $V = 32a^3$. The second volume was used to get more fidelity into the possible values of the external magnetic fields due to its magnitude being quantized as described shortly in section 3.2. We did investigate the finite size and volume effects in [1] which were observed to be small or negligible. Thus, we did

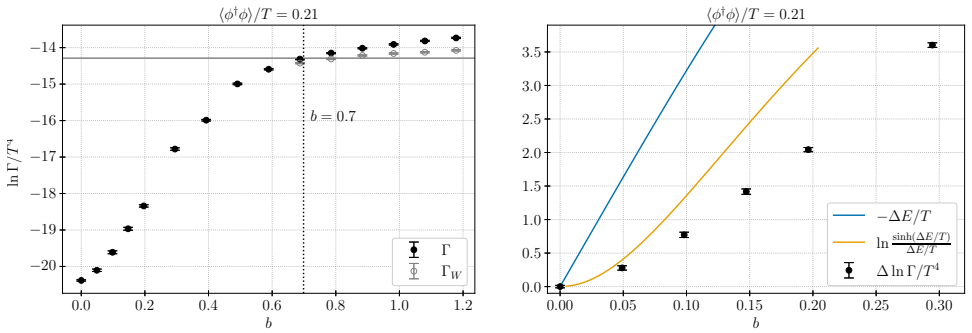

Figure 3.6. **(Left)** The full rate with constant Higgs condensate. The vertical dotted line marks the b value where the $\langle\phi^\dagger\phi\rangle/T = 0.21$ corresponds to the value at the pseudocritical temperature. The horizontal line is the symmetric $b = 0$ fit. **(Right)** Comparing the difference $\Delta\ln\Gamma/T^4 = \ln\Gamma(b)/T^4 - \ln\Gamma(0)/T^4$ of rates with and without magnetic field. Black data points are from the dynamical lattice simulations. Orange solid line is the semianalytical estimate computed using the spherical ansatz of the sphaleron, see section 1.4. From [1].

not pursue the full continuum limit since it needs considerably more computational effort due to the multicanonical method becoming inefficient. The inefficiency of the multicanonical method for small lattice spacings and large lattices was noted in the previous studies which were similarly not able to compute the continuum limit. In our case this seems to be worsened due to extra noise in the Chern–Simons number measurement coming from the U(1) field.

In summary, the sphaleron rate in an external magnetic field changes due to two main effects: the interactions between the sphalerons magnetic dipole moment and the external field which lowers the sphalerons energy, and from the external field changing the form of the electroweak transition. For small magnetic fields the sphaleron dipole moment gives the dominant effect which can lower the freeze-out temperature down by around $\lesssim 1$ GeV. For larger magnetic fields the changes to the electroweak crossover gives the dominant effect which can lower the freeze-out temperature down considerably by orders of 10 GeV. Thus, for large magnetic fields $B_Y^{\mathrm{4d}} \sim T^2$ the effects to the sphaleron rates suppression can be quite large.

Part II

Gravitation

"*In right angled triangles the square on the side subtending the right angle is equal to the squares on the sides containing the right angle.*"
— Euclid, *The Elements, Proposition 47*
Translated by Sir Thomas L. Heath

Chapter 4

Palatini formulation of General Relativity

In the usual metric formulation of General Relativity the geometry of the spacetime manifold is completely described by the metric. This includes the assumption that the connection on the manifold is the Levi–Civita connection, i.e. it is derived from the metric. The Einstein field equations can be derived from the Einstein–Hilbert action given by (first proposed by Hilbert [149])

$$\begin{aligned} S &= \int \mathrm{d}^4x \, \frac{1}{2}\sqrt{-g}R(g_{\alpha\beta}, \Gamma^{\alpha}_{\beta\gamma}) - \int \mathrm{d}^4x \, \sqrt{-g}\Lambda + S_{\mathrm{m}} \, , \\ &\equiv S_{EH} + S_{\Lambda} + S_{\mathrm{m}} \end{aligned} \tag{4.1}$$

where $g = \det g_{\alpha\beta}$ is the determinant of the metric $g_{\alpha\beta}$, and R is the Ricci scalar. Finally, we have also included the cosmological constant term Λ and a matter part of the action S_{m} that describes the matter content of the theory. In the metric formulation the Ricci scalar is constructed using the Levi–Civita connection and is thus derived from the metric $R = \mathring{R}(g_{\alpha\beta}, \partial_\gamma g_{\alpha\beta}, \partial_\gamma\partial_\delta g_{\alpha\beta})$. We use the symbol $\mathring{}$ to denote metric quantities and operators, i.e. in this case that the Ricci scalar $\mathring{R}$ is constructed using the Levi–Civita connection $\mathring{\Gamma}^{\alpha}_{\beta\gamma}$.

However, the metric and the connection describe different properties of the manifold. The metric describes distances and angles on the manifold as it defines the dot product of vectors on the tangent spaces. The connection on the other hand describes the curvature of the manifold, defining straight lines and covariant derivatives of tensor fields. In general the metric and the connection of a manifold can be independent quantities. This idea leads to the Palatini formulation of General Relativity (also referred as the first order formulation or the metric-affine formulation).

In the Palatini formulation the metric and the connection are taken to be inde-

pendent degrees of freedom (which was in fact first studied by Einstein [150, 151]). The nomenclature is, unfortunately, not fully agreed upon. Often in the literature the metric-affine refers to the case when the general connection is used both in the matter and gravitational sectors and Palatini to the case when the general connection is used in the gravitational sector only while the Levi–Civita connection is used for the matter sector.[16] In our works we do allow for the connection to mix with the matter fields but only via the curvature tensors. Fermions naturally couple directly to the connection unlike scalar fields and gauge fields. We do not explicitly discuss fermion fields further in our works, however, the connection used in fermionic terms could be taken to be the Levi–Civita connection [152–160].

In the Palatini formulation varying the Einstein–Hilbert action (4.1) with respect to both the metric and the general connection results into equations of motion that fix the connection to be the Levi–Civita connection. The field equations then reduce to the Einstein field equations

$$\mathring{R}_{\alpha\beta} - \frac{1}{2} g_{\alpha\beta} \mathring{R} + \Lambda g_{\alpha\beta} = \mathcal{T}_{\alpha\beta} \ , \tag{4.2}$$

where the energy momentum tensor is given by the variation of the matter part of the action with respect to the metric

$$\mathcal{T}_{\alpha\beta} \equiv \frac{-2}{\sqrt{-g}} \frac{\delta S_{\mathrm{m}}}{\delta g^{\alpha\beta}} \ . \tag{4.3}$$

The two formulations give rise to the same equations of motion and are thus classically equivalent.

By using the Palatini formulation fewer assumptions are needed to arrive at equivalent dynamics compared to the metric formulation. However, there are subtle differences even on the level of the Einstein–Hilbert action. In the metric formulation to obtain the Einstein field equations without further assumptions about boundaries a York-Gibbons-Hawking boundary term needs to be added to the action [161, 162]. In contrast, in the Palatini formulation such a term is not needed, see e.g. [163].

When gravity is modified by introducing new terms to the Einstein–Hilbert action the equivalence between different formulations break down and the different formulations yield different dynamics.

[16] In some older literature Palatini also implies the assumption that the general connection is restricted to be symmetric.

4.1 Geometrical quantities

Before discussing modifications, let us describe the richer structure of the spacetime manifold allowed by considering a general connection. The connection defines the covariant derivative ∇_α which acts on an arbitrary tensor $A^\alpha{}_\beta$ as

$$\nabla_\gamma A^\alpha{}_\beta = \partial_\gamma A^\alpha{}_\beta + \Gamma^\alpha_{\gamma\delta} A^\delta{}_\beta - \Gamma^\delta_{\gamma\beta} A^\alpha{}_\delta \ . \tag{4.4}$$

Note that the general connection does not have any symmetries, thus, the order of the indices appearing in the definition of the covariant derivative are important.[17]

A general connection allows for non-metricity and torsion. Non-metricity measures the covariant non-conservation of the metric by the connection. The non-metricity tensor and its contractions, the two non-metricity vectors, are defined as

$$Q_{\gamma\alpha\beta} \equiv \nabla_\gamma g_{\alpha\beta} \ , \quad Q_\gamma \equiv Q_{\gamma\alpha\beta} g^{\alpha\beta} \ , \quad \hat{Q}_\beta \equiv Q_{\gamma\alpha\beta} g^{\gamma\alpha} \ . \tag{4.5}$$

In geometrical terms the length of vectors change under parallel transport when a connection has non vanishing non-metricity.

Torsion describes the antisymmetricity of the connection. The torsion tensor and vector are defined as[18]

$$T^\gamma{}_{\alpha\beta} \equiv 2\Gamma^\gamma_{[\alpha\beta]} \ , \quad T_\beta \equiv T^\alpha{}_{\beta\alpha} \ . \tag{4.6}$$

Note that torsion does not depend on the metric. Geometrically torsion describes the non-closure of an infinitesimal parallellogram formed by parallel transporting vectors. Furthermore, straight lines described by the connection and shortest/longest paths described by the metric are equivalent if and only if the non-metricity vanishes and the torsion is totally antisymmetric [164]. See the figure 4.1 for schematic illustrations of the meaning of the different geometrical quantities.

It is often useful to perform a decomposition of the connection into a metric part and a difference from it

$$\Gamma^\gamma_{\alpha\beta} = \mathring{\Gamma}^\gamma_{\alpha\beta} + L^\gamma{}_{\alpha\beta} \ , \tag{4.7}$$

where the Levi–Civita connection of the metric $g_{\alpha\beta}$ is

$$\mathring{\Gamma}^\gamma_{\alpha\beta} = \tfrac{1}{2} g^{\gamma\delta} (\partial_\alpha g_{\delta\beta} + \partial_\beta g_{\alpha\delta} - \partial_\delta g_{\alpha\beta}) \ , \tag{4.8}$$

and $L^\gamma{}_{\alpha\beta}$ is the distortion tensor. This decomposition can be done with respect

[17] There are differing conventions in the literature for the order of indices and signs in the covariant derivative and so one has to take care to keep things consistent.

[18] It is also possible to construct an axial torsion vector $\hat{T}^\alpha = \frac{1}{6}\epsilon^{\alpha\beta\gamma\delta} T_{\beta\gamma\delta}$, but we will not need it.

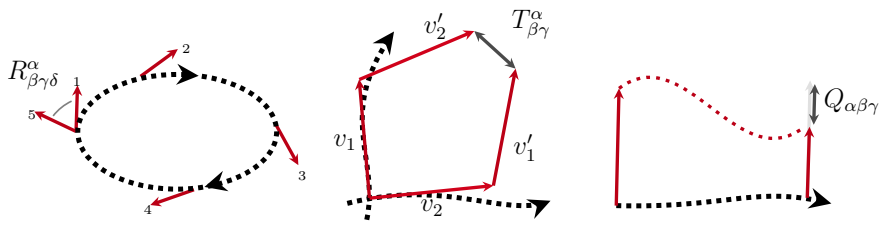

Figure 4.1. Illustrations of the different geometrical quantities derived from the connection. The dashed lines represent paths along which the vectors (solid arrows) are parallel transported. **(Left)** In a manifold with non-zero curvature parallel transporting a vector around a closed loop in general changes the direction of the vector. **(Middle)** With non-zero torsion trying to form a parallellogram by parallel transporting vectors infinitesimally along two paths will not necesarily form a closed parallellogram. **(Right)** With non-zero non-metricity parallel transporting a vector in general changes the length of the vector.

to any metric, not necessarily the original spacetime metric. Both the Levi–Civita connection and the distortion tensor $L^{\gamma}{}_{\alpha\beta}$ depend on the choice of the metric used in the decomposition. The sum of the two, i.e. the general connection, obviously does not.

The distortion tensor can be expressed in terms of non-metricity and torsion as

$$L^{\gamma}{}_{\alpha\beta} = J^{\gamma}{}_{\alpha\beta} + K^{\gamma}{}_{\alpha\beta} \ , \tag{4.9}$$

where the non-metricity part called the disformation is given by

$$J^{\alpha}{}_{\beta\gamma} \equiv \frac{1}{2} g^{\alpha\mu}(Q_{\mu\beta\gamma} - Q_{\gamma\mu\beta} - Q_{\beta\mu\gamma}) \ , \tag{4.10}$$

and the torsion part called the contortion is given by

$$K^{\alpha}{}_{\beta\gamma} \equiv \frac{1}{2}(T^{\alpha}{}_{\beta\gamma} + g_{\gamma\mu} g^{\alpha\nu} T^{\mu}{}_{\nu\beta} + g_{\beta\mu} g^{\alpha\nu} T^{\mu}{}_{\nu\gamma}) \ . \tag{4.11}$$

Note that these tensors have the symmetries $J_{\alpha\beta\gamma} = J_{\alpha(\beta\gamma)}$ and $K^{\alpha}{}_{\beta}{}^{\gamma} = K^{[\alpha}{}_{\beta}{}^{\gamma]}$, where the indices are raised and lowered with the metric $g_{\alpha\beta}$. In terms of distortion the non-metricity can be written as $Q_{\alpha\beta\gamma} = -2L_{(\alpha|\gamma|\beta)}$. Likewise, torsion can be expressed in terms of distortion as $2L^{\gamma}{}_{[\alpha\beta]}$. All the tensors $L^{\alpha}{}_{\beta\gamma}$, $J^{\alpha}{}_{\beta\gamma}$ and $K^{\alpha}{}_{\beta\gamma}$ depend on the metric chosen to do the decomposition with. Performing different metric transformations moves different pieces of the general connection between $\mathring{\Gamma}^{\alpha}_{\beta\gamma}$, $J^{\alpha}{}_{\beta\gamma}$ and $K^{\alpha}{}_{\beta\gamma}$.

4.2 Riemann and Ricci-type tensors

The Riemann tensor is constructed from the connection and is defined as

$$R^{\alpha}{}_{\beta\gamma\delta} \equiv \partial_\gamma \Gamma^{\alpha}_{\delta\beta} - \partial_\delta \Gamma^{\alpha}_{\gamma\beta} + \Gamma^{\alpha}_{\gamma\mu}\Gamma^{\mu}_{\delta\beta} - \Gamma^{\alpha}_{\delta\mu}\Gamma^{\mu}_{\gamma\beta} \ . \tag{4.12}$$

With a general connection the Riemann tensor has only one symmetry: it is antisymmetric in its last two indices $R^{\alpha}{}_{\beta\gamma\delta} = R^{\alpha}{}_{\beta[\gamma\delta]}$. This makes it possible to have more than one different first contraction of the Riemann tensor, not just the Ricci tensor. The three different possible first contractions are the Ricci tensor, the co-Ricci tensor, and the homothetic curvature tensor. We call these collectively the Ricci-type tensors, which are defined as:

$$R_{\alpha\beta} \equiv R^{\mu}{}_{\alpha\mu\beta} \qquad \text{(Ricci tensor)}, \tag{4.13a}$$

$$\hat{R}^{\alpha}{}_{\beta} \equiv g^{\mu\nu} R^{\alpha}{}_{\mu\nu\beta} \quad \text{(co-Ricci tensor)}, \tag{4.13b}$$

$$\widetilde{R}_{\alpha\beta} \equiv R^{\mu}{}_{\mu\alpha\beta} \qquad \text{(homothetic curvature tensor)}. \tag{4.13c}$$

In general the Ricci and co-Ricci tensor do not have any symmetries, while the homothetic curvature tensor is antisymmetric which originates from the Riemann tensor. The Ricci and homothetic tensors are independent of the metric, while the co-Ricci tensor depends on the metric. Furthermore, note that the Ricci scalar $R \equiv g^{\alpha\beta}R_{\alpha\beta}$ remains unique since $\hat{R}^{\alpha}{}_{\alpha} = -R$ and $g^{\alpha\beta}\widetilde{R}_{\alpha\beta} = 0$.[19]

It is also possible to construct many different scalars from contracting torsion and non-metricity tensors and combine them into actions that lead to second order field equations. Here we restrict our attention to theories where the connection appears only through the Riemann tensor.

Decomposing the connection as (4.7) the Riemann tensor decomposes into a metric and disformation parts, sometimes in the literature referred as post-Riemannian expansion:

$$R^{\alpha}{}_{\beta\gamma\delta} = \mathring{R}^{\alpha}{}_{\beta\gamma\delta} + 2\mathring{\nabla}_{[\gamma} L^{\alpha}{}_{\delta]\beta} + 2L^{\alpha}{}_{[\gamma|\mu|}L^{\mu}{}_{\delta]\beta} \ . \tag{4.14}$$

Using this decomposition for the Riemann tensor we can write the homothetic curvature as

$$\widetilde{R}_{\alpha\beta} = \partial_{[\alpha} Q_{\beta]} \ , \tag{4.15}$$

[19] There is another possible (pseudo)scalar that is linear in the Riemann tensor, called the Holst term: $R_h = \frac{1}{2} g_{\alpha\mu}\epsilon^{\mu\beta\gamma\delta} R^{\alpha}{}_{\beta\gamma\delta} = -3\mathring{\nabla}_\alpha \hat{T}^\alpha + \frac{1}{4}\epsilon^{\alpha\beta\gamma\delta} T_{\mu\alpha\beta} T^{\mu}{}_{\gamma\delta} + \frac{1}{2}\epsilon^{\alpha\beta\gamma\delta} Q_{\alpha\beta\mu} T^{\mu}{}_{\gamma\delta}$ [165]. With the Einstein–Hilbert action (with no matter couplings to the connection) adding the Holst term does not change the equations of motion and thus it has no effect on classical dynamics. If, however, the Einstein–Hilbert action is modified the Holst term becomes dynamical, see [166] for its effects in the context of inflation.

i.e. the homothetic curvature tensor is the exterior derivative of the non-metricity vector. The homothetic curvature tensor thus has to do with the change of length of vectors under parallel transport [167].

We can similarly use the decomposition (4.14) to write the co-Ricci tensor as

$$\hat{R}_{\alpha\beta} = -R_{\alpha\beta} + 2g^{\mu\nu}\nabla_{[\beta}Q_{\mu]\nu\alpha} - T^{\mu\nu}{}_{\beta}Q_{\mu\nu\alpha} \ , \tag{4.16}$$

from which it is apparent that the Ricci and co-Ricci tensors depend on each other. For our analysis it turns out to be useful to define an average of the Ricci and co-Ricci tensors

$$\overset{\Delta}{R}_{\alpha\beta} \equiv \frac{1}{2}(\hat{R}_{\alpha\beta} + R_{\alpha\beta}) = g^{\mu\nu}\nabla_{[\beta}Q_{\mu]\nu\alpha} - \frac{1}{2}T^{\mu\nu}{}_{\beta}Q_{\mu\nu\alpha} \ . \tag{4.17}$$

4.3 Projective transformation

Solving the connection from the Einstein–Hilbert action sets the connection to be the Levi–Civita connection up to an arbitrary vector $\Gamma^{\gamma}_{\alpha\beta} = \mathring{\Gamma}^{\gamma}_{\alpha\beta} + \delta^{\gamma}{}_{\beta}V_{\alpha}$ [168, 169]. This is due to a well known symmetry of the Einstein–Hilbert action: it is invariant under the projective transformation [168]

$$\Gamma^{\gamma}_{\alpha\beta} \to \Gamma^{\gamma}_{\alpha\beta} + \delta^{\gamma}{}_{\beta}V_{\alpha} \ , \tag{4.18}$$

where V_{α} is an arbitrary vector field. The projective part of the connection is left unconstrained by the field equations.

In some modified actions requiring projective invariance makes the theory ghost free [170–172]. However, ghost free theories without this symmetry are also known [171–173]. Furthermore, in [2] we have found theories that have ghosts which have this symmetry. A more complex type of symmetry is needed to guarantee a theory to be free of ghosts, see e.g. [174]. We discuss issues of ghost degrees of freedom in more detail in chapter 5. Additionally, if the gravitational sector is projectively invariant and the matter sector is not will in general lead to problems [163].

Under the projective transformation the Ricci-type tensors transform as

$$\begin{aligned}
R_{\alpha\beta} &\to R_{\alpha\beta} + 2\partial_{[\alpha}V_{\beta]} \ , \\
\hat{R}_{\alpha\beta} &\to \hat{R}_{\alpha\beta} + 2\partial_{[\alpha}V_{\beta]} \ , \\
\widetilde{R}_{\alpha\beta} &\to \widetilde{R}_{\alpha\beta} + 8\partial_{[\alpha}V_{\beta]} \ , \\
\overset{\Delta}{R}_{\alpha\beta} &\to \overset{\Delta}{R}_{\alpha\beta} + 2\partial_{[\alpha}V_{\beta]} \ .
\end{aligned} \tag{4.19}$$

Note that only the antisymmetric parts of the Ricci-type tensors change under the projective transformation. Thus, the symmetric parts of the Ricci-type tensors re-

main invariant. This makes the fact that Einstein–Hilbert action is symmetric under the projective transformation evident, since only the symmetric part of the Ricci tensor appears in the action. We can also construct a linear combination from the antisymmetric parts which is invariant under the projective transformation

$$\overset{P}{R}_{\alpha\beta} \equiv (\alpha + 4\beta)R_{[\alpha\beta]} - \alpha\overset{\hat{\Delta}}{R}_{[\alpha\beta]} - \beta\widetilde{R}_{\alpha\beta} \ , \tag{4.20}$$

where α and β can be any quantities that are invariant under the projective transformation.

The projective symmetry will play a role in the next chapter where we will investigate the stability of Ricci-type theories.

Chapter 5

Stability of higher order curvature theories

In our work we investigated the perturbative degrees of freedom propagating around specific backgrounds. This is distinct from investigating the degrees of freedom of the full nonlinear theories where one would obtain a complete picture of all propagating degrees of freedom and their nature. The full nonlinear Hamiltonian analysis to obtain this full picture for a given modified gravity theory is a highly nontrivial task, see e.g. [175]. So, one can first investigate the easier path and look at degrees of freedom around specific backgrounds.

The stability of physically relevant backgrounds is an important requirement for any physically sensible theory to have. In addition, finding that different number of degrees of freedom propagate around different backgrounds can indicate the existence of a strong coupling problem [176–179], bringing the viability of a theory into question.

To illustrate the stability of perturbations around a background let us look at a canonical scalar field around Minkowski space with the Lagrangian

$$\mathcal{L} = \frac{k}{2}\partial_0\phi\partial_0\phi - \frac{l}{2}\partial_i\phi\partial_i\phi - \frac{m^2}{2}\phi^2 + \mathcal{L}_{\phi\Psi} \ , \tag{5.1}$$

where k, l and m^2 are some constants, and $\mathcal{L}_{\phi\Psi}$ denotes couplings between the scalar ϕ and additional degrees of freedom in the theory. The usual stable canonical scalar corresponds to $k = 1$, $l = 1$ and $m^2 \geq 0$.

There can be different types of instabilities depending on the signs of k, l and m^2. If the gradient term has the wrong sign $l < 0$ there is a gradient (Laplacian) instability and if the mass term has the wrong sign $m^2 < 0$ there is a tachyonic instability, for more on these see e.g. [179–181]. Here we will focus on the instabilities

appearing when $k < 0$, i.e. when the kinetic term has a negative sign.[20] Degrees of freedom with a negative sign kinetic term are called ghosts. The Hamiltonian is $H = \frac{1}{2}[k^{-1}\pi^2 + (\partial_i\phi)^2 + m^2\phi^2] + H_{\phi\Psi}$ with $\pi/k = \partial_0\phi$, which for $k < 0$ is not bounded from below. This is a problem, since if the field interacts with other fields, the ghost can decay to arbitrarily negative energies exciting the other fields to arbitrarily high energies.

Quantizing this theory one finds the background to be unstable. Due to the ghosts having negative energy, energy conservation does not forbid vacuum to produce ghost particles and particles it interacts with. This renders any candidate of a vacuum state to be unstable. Another choice is to define non-positive definite metric on the Hilbert space leading to bounded energies at the cost of introducing negatively normed states [182].

It is worth noting here that not all ghosts are necessarily problematic. One might be more familiar with the Faddeev–Popov ghosts in the context of gauge theories. In this context the ghosts are introduced to deal with unphysical gauge degrees of freedom. These ghosts do not appear in physical spectrum of the theory (the ghosts only appear in internal lines in Feynman diagrams) and thus these ghosts are not problematic. In effective field theory setting a perfectly healthy ultraviolet theory may lead to low energy effective field theory that contains ghosts. If the ghost appear at higher orders of the effective theory's expansion parameter they are not problematic since they cannot be excited while staying in the validity of the effective theory [183, 184].

There has been recent studies on how to make ghosts in the quantum theory viable [185–189]. The classical stability of ghosts has also been studied, see [190] and references therein.

It is worth noting here that there has been successful efforts in automating the computations needed to investigate perturbative degrees of freedom for the very complicated tensorial theories, at least around Minkowski space [191, 192].

5.1 Stability of non-degenerate Ricci-type theories

In [2] we studied the most general non-degenerate Palatini theory where the action depends algebraically on the Ricci-type tensors, focusing on if ghost degrees of freedom appear or not.

We take the action to be a function of any set of linearly independent combination of the Ricci-type tensors (4.13). For later convenience we choose this to be

[20] In the Lorentz invariant form it is often said that the kinetic terms has the *wrong* sign, since the correct sign leading to positive kinetic term depends on the convention for the metric signature in use, $-\frac{1}{2}(\partial_\alpha\phi)^2$ for $(-,+,+,+)$ signature and $+\frac{1}{2}(\partial_\alpha\phi)^2$ for $(+,-,-,-)$.

$\{R_{\alpha\beta}, \overset{\triangle}{R}_{(\alpha\beta)}, \overset{P}{R}_{\alpha\beta}, \widetilde{R}_{\alpha\beta}\}$. Furthermore, we choose $\alpha = 1$ and $\beta = 0$ in the definition (4.20) of $\overset{P}{R}_{\alpha\beta}$ without loss of generality. The action under consideration reads

$$S = \int \mathrm{d}^4x\sqrt{-g}\frac{1}{2}F(g_{\alpha\beta}, R_{\alpha\beta}, \overset{\triangle}{R}_{(\alpha\beta)}, \overset{P}{R}_{\alpha\beta}, \widetilde{R}_{\alpha\beta}, \Psi, \partial\Psi) \ , \tag{5.2}$$

where Ψ and $\partial\Psi$ denote collectively all the matter fields and their derivatives included in the theory. The matter fields are allowed to couple arbitrarily to the Ricci-type tensors. To make the analysis of this action more tractable, we perform a Legendre transformation to bring the action into a form that is linear in the Ricci-type tensors [193–197].

5.1.1 Legendre transformation

Performing a Legendre transformation to the action (5.2) we get

$$\begin{aligned} S = \int \mathrm{d}^4x\sqrt{-g}\frac{1}{2}\Bigg[& F\left(g_{\alpha\beta}, \Sigma_{\alpha\beta}, \Delta_{\alpha\beta}, \Pi_{\alpha\beta}, \Theta_{\alpha\beta}, \Psi, \partial\Psi\right) + \frac{\partial F}{\partial\Sigma_{\alpha\beta}}(R_{\alpha\beta} - \Sigma_{\alpha\beta}) \\ & + \frac{\partial F}{\partial\Delta_{\alpha\beta}}(\overset{\triangle}{R}_{(\alpha\beta)} - \Delta_{\alpha\beta}) + \frac{\partial F}{\partial\Pi_{\alpha\beta}}(\overset{P}{R}_{\alpha\beta} - \Pi_{\alpha\beta}) + \frac{\partial F}{\partial\Theta_{\alpha\beta}}(\widetilde{R}_{\alpha\beta} - \Theta_{\alpha\beta})\Bigg] \ , \end{aligned} \tag{5.3}$$

where $\Sigma_{\alpha\beta}$, $\Delta_{\alpha\beta} = \Delta_{(\alpha\beta)}$, $\Pi_{\alpha\beta} = \Pi_{[\alpha\beta]}$, and $\Theta_{\alpha\beta} = \Theta_{[\alpha\beta]}$ are auxiliary fields. Varying the action (5.3) with respect to the auxiliary fields lead to equations of motion of the form $\partial^2F/(\partial\Sigma_{\alpha\beta}\partial\Sigma_{\gamma\delta})[R_{\gamma\delta} - \Sigma_{\gamma\delta}] = 0$, which has the solution $\Sigma_{\alpha\beta} = R_{\alpha\beta}$, if $\partial^2F/(\partial\Sigma_{\alpha\beta}\partial\Sigma_{\gamma\delta})$ is invertible. Assuming that the second derivative of F with respect to each of the auxiliary fields is invertible, from the auxiliary fields equations of motion we get the solutions $\Sigma_{\alpha\beta} = R_{\alpha\beta}$, $\Delta_{\alpha\beta} = \overset{\triangle}{R}_{(\alpha\beta)}$, $\Pi_{\alpha\beta} = \overset{P}{R}_{\alpha\beta}$, and $\Theta_{\alpha\beta} = \widetilde{R}_{\alpha\beta}$, which when substituted back into the action gives the original action (5.2). Theories for which F satisfies these invertibility conditions, the original action (5.2) and the Legendre transformed one (5.3) are equivalent and we call them non-degenerate.

The action is simplified further by introducing the following field redefinitions

$$\sqrt{-g}\frac{\partial F}{\partial\Sigma_{(\alpha\beta)}} \equiv \sqrt{-q}q^{\alpha\beta} \ , \quad \sqrt{-g}\frac{\partial F}{\partial\Sigma_{[\alpha\beta]}} \equiv \sqrt{-q}B^{\alpha\beta} \tag{5.4a}$$

$$\sqrt{-g}\frac{\partial F}{\partial\Delta_{\alpha\beta}} \equiv \sqrt{-q}S^{\alpha\beta} \ , \quad \sqrt{-g}\frac{\partial F}{\partial\Pi_{\alpha\beta}} \equiv \sqrt{-q}P^{\alpha\beta} \tag{5.4b}$$

$$\sqrt{-g}\frac{\partial F}{\partial\Theta_{\alpha\beta}} \equiv \sqrt{-q}H^{\alpha\beta} \ , \tag{5.4c}$$

where $q = \det q_{\alpha\beta}$ and $q^{\alpha\beta}$ is the inverse of $q_{\alpha\beta}$, which has to exist for the field

redefinitions to be consistent. With these the action can be written as

$$S = \int \mathrm{d}^4x\sqrt{-q}\frac{1}{2}\Bigg[R^{\alpha}{}_{\beta\gamma\delta}f_{\alpha}{}^{\beta\gamma\delta} + \frac{\sqrt{-g}}{\sqrt{-q}}F - (q^{\alpha\beta}+B^{\alpha\beta})\Sigma_{\alpha\beta} - S^{\alpha\beta}\Delta_{\alpha\beta} - P^{\alpha\beta}\Pi_{\alpha\beta} - H^{\alpha\beta}\Theta_{\alpha\beta}\Bigg] , \quad (5.5)$$

where

$$f_{\alpha}{}^{\beta\gamma\delta} \equiv \left(q^{\beta[\delta} + B^{\beta[\delta} + \frac{1}{2}S^{\beta[\delta} + \frac{1}{2}P^{\beta[\delta}\right)\delta^{\gamma]}{}_{\alpha} + \frac{1}{2}S^{\mu[\delta}g^{\gamma]\beta}g_{\mu\alpha} - \frac{1}{2}P^{\mu[\delta}g^{\gamma]\beta}g_{\mu\alpha} + H^{\gamma\delta}\delta^{\beta}{}_{\alpha} . \quad (5.6)$$

The new auxiliary field $q_{\alpha\beta}$ plays the role of the metric. The original metric $g_{\alpha\beta}$ among the rest of the auxiliary fields $\Sigma_{\alpha\beta}$, $\Delta_{\alpha\beta}$, $\Pi_{\alpha\beta}$, $\Theta_{\alpha\beta}$ are to be solved algebraically from the field redefinitions (5.4) in terms of the new fields $q_{\alpha\beta}$, $B^{\alpha\beta}$, $S^{\alpha\beta}$, $P^{\alpha\beta}$, $H^{\alpha\beta}$.

We have managed to write the general action (5.2) depending non-degenerately on the Ricci-type tensors in a form which is linear in the Riemann tensor. Thus the action is quadratic in the connection, meaning that the action results into a linear equations of motion for the connection. We can thus solve the connection in terms of the rest of the fields and substitute it back into the action. We then obtain an action that depends only on $q_{\alpha\beta}$, $B^{\alpha\beta}$, $S^{\alpha\beta}$, $P^{\alpha\beta}$, $H^{\alpha\beta}$, the matter fields Ψ and possibly on the projective mode of the connection if it is left unconstrained by the equations of motion for the connection. From the resulting form of the action we can inspect if the new fields obtain kinetic terms and if they are ghosts or not.

In principle the connection is solvable in the full theory since it is a linear equation. However, it becomes untractable in general. Thus, we resorted into considering perturbations around different backgrounds and solving the connection to first order. We investigated different initial constraints for the connection: the general case where the initial connection is completely unconstrained, the case where the torsion is vanishing and the case where the non-metricity is vanishing.

5.1.2 General case around Minkowski background

Around Minkowski space the original metric is expanded as $g_{\alpha\beta} = \eta_{\alpha\beta} + \delta g_{\alpha\beta}$ where $\eta_{\alpha\beta}$ is the Minkowski metric. This results in the new metric being similarly expanded as $q_{\alpha\beta} = \eta_{\alpha\beta} + \delta q_{\alpha\beta}$. Furthermore, around Minkowski the connection $\Gamma^{\gamma}_{\alpha\beta}$ and the fields $B^{\alpha\beta}$, $S^{\alpha\beta}$, $P^{\alpha\beta}$ and $H^{\alpha\beta}$ are considered to be first order perturbations.

Solving the connection to first order in the general case leads to the action [2]

$$S = \int \mathrm{d}^4x \frac{1}{2}\Bigg[\mathring{R} - \frac{7}{2}\partial_\alpha B^{\alpha\beta}\partial^\gamma B_{\gamma\beta} - \frac{1}{4}\partial_\gamma B_{\alpha\beta}\partial^\gamma B^{\alpha\beta} - \frac{166}{3}\partial_\alpha H^{\alpha\beta}\partial^\gamma H_{\gamma\beta} \\ - \frac{82}{3}\partial_\alpha B^{\alpha\beta}\partial^\gamma H_{\gamma\beta} + \frac{1}{3}(-2T_\beta + \partial^\gamma S_{\gamma\beta} + \partial^\gamma P_{\gamma\beta})(\partial_\alpha B^{\alpha\beta} + 4\partial_\alpha H^{\alpha\beta}) \\ + \frac{\sqrt{-g}}{\sqrt{-q}}F - (q^{\alpha\beta} + B^{\alpha\beta})\Sigma_{\alpha\beta} - S^{\alpha\beta}\Delta_{\alpha\beta} - P^{\alpha\beta}\Pi_{\alpha\beta} - H^{\alpha\beta}\Theta_{\alpha\beta}\Bigg] . \tag{5.7}$$

Here T_β is the projective mode of the connection left unconstrained due to the projective symmetry of the field equations. The action does not have mixing between $\mathring{R}_{\alpha\beta}$ and the other fields due to us making the choice of using $\overset{\Delta}{R}_{\alpha\beta}$ as an variable instead of $\hat{R}_{\alpha\beta}$.

Analysing the kinetic terms of the action (5.7) results into the following conclusions. Kinetic terms for $B^{\alpha\beta}$, originating from $R_{[\alpha\beta]}$, lead to a pseudovector degree of freedom which is unstable. This ghost exists whether or not the action depends on the other fields or not. Action depending on $\overset{\Delta}{R}_{[\alpha\beta]}$ leads to a ghost in the same way as $R_{[\alpha\beta]}$. We can now note another projectively invariant action leading to a ghost. An action depending on the projectively invariant combination $4R_{[\alpha\beta]} - \widetilde{R}_{\alpha\beta}$ leads to the same pseudovector ghost as $R_{[\alpha\beta]}$, since the homothetic tensor only contributes to the vector sector and cannot thus affect the pseudovector sector. In contrast, both $R_{[\alpha\beta]}$ and $\overset{\Delta}{R}_{[\alpha\beta]}$ contribute to the pseudovector sector and in the combination $\overset{P}{R}_{\alpha\beta} = R_{[\alpha\beta]} - \overset{\Delta}{R}_{\alpha\beta}$ their contributions exactly cancels. Thus, we do not have a kinetic term for $P^{\alpha\beta}$ in the action (5.7).

We saw that if the action depends on $B^{\alpha\beta}$ there is always a ghost around Minkowski space. Now if the action does not depend on $B^{\alpha\beta}$, depending on the form of the function F in the action, it may either have: no new degrees of freedom or a new propagating vector field, which may be healthy or a ghost. These come from the projective mode T_β of the connection that appears in the action (5.7) as a Lagrange multiplier type term [2]. The new propagating vector field coming from the homothetic curvature has been found also previously in the literature [198].

5.1.3 General case around FLRW background

We found that around Minkowski background the Ricci-type tensors $\overset{\Delta}{R}_{\alpha\beta}$ and $\overset{P}{R}_{\alpha\beta}$ do not result in new degrees of freedom. This motivated us to look if it is a peculiarity of the maximally symmetric Minkowski space that no new degrees of freedom propagate due to these tensors. To investigate this further we chose to investigate perturbations around a cosmological spatially flat FLRW background (see section 6.1 for description of the FLRW background).

Expanding around the FLRW background is considerably more cumbersome than the Minkowski case. To make the computations more tractable we considered a simpler case where the action (5.2) is

$$S = \int \mathrm{d}^4x\sqrt{-g}\frac{1}{2}F(g_{\alpha\beta}, g^{\alpha\beta}R_{\alpha\beta}, \overset{\Delta}{R}_{(\alpha\beta)}, \overset{P}{R}_{\alpha\beta}, \Psi, \partial\Psi) \ . \tag{5.8}$$

After performing the same Legendre transformation procedure described above, the metric is split into background plus perturbations as $q_{\alpha\beta} = \bar{q}_{\alpha\beta} + \delta q_{\alpha\beta}$ where the background metric is $\bar{q}_{\alpha\beta} = a(\eta)^2\eta_{\alpha\beta}$ where η is the conformal time. The connection is also divided into a non-zero background part and perturbations. For the non-metric part, i.e. the distortion, $L^\gamma{}_{\alpha\beta} = \bar{L}^\gamma{}_{\alpha\beta} + \delta L^\gamma{}_{\alpha\beta}$. By symmetries the background part of distortion is of the form

$$\bar{L}^\gamma{}_{\alpha\beta} = L_1(\eta)u^\gamma\bar{q}_{\alpha\beta} + L_2(\eta)u_\alpha\delta^\gamma{}_\beta + L_3(\eta)u_\beta\delta^\gamma{}_\alpha + L_4(\eta)u^\gamma u_\alpha u_\beta + L_5(\eta)\epsilon^\gamma{}_{\alpha\beta\delta}u^\delta \ , \tag{5.9}$$

where $u^\alpha = (a^{-1}, 0, 0, 0)$ and $\epsilon_{\alpha\beta\gamma\delta}$ is the totally antisymmetric Levi–Civita tensor. The new field $S^{\alpha\beta}$ is split into background and perturbations $S^{\alpha\beta} = \bar{S}^{\alpha\beta} + \delta S^{\alpha\beta}$ with $\bar{S}^{\alpha\beta} = S_1(\eta)\bar{q}^{\alpha\beta} + S_2(\eta)u^\alpha u^\beta$. Finally, the antisymmetric field is zero on the background and thus $P^{\alpha\beta} = \delta P^{\alpha\beta}$. With these we can solve the background connection and substitute it back into the action, which results into $R^\alpha{}_{\beta\gamma\delta}f_\alpha{}^{\beta\gamma\delta}$ part of the action becoming [2]

$$S \supset \int \mathrm{d}^4x a^4 \left[\frac{1}{2}\mathring{R}(\bar{q}) + \frac{3}{4}H^2S_2^2 + \frac{3S_2^2}{16a^2(S_2^2-4)}S_2'S_2' + \frac{3HS_2}{4a}S_2'\right] \ , \tag{5.10}$$

where $\mathring{R}(\bar{q})$ in the Ricci scalar of the background metric $\bar{q}_{\alpha\beta}$, the prime denotes $' \equiv \frac{\mathrm{d}}{\mathrm{d}\eta}$ and $H \equiv a'/a^2$ is the Hubble parameter. We can note that the action turns out not to depend on $S_1(\eta)$ part of the $\bar{S}^{\alpha\beta}$ background. This implies that for maximally symmetric backgrounds with no preferred time directions (i.e. no u^α exist) there is no kinetic terms for the $S^{\alpha\beta}$. Which is the case in Minkowski background as we saw earlier. Inspecting the action we note that the kinetic term of S_2 has the wrong sign for $|S_2| < 2$, thus $S_2 = 0$ is unstable.

Obtaining the second order action for the perturbations around FLRW background is in principle straightforward, but very cumbersome. To second order perturbations transforming differently under spatial rotations tensors, vectors and scalars decouple and can be treated separately. The tensor modes turn out to be simplest to analyse. After a lengthy cumbersome calculation the kinetic terms for the tensor

perturbations turn out to be

$$S \supset \int \mathrm{d}^4x a^4 \left[\frac{1}{2a^2}\partial_0 h_{ij}\partial_0 h^{ij} - \frac{1}{4}\partial_k h_{ij}\partial^k h^{ij} + \frac{S_2^2}{4a^2(S_2^2-4)}\partial_0 s_{ij}\partial_0 s^{ij} \right] , \qquad (5.11)$$

where $\delta q_{ij} = h_{ij}$, with $h^i{}_i = 0,\ \partial^i h_{ij} = 0$; and $\delta S^{ij} = s^{ij}$, with $s^i{}_i = 0,\ \partial_i s^{ij} = 0$. Spatial indices are raised and lowered using the background metric $\bar{q}_{\alpha\beta}$. We find the same conclusion as for the background kinetic term: the kinetic term for the tensor modes s_{ij} have the wrong sign when $|S_2| < 2$. We have found that whether or not $S^{\alpha\beta}$ leads to new degrees of freedom depends on the background. This may be an indication of a strong coupling problem, as noted earlier.

5.1.4 Case of zero torsion around Minkowski background

Let us assume that the torsion vanishes a priori $T^\alpha{}_{\beta\gamma} = 0$, as often historically assumed in the Palatini formulation. With zero torsion one finds $\widetilde{R}_{\alpha\beta} = 2R_{[\alpha\beta]}$ and thus the homothetic curvature is not linearly independent and we can drop its dependence setting $H^{\alpha\beta} = 0$.

Solving the connection to first order as explained at the beginning of section 5.1.2 now results into a second order action for the perturbations around Minkowski

$$\begin{aligned} S = \int \mathrm{d}^4x \frac{1}{2} \Bigg[& \mathring{R}(q) + \frac{1}{6}\partial_\alpha \hat{B}^{\alpha\beta}\partial_\gamma \hat{B}^\gamma{}_\beta - \frac{1}{2}\partial_\alpha P^{\alpha\beta}\partial_\gamma P^\gamma{}_\beta - \frac{1}{16}\partial_\gamma P_{\alpha\beta}\partial^\gamma P^{\alpha\beta} \\ & + \frac{1}{16}\partial_\gamma S_{\alpha\beta}\partial^\gamma S^{\alpha\beta} - \frac{1}{48}\partial_\alpha S^\beta{}_\beta \partial^\alpha S^\gamma{}_\gamma - \frac{1}{12}\partial_\alpha S^{\alpha\beta}\partial_\gamma S^\gamma{}_\beta + \frac{1}{24}\partial_\beta S^{\beta\gamma}\partial_\gamma S^\alpha{}_\alpha \\ & - \frac{5}{4}\partial_\alpha P^{\alpha\beta}\partial_\gamma S^\gamma{}_\beta + \frac{2}{3}\partial_\alpha \hat{B}^{\alpha\beta}\partial_\gamma S^\gamma{}_\beta \\ & + \frac{\sqrt{-g}}{\sqrt{-q}}F - (q^{\alpha\beta} + \hat{B}^{\alpha\beta} + 2P^{\alpha\beta})\Sigma_{\alpha\beta} - S^{\alpha\beta}\Delta_{\alpha\beta} - P^{\alpha\beta}\Pi_{\alpha\beta} \Bigg] , \end{aligned} \qquad (5.12)$$

where the $P^{\alpha\beta}$ and $B^{\alpha\beta}$ kinetic terms have been diagonalized using a redefinition $\hat{B}_{\alpha\beta} = B_{\alpha\beta} + 2P_{\alpha\beta}$. Ignoring cross terms $B^{\alpha\beta}$ has a healthy kinetic term, but $P^{\alpha\beta}$ and $S^{\alpha\beta}$ lead to ghosts [199]. If we set $P^{\alpha\beta} = 0$ the remaining kinetic terms are easy to diagonalize and one sees that ghosts appear. If the action does not depend on $\overset{P}{R}_{\alpha\beta}$ nor $\overset{\hat{A}}{R}_{\alpha\beta}$ (i.e. $P^{\alpha\beta} = S^{\alpha\beta} = 0$) it is possible to solve the connection exactly and the extra degree of freedom coming from $R_{[\alpha\beta]}$ ($B^{\alpha\beta}$) corresponds to a vector field with positive definite kinetic term [171].

5.1.5 Case of zero non-metricity around Minkowski background

Theories where the non-metricity is assumed to vanish are called Einstein-Cartan theories, a common assumption in loop quantum gravity [200].

Tensor	General case Minkowski	FLRW	Zero torsion Minkowski	Zero non-metricity Minkowski
$R_{(\alpha\beta)}$	no new dofs	-	no new dofs	no new dofs
$R_{[\alpha\beta]}$	ghosts	-	healthy vector	no new dofs
$\overset{\Delta}{R}_{(\alpha\beta)}$	no new dofs	ghosts	ghosts	0
$\overset{P}{R}_{\alpha\beta}$	no new dofs	no new dofs	ghosts	not independent
$\widetilde{R}_{\alpha\beta}$	no new dofs, healthy vector, or ghosts	-	not independent	0

Table 5.1. Table summarising which Ricci-type tensors lead to new degrees of freedom (dofs) and if they include ghosts. Entry of 0 means the tensor is identically zero and "not independent" means the tensor depends linearly on the other tensors. In the general case $\widetilde{R}_{\alpha\beta}$ can lead either one of the listed entries, depending on the form of the function F in the action (5.2). In the FLRW case $\overset{\Delta}{R}_{\alpha\beta}$ leads to ghost or healthy degrees of freedom depending on the background solution. Table from [2].

Assuming $\nabla_\alpha g_{\beta\gamma} = Q_{\alpha\beta\gamma} = 0$ the disformation vanishes, thus the distortion is given solely by the contortion $L^\alpha{}_{\beta\gamma} = K^\alpha{}_{\beta\gamma}$. Recalling the symmetry $K^{[\alpha}{}_\beta{}^{\gamma]} = K^\alpha{}_\beta{}^\gamma$ we see from (4.14) that $\widetilde{R}_{\alpha\beta} = 0$. From (4.17) we also see that $\overset{\Delta}{R}_{\alpha\beta} = 0$. Now since we have only $R_{\alpha\beta}$ left we can also drop dependence on $\overset{P}{R}_{\alpha\beta}$ since it is not independent. Thus, the only remaining non trivial Ricci-type tensor is $R_{\alpha\beta}$ and we thus have only the $q_{\alpha\beta}$ and $B^{\alpha\beta}$ fields.[21]

Solving for the connection to first order as described in section 5.1.2 we obtain an action with only kinetic terms coming from the Einstein–Hilbert term $\mathring{R}(q)$ for the metric $q_{\alpha\beta}$. The new field $B^{\alpha\beta}$ does not propagate around Minkowski space.

We did not investigate this case around FLRW background since it is known that Einstein-Cartan theory quadratic in $R_{[\alpha\beta]}$ has a ghost in the full nonlinear theory [201–204].

The main findings reviewed in this chapter are summarised in the Table 5.1.

[21] Assuming $\nabla_\alpha g_{\beta\gamma} = Q^{(g)}_{\alpha\beta\gamma} = 0$ is the most natural choice since the original theory is formulated with the metric $g_{\alpha\beta}$. We could also ask what if we assume the non-metricity with respect to the Einstein frame metric $q_{\alpha\beta}$ vanishes instead $\nabla_\alpha q_{\beta\gamma} = Q^{(q)}_{\alpha\beta\gamma} = 0$. The end result, to first order, turns out to be the same [2].

Chapter 6

Cosmic Inflation and Ricci-type theories

The most promising observational probe of higher order curvature effects is the primordial universe, most notably the period of cosmic inflation. In this chapter we will review our results found in [3] starting with a brief introduction to inflation.

6.1 Inflationary paradigm

Cosmic inflation [205–210] is a hypothetical period of accelerated expansion of spacetime, which is a very successful scenario of the very early universe. It is able to explain features that are left unaddressed by the hot Big Bang model of cosmology. It can explain: the homogeneity and isotropy problem, the observed spatial flatness and alleviate possible problematic relic problems.[22]

Most notably, and what we are going to focus on here, is the ability to explain the origin of primordial perturbations. Many inflationary models are able to generate primordial perturbations that are (to a good approximation) Gaussian, adiabatic and close to scale invariant, which is in very good agreement with observations [212]. These primordial perturbations act as seeds for large scale structure formation in the later evolution of the universe.

Inflating universe rapidly becomes spatially homogeneous and isotropic to a high degree. A spacetime manifold with the latter symmetries can be foliated into maximally symmetric spacelike slices. The most general metric on such a manifold is the Friedmann-Lemaître-Robertson-Walker (FLRW) metric

$$\mathrm{d}s^2 = -\mathrm{d}t^2 + a^2(t)\left[\frac{\mathrm{d}r^2}{1-Kr^2} + r^2(\mathrm{d}\theta^2 + \sin^2\theta\mathrm{d}\phi^2)\right], \tag{6.1}$$

[22] For detailed explanations and how inflation is able to solve these problems see any introductory text on inflation, e.g. [211].

where t is the time coordinate, $a(t)$ the scale factor describing the expansion of the universe, $\{r, \theta, \phi\}$ are the spherical coordinates on the maximally symmetric spatial slice and K describes the curvature of the slices. Since inflation drives the universe to be spatially flat we can set $K = 0$. Universe is in accelerated expansion, i.e. inflating, when the second time derivative of the scale factor is positive $\ddot{a} > 0$. The dots denote time derivatives $\frac{\mathrm{d}}{\mathrm{d}t}$.

As the famous quote by Wheeler says *"Spacetime tells matter how to move; matter tells spacetime how to curve"* [213], let us inspect what kind of matter can curve spacetime in such a way that it is accelerated expansion of space. Homogeneity and isotropy restricts the matter content to be described by a perfect fluid, for which the energy momentum tensor can be written as

$$\mathcal{T}_{\alpha\beta} = p g_{\alpha\beta} + (\rho + p) u_\alpha u_\beta \ , \tag{6.2}$$

where u_α is the four-velocity, $p = p(t)$ is the pressure, and $\rho = \rho(t)$ is the energy density of the fluid. With the FLRW metric (6.1) and the perfect fluid (6.2) the Einstein equations reduce to the Friedmann equations

$$\begin{aligned} H^2 &= \frac{\rho}{3}, \\ \frac{\ddot{a}}{a} &= -\frac{1}{6}(\rho + 3p) \ , \end{aligned} \tag{6.3}$$

where $H \equiv \dot{a}/a$ is the Hubble parameter. In terms of the Hubble parameter the requirement for inflation can be written as $\epsilon_H \equiv -\dot{H}/H^2 < 1$. In other words, during inflation the comoving Hubble radius $(aH)^{-1}$ decreases, in contrast during matter and radiation domination it increases. From the second Friedmann equation it is clear that we get accelerated expansion when $\rho + 3p < 0$. For non-relativistic matter and radiation $\rho + 3p > 0$.

6.2 Scalar field driven inflation

A simple way of realising accelerated expansion is by adding a single scalar field to the Einsten-Hilbert action. Consider the matter part of the action (4.1) to be dominated by

$$S_{\mathrm{m}} = \int \mathrm{d}^4x\sqrt{-g}\left[-\frac{1}{2}g^{\alpha\beta}\partial_\alpha\varphi\partial_\beta\varphi - V(\varphi)\right] \ . \tag{6.4}$$

Assuming that the scalar is homogeneous and isotropic $\varphi = \varphi(t)$, the equations of motion for the scalar field are given by

$$\ddot{\varphi} + 3H\dot{\varphi} + V(\varphi)_{,\varphi} = 0 \ , \tag{6.5}$$

and we have $\rho = \frac{1}{2}\dot{\varphi}^2 + V(\varphi)$ and $p = \frac{1}{2}\dot{\varphi}^2 - V(\varphi)$. We have introduced a shorthand notation for partial derivatives $\partial_\varphi V(\varphi) \equiv V(\varphi)_{,\varphi}$. Thus, the Friedmann equations now read

$$H^2 = \frac{1}{3}\left[\frac{1}{2}\dot{\varphi}^2 + V(\varphi)\right], \tag{6.6}$$

$$\frac{\ddot{a}}{a} = -\frac{1}{3}\left[\dot{\varphi}^2 - V(\varphi)\right] \ , \tag{6.7}$$

from which it is evident that we get accelerated expansion when the kinetic energy of the scalar is smaller than its potential energy $\dot{\varphi}^2 < V(\varphi)$. The scalar field that drives inflation is called the inflaton.

For inflation to be able to solve the various problems mentioned previously, the universe has to inflate for sufficiently long. We can imagine that in a scenario where the scalar field is slowly rolling down a sufficiently flat potential the condition $\dot{\varphi}^2 < V(\varphi)$ will be satisfied for non-negligible time. This leads us to the scenario of slow-roll inflation.

In the slow-roll approximation we assume that

$$\dot{\varphi}^2 \ll V(\varphi), \quad |\ddot{\varphi}| \ll |3H\dot{\varphi}| \ , \tag{6.8}$$

With the above assumptions (6.6) and (6.5) simplify to the slow-roll equations

$$H^2 = \frac{V(\varphi)}{3} \ , \tag{6.9}$$

$$3H\dot{\varphi} = -V(\varphi)_{,\varphi} \ . \tag{6.10}$$

Let us define the first two slow-roll parameters

$$\epsilon = \frac{1}{2}\left(\frac{V_{,\varphi}}{V}\right)^2 , \tag{6.11}$$

$$\eta = \frac{V_{,\varphi\varphi}}{V} \ . \tag{6.12}$$

When the slow-roll approximation is valid $\epsilon_H \approx \epsilon \ll 1$ and $|\eta| \ll 1$, or in other words these two conditions imply (6.8). The second and further slow-roll parameters are needed to be small to get long period of inflation. Slow-roll is an attractor of the equations of motion, thus a wide range of different initial conditions tend to rapidly flow to the slow-roll region of the phase space, see e.g. [214]. The amount of inflation is customarily measured by the number of e-folds of the scale factor, given by

$$N \equiv \ln\frac{a(t_{\rm end})}{a(t)} = \int_t^{t_{\rm end}} H\mathrm{d}t \approx \int_{\varphi_{\rm end}}^{\varphi} \frac{\mathrm{d}\varphi}{\sqrt{2\epsilon}} \ . \tag{6.13}$$

The end of inflation is often approximated to be at the end of slow-roll, i.e. when $\epsilon(\varphi_{\rm end}) = 1$ or $|\eta(\varphi_{\rm end})| = 1$ which ever happens first. The exact number of e-folds of inflation needed depends on the details of the model and length of the graceful exit from inflation to the hot primordial universe, i.e. (p)reheating [215–217]. A typical amount is of order 50 e-folds [218].

6.3 Inflationary observables

As stated earlier, inflation gives us a mechanism of generating primordial perturbations whose statistical properties can be computed in a given inflationary model and compared with observations. These perturbations are generated by quantum vacuum fluctuations, which get stretched to large scales and classicalised during inflation. With additional knowledge of the history of the universe we can evolve these initial perturbations to later times and compare them with observations.

We give here a high-level description on the analysis. For later it is also important to note that the perturbations in the metric formulation are equivalent with the perturbations in the Palatini formulation [219, 220].

We consider small perturbations around the FLRW metric and a homogeneous and isotropic inflaton field: $\varphi \to \bar{\varphi}(t) + \delta\varphi(t,x)$ and $g_{\alpha\beta} \to \bar{g}_{\alpha\beta} + \delta g_{\alpha\beta}(t,x)$. We denote the background quantities $\bar{\varphi}$, $\bar{g}_{\alpha\beta}$ with an overbar. Due to the diffeomorphism invariance in General Relativity the perturbations $\delta\varphi$ and $\delta g_{\alpha\beta}$ have gauge freedom. For introductory treatments to cosmological perturbation theory see e.g. [221, 222]. To get something physical from our computations we must fix a gauge or construct gauge invariant quantities.

To first order in perturbation theory parts transforming differently under spatial rotations, i.e. scalars, vectors and tensor modes, do not mix with one another. This is called the decomposition theorem [223, ch. 5]. We can thus consider separately each of the different sectors. It turns out that vector perturbations decay as $1/a^2$ and thus have vanishing effect on cosmology. For scalar perturbations an useful quantity is the Mukhanov-Sasaki variable $v(\eta, x)$ [224–226]. In spatial flat gauge it reads $v = a\delta\varphi$. The Einstein–Hilbert action (4.1) with the added scalar field (6.4) can be expanded to second order in the perturbations resulting into an action which in terms of v reads [227–229]

$$S^{(\rm s)}_{2^{\rm nd}} = \int {\rm d}\eta {\rm d}^3x \left[(\partial_\eta v)^2 - (\partial_i v)^2 + \frac{\partial^2_\eta z}{z} \right] , \tag{6.14}$$

where ${\rm d}\eta = {\rm d}t/a(t)$ is conformal time and $z^2 \equiv a^2\dot{\varphi}^2/H^2 = 2a^2\epsilon$. The Mukhanov-Sasaki variable is related to the curvature perturbation on uniform-density spatial

slices $\mathcal{R} = v/z$, which is gauge invariant.[23]

From the action we obtain the equations of motion for the Fourier modes of $v = v(k)$:

$$\partial_\eta^2 v + \left[k^2 - \frac{\partial_\eta^2 z}{z}\right] v = 0 \ , \tag{6.15}$$

where k is the comoving wave number. During slow-roll inflation spacetime is close to de Sitter space. We can choose the initial vacuum state to be the adiabatic Bunch-Davies vacuum $v_0(\eta, k) = i(aH)e^{-ik\eta}(1+ik\eta)/\sqrt{2k^3}$ [230, 231]. An important fact that allows inflationary scenarios to make predictions about the form of the perturbations is that the initially adiabatic perturbations of the scalar and tensor modes are conserved after the wave length becomes larger than the Hubble radius, i.e. $k < aH$ [223, 232, 233]. This is also where the quantum fluctuations decohere and make the fluctuations appear classical [234].

With the above ingredients one can compute the correlation functions of the perturbations describing their statistical properties. To first order the perturbations are Gaussian. The two point correlation function, i.e. the power spectrum, for the scalar curvature perturbations to first order in slow-roll is given by[24]

$$\mathcal{P}_\mathcal{R} = \left[\frac{1}{2\epsilon}\left(\frac{H}{2\pi}\right)^2\right]_{k=aH} = A_s \left(\frac{k}{k_*}\right)^{n_s - 1} \ . \tag{6.16}$$

The power spectrum is computed at Hubble horizon crossing $k = aH$, meaning at the point when the modes freeze-out. On the second line of (6.16) we have introduced the usual parametrization of the spectrum in a nearly scale invariant form, where A_s is the amplitude of the spectrum, n_s is the scalar spectrum tilt and k_* is some reference (pivot) scale. The spectrum is thus scale invariant if $n_s = 1$. Looking at the CMB the spectral tilt is observed to be slightly red tilted $n_s \simeq 0.9649$ [212]. In the slow-roll approximation

$$A_s \approx \frac{1}{24\pi^2}\frac{V}{\epsilon} \ , \tag{6.17}$$

$$n_s = 1 + \frac{\mathrm{d}\ln \mathcal{P}_\mathcal{R}}{\mathrm{d}\ln k} \approx 1 + 2\eta - 6\epsilon. \tag{6.18}$$

For tensor perturbations the analysis is analogous to what we described above. The spectrum for the tensor perturbations, i.e. for gravitational waves, to first order

[23] Another gauge invariant scalar often used in the literature is the curvature perturbation on uniform-density spatial slices ζ, which is equal to the comoving curvature perturbation $\mathcal{R}$ on super-horizon scales, i.e. for modes with comoving wave number much smaller than the inverse Hubble radius $k \ll aH$, see e.g. [223]. The two quantities $\mathcal{R}$ and ζ are also equal during slow-roll inflation.

[24] Beyond slow-roll approximation, analytical expressions can also be obtained, see e.g. [222, 235].

in slow-roll is

$$\mathcal{P}_t = \left[8\left(\frac{H}{2\pi}\right)^2\right]_{k=aH} . \tag{6.19}$$

The tensor modes have not been observed to date. An important quantity that current observations can put bounds on is the tensor-to-scalar ratio r, which in slow-roll is

$$r \equiv \frac{\mathcal{P}_t}{\mathcal{P}_\mathcal{R}} \approx 16\epsilon . \tag{6.20}$$

The current best bound is given by the efforts of Planck and BICEP/Keck collaborations: $r < 0.036$ at two sigma confidence [236]. How these parameters are related to the CMB observables measured is highly non-trivial task and thus we will not go into the details here, for introductory treatments see e.g. [211].

We have reviewed the generation of primordial perturbations and the predictions of important observables in single scalar field inflation with the Einstein–Hilbert action. We will be able to reuse this analysis on the next section when discussing higher order curvature modifications of gravity.

6.4 Effects of Higher order curvature on Inflation

As we saw in the chapter 5 many higher order curvature terms lead to possible theoretical problems. A theory that does not suffer from the previously discussed problems is one that depends only on the symmetric Ricci tensor $R_{(\alpha\beta)}$, which is also particularly simple since it does not lead to new degrees of freedom.

Next we will review our work on the effects of higher order $R_{(\alpha\beta)}$ terms on inflation.

6.4.1 Non-degenerate $R_{(\alpha\beta)}$ gravity theory

The quadratic case of non-degenerate $R_{(\alpha\beta)}$ gravity and its effects on inflation were first investigated in [237] and later expanded upon in [238].

In [3] we investigated how a general non-degenerate $R_{(\alpha\beta)}$ Palatini gravity theory affects single scalar field driven inflation. The action we consider reads

$$S = \int \mathrm{d}^4x\sqrt{-g}\left[\frac{1}{2}F(g_{\alpha\beta}, R_{(\alpha\beta)}, \varphi) - \frac{1}{2}g^{\alpha\beta}X_{\alpha\beta} - U(\varphi)\right] , \tag{6.21}$$

where $X_{\alpha\beta} \equiv \partial_\alpha\varphi\partial_\beta\varphi$ and we emphasise that non-minimal couplings between gravity and the scalar field are allowed. However, we do not allow derivative couplings between the scalar and $R_{(\alpha\beta)}$, for example $\partial^\alpha\varphi\partial^\beta\varphi R_{(\alpha\beta)}$ is excluded. (For derivative couplings to Ricci-type tensors in Palatini formulation see [239].)

We use the same Legendre transform approach, as described in section 5.1.1. Using a Legendre transformation we bring the action in a form linear in the Riemann tensor and then introduce a field redefinition to bring the action into an Einstein frame. With this procedure the action becomes

$$S = \int \mathrm{d}^4x\sqrt{-q}\frac{1}{2}\Big\{q^{\alpha\beta}R_{(\alpha\beta)} \\ - q^{\alpha\beta}\Sigma_{\alpha\beta}(g_{\alpha\beta},\varphi) + \frac{\sqrt{-g}}{\sqrt{-q}}\left[F(g_{\alpha\beta},\Sigma_{\alpha\beta},\varphi) - g^{\alpha\beta}X_{\alpha\beta} - 2U(\varphi)\right]\Big\}\ , \quad (6.22)$$

with the field redefinition $\sqrt{-g}\partial F/\partial\Sigma_{\alpha\beta} = \sqrt{-q}q^{\alpha\beta}$. We again have the restriction on the form of F that it has to be non-degenerate, meaning that $\partial^2 F/(\partial\Sigma_{\alpha\beta}\partial\Sigma_{\gamma\delta})$ has to be invertible for the Legendre transformed action (6.22) and the original action (6.21) to be equivalent.

In the previous section when we investigated the degrees of freedom, we were not concerned by the form of the potential terms in the action. As we saw in section 6.3, single scalar field inflation observables can be computed solely from the potential of the scalar field. So, here we are interested in the potential terms. Thus, we have to explicitly solve $q_{\alpha\beta}$ and $\Sigma_{\alpha\beta}$ in terms of $g_{\alpha\beta}$ and φ.

The original metric $g_{\alpha\beta}$ and the Einstein frame metric $q_{\alpha\beta}$ turn out to be related by a disformal transformation. To solve $q_{\alpha\beta}$ and $\Sigma_{\alpha\beta}$ in terms of $g_{\alpha\beta}$ and φ we introduce an ansatz for the disformal transformation

$$g_{\alpha\beta} = \gamma_1(\varphi, X_q)q_{\alpha\beta} + \gamma_2(\varphi, X_q)X_{\alpha\beta}\ , \quad (6.23)$$

where $X_q \equiv q^{\alpha\beta}X_{\alpha\beta}$. The functions γ_1 and γ_2 have to satisfy the following requirements for the disformal transformation to map between two pseudo-Riemannian manifolds that are physically equivalent [240–248]:

$$\gamma_1 > 0, \quad \gamma_2 \geq 0, \quad \gamma_1 + X_q\gamma_2 > 0, \\ \gamma_1\left(\gamma_1 - X_q\frac{\partial\gamma_1}{\partial X_q} - X_q^2\frac{\partial\gamma_2}{\partial X_q}\right) \neq 0\ . \quad (6.24)$$

These come from the requirements that: the transformation is invertible, the metric $q_{\alpha\beta}$ has Lorentzian signature and causal trajectories map to causal trajectories. Using (6.23) and introducing the ansatz $\Sigma_{\alpha\beta} = C(\varphi, X_q)q_{\alpha\beta} + D(\varphi, X_q)X_{\alpha\beta}$ we can substitute them to the action and find algebraic equations for γ_1, γ_2 and the ansatz coefficients C and D. Finding exact solutions for these equations is difficult. However, we can solve them approximately in the limit of small X_q. The kinetic term X_q is required to be small for the classical theory to be applicable. Furthermore, during slow-roll inflation in the long wavelength limit the kinetic term is further suppressed.

Solving $q_{\alpha\beta}$ and $\Sigma_{\alpha\beta}$ perturbatively to first order in X_q the action can be written in a simple form

$$S = \int \mathrm{d}^4x\sqrt{-q}\left[\frac{1}{2}q^{\alpha\beta}R_{(\alpha\beta)} - \frac{4\sigma_0(U,\varphi)}{F_{,\sigma}(\sigma_0,\varphi)} - \frac{2}{F_{,\sigma}(\sigma_0,\varphi)}X_q + \mathcal{O}(X_q^2)\right] , \qquad (6.25)$$

where the function F to first order in X_q is $F(g^{\alpha\beta},\Sigma_{\alpha\beta},\varphi) = F(\sigma,\varphi) + \mathcal{O}(X_q^2)$. Here $\sigma \equiv \sigma_0(\varphi)+\sigma_1(\varphi)X_q$, where σ_0 and σ_1 are functions of the series expansion coefficients for small X_q of γ_1, γ_2, C and D. To first order the requirements (6.24) simplify to $F_{,\sigma}(\sigma_0) > 0$. Finally, the auxiliary field σ_0 is to be solved from the algebraic equation

$$2F(\sigma_0,\varphi) - \sigma_0 F_{,\sigma}(\sigma_0,\varphi) = 4U(\varphi) \ . \qquad (6.26)$$

The action is now in a simple Einstein frame form with all the effects of the modified gravity sector transformed into the matter sector. We can now find how the inflationary observables change due to the modified gravity by simply looking at the modified scalar potential in the Einstein frame.

To do this we can bring the scalars kinetic term to canonical form with a field redefinition $\mathrm{d}\chi/\mathrm{d}\varphi = \pm\sqrt{F_{,\sigma}(\sigma_0)}/2$. Now to first order in slow-roll the observables n_s (6.18) and r (6.20) are simple functions of the two first slow-roll parameters ϵ (6.11) and η (6.12). The computation boils down to just taking derivatives of the effective potential $U(\chi) = 4\sigma_0/F_{,\sigma}$ with respect to the canonicalized scalar field χ.

In general both the scalar spectrum tilt n_s and the tensor-to-scalar ratio r change. The lengthy expressions for the change of these observables can be found in [3]. Let us describe a few applications of the general result by choosing the form of the function F.

Quadratic action: In Palatini formulation the quadratic action $R + \alpha R^2$ was first analysed in the framework of inflation in [237]. This was then extended to $R+\alpha R^2+\beta R_{(\alpha\beta)}R^{(\alpha\beta)}$ in [238].

With the above simple form for the general action (6.25) we can easily analyse this case. We take the functional dependence to be

$$F(g_{\alpha\beta}, R_{(\alpha\beta)}, \varphi) = R + \alpha R^2 + \beta R_{(\alpha\beta)}R^{(\alpha\beta)} \ . \qquad (6.27)$$

Leaving out the non-minimal coupling of the scalar to the Ricci tensor does not lead to loss of generality. This is because the non-minimal coupling $f(\varphi)R$ can be removed via a conformal transformation $g_{\alpha\beta} \to f^{-1}(\varphi)g_{\alpha\beta}$, which just leads to redefinitions of φ and U.

Now the quadratic action to first order in X_q becomes simply

$$F(\sigma) = 4\sigma + 4(4\alpha + \beta)\sigma^2 \ . \tag{6.28}$$

From (6.26) we find $\sigma_0 = U$ and the requirements (6.24) reduces to $U > 0$ and $4\alpha + \beta > 0$. The effective potential then reads

$$\widetilde{U}(\chi) \equiv \frac{U[\varphi(\chi)]}{1 + 2(4\alpha + \beta)U[\varphi(\chi)]} \ , \tag{6.29}$$

which leads to the first slow-roll parameter becoming

$$\tilde{\epsilon} \equiv \frac{1}{2}\left(\frac{\widetilde{U}_{,\chi}}{\widetilde{U}}\right)^2 = \frac{\epsilon}{1 + 2(4\alpha + \beta)U} \ , \tag{6.30}$$

where $\epsilon = \frac{1}{2}\left(\frac{U_{,\varphi}}{U}\right)^2$.

From these we see that since the potential $\widetilde{U}$ and the first slow-roll parameter $\tilde{\epsilon}$ are suppressed by the same factor, the scalar spectrum (6.17) is left unchanged $\widetilde{U}/\tilde{\epsilon} = U/\epsilon$. From (6.13) we also see that the number of e-folds is unaffected to first order. Looking at the tensor spectrum (6.19), however, we see that it does change. We see that it is supressed by the factor $1 + 2(4\alpha + \beta)U$.

To summarize: the effect of quadratic terms in $R_{(\alpha\beta)}$ has the effect of keeping the scalar spectrum (A_s, n_s) unchanged to first order, while the tensor spectum and thus the tensor-to-scalar ratio r can be suppressed without limit.

Cubic action: We also investigated an action cubic in $R_{(\alpha\beta)}$. Taking the functional dependence to be

$$F(g^{\alpha\beta}, R_{(\alpha\beta)}, \varphi) = R + \kappa_1 R^3 + \kappa_2 R R_{(\alpha\beta)} R^{(\alpha\beta)} + \kappa_3 g^{\alpha\gamma} g^{\beta\mu} g^{\delta\nu} R_{(\alpha\beta)} R_{(\gamma\delta)} R_{(\mu\nu)} \ . \tag{6.31}$$

Here for simplicity we take κ_i to be constants which excludes non-minimal couplings of the scalar. Again writing the function to first order in X_q we have $F(\sigma) = 4\sigma + 4\kappa\sigma^3$ where $\kappa \equiv 16\kappa_1 + 4\kappa_2 + \kappa_3$. The conditions (6.24) now reduce to $\kappa > 0$.

Now from (6.26) we get an cubic equation for σ_0: $\kappa\sigma_0^3 - \sigma_0 + U = 0$. This has three different branches of solutions. One of the branches does not have a sensible $\kappa \to 0$ limit and one of them leads to an effective potential not bounded from below. Here we choose to analyse the least problematic case where $\kappa > 0$ and $4/\kappa - 27U^2 > 0$, which leads to the bound for the potential $-3/(3\sqrt{3\kappa}) < U < 3/(3\sqrt{3\kappa})$.

With these assumptions one can solve σ_0 from the third order equation and

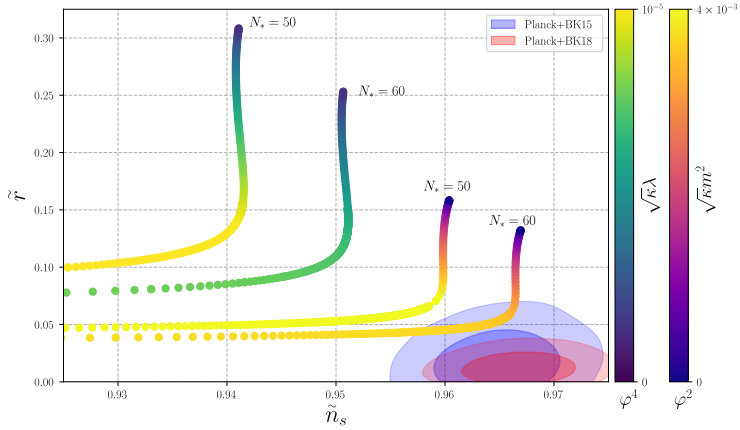

Figure 6.1. The spectral tilt against the tensor-to-scalar ratio. The changes of inflationary observables due to cubic $R_{(\alpha\beta)}$ terms. The two leftmost curves correspond to the potential $U = \lambda\varphi^4/4$ with 50 and 60 e-folds and varying coupling $\sqrt{\kappa}\lambda$. The two rightmost curves correspond to the potential $U = m^2\varphi^2/2$. Figure from [3], here we have added the most recent BICEP/Keck (BK18) confidence contours [236].

find the form of the effective potential. After which we can obtain the inflationary observables. For this branch we found that: r can again be suppressed but at most a factor of 2/9 due to the bound put on the potential in this branch. Furthermore, the scalar spectrum changes and in particular n_s can decrease without limit.

To illustrate these further we picked two forms for the potential $U = \frac{\lambda}{4}\varphi^2$ and $U = \frac{m^2}{2}\varphi^2$. Due to the assumed bound on the potential given in this branch these two choices for the potentials cannot be global, however, we can use them as approximating the full potential valid after some field amplitude.

We computed numerically the relations between the number of e-folds and the field value and evaluated the observables for different values of the couplings. The couplings turn out to appear only in the combinations $\sqrt{\kappa}\lambda$ for quadratic and $\sqrt{\kappa}m^2$ for quartic potential. The results are shown in figure 6.1 where we used two different values for the number of e-folds $N = 50, 60$ and varied the couplings.

We can see that by increasing the size of the coupling the tensor-to-scalar ratio starts to get suppressed, however, increasing it further the tensor spectrums suppression starts to get closer to the maximum suppression 2/9 which is where the scalar tilt n_s starts to get more and more red tilted without bound. At the time of working on [3] the best bound on r was $r < 0.067$ and with $N = 60$ e-folds the quartic potential could be just pushed below the observational bound (blue contour in the figure 6.1). Now adding the most recent bound $r < 0.036$ (the red contour in figure 6.1) it also falls outside the bound.

Chapter 7

Conclusions

In this thesis we have investigated possible phenomena taking place in the very early universe both in the matter and gravitational sectors. The future prospects of gaining a better understanding of the fundamental laws governing our universe from cosmological observations are exciting. There are many planned new experiments that require us to get a better theoretical understanding of possible signals we could detect.

In the first part of this thesis we focused on the sphaleron processes that are able to change the baryon number in the Standard Model. Getting a good understanding of the baryon number violation or sphaleron rate is important for possible explanations of the observed matter-antimatter asymmetry. We reviewed the results found in [1] and showed that having strong magnetic fields around the phase transition can change the details of the suppression of the rate considerably. Furthermore, in the broken phase for small magnetic fields the sphaleron dipole moment is the dominant effect giving rise to the sphaleron rate being suppressed slightly less. With bigger magnetic fields the dominant effect is the shifting of the pseudocritical temperature to lower temperatures, e.g. having a magnetic field $B_Y \simeq 2.0T^2$ shifts the pseudocritical temperature from 160 GeV down to 145 GeV. Thus, the start of the exponential suppression of the sphaleron rate shifts to lower temperatures accordingly.

In the second part of the thesis we investigated the stability of higher order curvature terms in Palatini formulation of General Relativity. We studied a theory that depends on the connection only through the first contractions of the Riemann tensor, the Ricci type tensors. We reviewed the perturbative stability of the different terms that we investigated in [2], which can be most concisely seen in the table 5.1. The question of which is the most general higher order Palatini theory that does not lead to instabilities remains open.

We then reviewed how higher order terms in the symmetric Ricci tensor affect the inflationary predictions that we studied in [3]. A valuable result is the quite simple form of the action found for a single scalar field driven inflation in slow-roll with quite general form of the action containing higher order symmetric Ricci tensor terms. We also reviewed the quadratic and cubic actions in $R_{(\alpha\beta)}$ as examples.

Bibliography

[1] J. Annala and K. Rummukainen, *Electroweak sphaleron in a magnetic field*, *Phys. Rev. D* **107** (2023) 073006, [2301.08626].

[2] J. Annala and S. Rasanen, *Stability of non-degenerate Ricci-type Palatini theories*, *JCAP* **04** (2023) 014, [2212.09820].

[3] J. Annala and S. Räsänen, *Inflation with R ($\alpha\beta$) terms in the Palatini formulation*, *JCAP* **09** (2021) 032, [2106.12422].

[4] ATLAS collaboration, G. Aad et al., *Observation of a new particle in the search for the Standard Model Higgs boson with the ATLAS detector at the LHC*, *Phys. Lett. B* **716** (2012) 1–29, [1207.7214].

[5] CMS collaboration, S. Chatrchyan et al., *Observation of a New Boson at a Mass of 125 GeV with the CMS Experiment at the LHC*, *Phys. Lett. B* **716** (2012) 30–61, [1207.7235].

[6] LIGO Scientific, Virgo collaboration, B. P. Abbott et al., *Observation of Gravitational Waves from a Binary Black Hole Merger*, *Phys. Rev. Lett.* **116** (2016) 061102, [1602.03837].

[7] S. Kawamura et al., *The Japanese space gravitational wave antenna DECIGO*, *Class. Quant. Grav.* **23** (2006) S125–S132.

[8] G. M. Harry, P. Fritschel, D. A. Shaddock, W. Folkner and E. S. Phinney, *Laser interferometry for the big bang observer*, *Class. Quant. Grav.* **23** (2006) 4887–4894.

[9] W.-H. Ruan, Z.-K. Guo, R.-G. Cai and Y.-Z. Zhang, *Taiji program: Gravitational-wave sources*, *Int. J. Mod. Phys. A* **35** (2020) 2050075, [1807.09495].

[10] C. Caprini et al., *Detecting gravitational waves from cosmological phase transitions with LISA: an update*, *JCAP* **03** (2020) 024, [1910.13125].

[11] K. Subramanian, *The origin, evolution and signatures of primordial magnetic fields*, *Rept. Prog. Phys.* **79** (2016) 076901, [1504.02311].

[12] T. Vachaspati, *Progress on cosmological magnetic fields*, *Rept. Prog. Phys.* **84** (2021) 074901, [2010.10525].

[13] D. Grasso and H. R. Rubinstein, *Magnetic fields in the early universe*, *Phys. Rept.* **348** (2001) 163–266, [astro-ph/0009061].

[14] J. D. Barrow and C. G. Tsagas, *Cosmological magnetic field survival*, *Mon. Not. Roy. Astron. Soc.* **414** (2011) 512, [1101.2390].

[15] K. Kamada, F. Uchida and J. Yokoyama, *Baryon isocurvature constraints on the primordial hypermagnetic fields*, *JCAP* **04** (2021) 034, [2012.14435].

[16] M. Giovannini and M. E. Shaposhnikov, *Primordial hypermagnetic fields and triangle anomaly*, *Phys. Rev. D* **57** (1998) 2186–2206, [hep-ph/9710234].

[17] M. Joyce and M. E. Shaposhnikov, *Primordial magnetic fields, right-handed electrons, and the Abelian anomaly*, *Phys. Rev. Lett.* **79** (1997) 1193–1196, [astro-ph/9703005].

[18] D. G. Figueroa and M. Shaposhnikov, *Anomalous non-conservation of fermion/chiral number in Abelian gauge theories at finite temperature*, *JHEP* **04** (2018) 026, [1707.09967].

[19] D. G. Figueroa, A. Florio and M. Shaposhnikov, *Chiral charge dynamics in Abelian gauge theories at finite temperature*, *JHEP* **10** (2019) 142, [1904.11892].

[20] K. Kamada and A. J. Long, *Baryogenesis from decaying magnetic helicity*, *Phys. Rev. D* **94** (2016) 063501, [1606.08891].

[21] K. Kamada and A. J. Long, *Evolution of the Baryon Asymmetry through the Electroweak Crossover in the Presence of a Helical Magnetic Field*, *Phys. Rev. D* **94** (2016) 123509, [1610.03074].

[22] K. Kamada, *Return of grand unified theory baryogenesis: Source of helical hypermagnetic fields for the baryon asymmetry of the universe*, *Phys. Rev. D* **97** (2018) 103506, [1802.03055].

[23] K. Kajantie, M. Laine, J. Peisa, K. Rummukainen and M. E. Shaposhnikov, *The Electroweak phase transition in a magnetic field*, *Nucl. Phys. B* **544** (1999) 357–373, [hep-lat/9809004].

[24] S. Capozziello and M. De Laurentis, *Extended Theories of Gravity*, *Phys. Rept.* **509** (2011) 167–321, [1108.6266].

[25] T. Clifton, P. G. Ferreira, A. Padilla and C. Skordis, *Modified Gravity and Cosmology*, *Phys. Rept.* **513** (2012) 1–189, [1106.2476].

[26] CANTATA collaboration, Y. Akrami et al., *Modified Gravity and Cosmology. An Update by the CANTATA Network*. Springer, 2021, 10.1007/978-3-030-83715-0.

[27] F. L. Bezrukov and M. Shaposhnikov, *The Standard Model Higgs boson as the inflaton*, *Phys. Lett. B* **659** (2008) 703–706, [0710.3755].

[28] J. Rubio, *Higgs inflation*, *Front. Astron. Space Sci.* **5** (2019) 50, [1807.02376].

[29] S. Bahamonde, K. F. Dialektopoulos, C. Escamilla-Rivera, G. Farrugia, V. Gakis, M. Hendry et al., *Teleparallel gravity: from theory to cosmology*, *Rept. Prog. Phys.* **86** (2023) 026901, [2106.13793].

[30] F. Bauer and D. A. Demir, *Inflation with Non-Minimal Coupling: Metric versus Palatini Formulations*, *Phys. Lett. B* **665** (2008) 222–226, [0803.2664].

[31] D. Lovelock, *The uniqueness of the einstein field equations in a four-dimensional space*, *Archive for Rational Mechanics and Analysis* **33** (Jan, 1969) 54–70.

[32] T. P. Sotiriou and V. Faraoni, *f(R) Theories Of Gravity*, *Rev. Mod. Phys.* **82** (2010) 451–497, [0805.1726].

[33] T. Kobayashi, *Horndeski theory and beyond: a review*, *Rept. Prog. Phys.* **82** (2019) 086901, [1901.07183].

[34] S. Elitzur, *Impossibility of spontaneously breaking local symmetries*, *Phys. Rev. D* **12** (Dec, 1975) 3978–3982.

[35] T. T. Wu and C. N. Yang, *Concept of nonintegrable phase factors and global formulation of gauge fields*, *Phys. Rev. D* **12** (Dec, 1975) 3845–3857.

[36] M. Nakahara, *Geometry, topology and physics*. 2003.

[37] G. Naber, *Topology, Geometry and Gauge fields: Foundations*. Texts in Applied Mathematics. Springer New York, 2010.

[38] F. Strocchi, *Symmetry Breaking in the Standard Model: A Non-Perturbative Outlook*. Publications of the Scuola Normale Superiore. Scuola Normale Superiore, 2019.

[39] H. Gomes and A. Riello, *Large gauge transformations, gauge invariance, and the QCD θ_{YM}-term*, 2007.04013.

[40] S. Coleman, *Aspects of Symmetry: Selected Erice Lectures*. Cambridge University Press, Cambridge, U.K., 1985, 10.1017/CBO9780511565045.

[41] A. Hatcher, *Algebraic Topology*. Algebraic Topology. Cambridge University Press, 2002.

[42] A. Belavin, A. Polyakov, A. Schwartz and Y. Tyupkin, *Pseudoparticle solutions of the yang-mills equations*, *Physics Letters B* **59** (1975) 85–87.

[43] N. S. Manton and P. Sutcliffe, *Topological solitons*. Cambridge Monographs on Mathematical Physics. Cambridge University Press, 2004, 10.1017/CBO9780511617034.

[44] A. Maas, *Brout-Englert-Higgs physics: From foundations to phenomenology*, *Prog. Part. Nucl. Phys.* **106** (2019) 132–209, [1712.04721].

[45] M. D. Schwartz, *Quantum Field Theory and the Standard Model*. Cambridge University Press, 3, 2014.

[46] D. Tong, *Lectures on the standard model, chapter 2.*, *https://www.damtp.cam.ac.uk/user/tong/standardmodel.html* (2019) .

[47] K. Kajantie, M. Laine, K. Rummukainen and M. E. Shaposhnikov, *Is there a hot electroweak phase transition at $m_H \gtrsim m_W$?*, *Phys. Rev. Lett.* **77** (1996) 2887–2890, [hep-ph/9605288].

[48] Y. Aoki, *Four-dimensional simulation of the hot electroweak phase transition with the SU(2) gauge Higgs model*, *Phys. Rev. D* **56** (1997) 3860–3865, [hep-lat/9612023].

[49] M. Gurtler, E.-M. Ilgenfritz and A. Schiller, *Where the electroweak phase transition ends*, *Phys. Rev. D* **56** (1997) 3888–3895, [hep-lat/9704013].

[50] F. Csikor, Z. Fodor and J. Heitger, *Endpoint of the hot electroweak phase transition*, *Phys. Rev. Lett.* **82** (1999) 21–24, [hep-ph/9809291].

[51] K. Rummukainen, M. Tsypin, K. Kajantie, M. Laine and M. E. Shaposhnikov, *The Universality class of the electroweak theory*, *Nucl. Phys. B* **532** (1998) 283–314, [hep-lat/9805013].

[52] M. D'Onofrio and K. Rummukainen, *Standard model cross-over on the lattice*, *Phys. Rev. D* **93** (2016) 025003, [1508.07161].

[53] F. R. Klinkhamer and N. S. Manton, *A Saddle Point Solution in the Weinberg-Salam Theory*, *Phys. Rev. D* **30** (1984) 2212.

[54] R. F. Dashen, B. Hasslacher and A. Neveu, *Nonperturbative methods and extended-hadron models in field theory. iii. four-dimensional non-abelian models*, *Phys. Rev. D* **10** (Dec, 1974) 4138–4142.

[55] N. S. Manton, *Topology in the Weinberg-Salam Theory*, *Phys. Rev. D* **28** (1983) 2019.

[56] V. Rubakov and S. S. Wilson, *Classical Theory of Gauge Fields*. Princeton University Press, 2002.

[57] C. W. Bernard and E. J. Weinberg, *The Interpretation of Pseudoparticles in Physical Gauges*, *Phys. Rev. D* **15** (1977) 3656.

[58] R. Jackiw, *Introduction to the Yang-Mills Quantum Theory*, *Rev. Mod. Phys.* **52** (1980) 661–673.

[59] G. G. van Marion, *Sphalerons and the vacuum structure of gauge theories*, *Master's Thesis, University of Groningen,* *https://fse.studenttheses.ub.rug.nl/id/eprint/22678* (July, 2020) .

[60] B. Kleihaus, J. Kunz and Y. Brihaye, *The Electroweak sphaleron at physical mixing angle*, *Phys. Lett. B* **273** (1991) 100–104.

[61] J. Kunz, B. Kleihaus and Y. Brihaye, *Sphalerons at finite mixing angle*, *Phys. Rev. D* **46** (1992) 3587–3600.

[62] F. R. Klinkhamer and R. Laterveer, *The Sphaleron at finite mixing angle*, *Z. Phys. C* **53** (1992) 247–252.

[63] S. H. H. Tye and S. S. C. Wong, *Bloch Wave Function for the Periodic Sphaleron Potential and Unsuppressed Baryon and Lepton Number Violating Processes*, *Phys. Rev. D* **92** (2015) 045005, [1505.03690].

[64] J. Kunz and Y. Brihaye, *New Sphalerons in the Weinberg-Salam Theory*, *Phys. Lett. B* **216** (1989) 353–359.

[65] L. G. Yaffe, *Static Solutions of SU(2) Higgs Theory*, *Phys. Rev. D* **40** (1989) 3463.

[66] S. Skadhauge, *Sphalerons and electroweak baryogenesis*, Ph.D. thesis, Copenhagen U., 1996.

[67] M. Hindmarsh and M. James, *The Origin of the sphaleron dipole moment*, *Phys. Rev. D* **49** (1994) 6109–6114, [hep-ph/9307205].

[68] D. Comelli, D. Grasso, M. Pietroni and A. Riotto, *The Sphaleron in a magnetic field and electroweak baryogenesis*, *Phys. Lett. B* **458** (1999) 304–309, [hep-ph/9903227].

[69] D. L. J. Ho and A. Rajantie, *Electroweak sphaleron in a strong magnetic field*, *Phys. Rev. D* **102** (2020) 053002, [2005.03125].

[70] J. Ambjorn and P. Olesen, *Antiscreening of Large Magnetic Fields by Vector Bosons*, *Phys. Lett. B* **214** (1988) 565–569.

[71] J. Ambjorn and P. Olesen, *A Condensate Solution of the Electroweak Theory Which Interpolates Between the Broken and the Symmetric Phase*, *Nucl. Phys. B* **330** (1990) 193–204.

[72] M. N. Chernodub, V. A. Goy and A. V. Molochkov, *Phase Structure of Electroweak Vacuum in a Strong Magnetic Field: The Lattice Results*, *Phys. Rev. Lett.* **130** (2023) 111802, [2206.14008].

[73] K. Fujikawa, *Path-integral measure for gauge-invariant fermion theories*, *Phys. Rev. Lett.* **42** (Apr, 1979) 1195–1198.

[74] S. L. Adler, *Axial-vector vertex in spinor electrodynamics*, *Phys. Rev.* **177** (Jan, 1969) 2426–2438.

[75] J. S. Bell and R. Jackiw, *A PCAC puzzle: $\pi 0 \to \gamma\gamma$ in the σ-model*, *Nuovo Cimento A Serie* **60** (Mar., 1969) 47–61.

[76] D. Tong, *Lectures on gauge theory, chapter 3.*, *https://www.damtp.cam.ac.uk/user/tong/gaugetheory.html* (2018) .

[77] G. 't Hooft, *Symmetry Breaking Through Bell-Jackiw Anomalies*, *Phys. Rev. Lett.* **37** (1976) 8–11.

[78] A. Ringwald, *Sphaleron and Level Crossing*, *Phys. Lett. B* **213** (1988) 61–63.

[79] A. A. Anselm and A. A. Johansen, *Can electroweak theta term be observable?*, *Nucl. Phys. B* **412** (1994) 553–573, [hep-ph/9305271].

[80] M. Axenides, A. Johansen and H. B. Nielsen, *The Level crossing phenomenon with Yukawa interactions*, *Nucl. Phys. B* **414** (1994) 53–72, [hep-ph/9308299].

[81] G. 't Hooft, *Computation of the Quantum Effects Due to a Four-Dimensional Pseudoparticle*, *Phys. Rev. D* **14** (1976) 3432–3450.

[82] I. Affleck, *On Constrained Instantons*, *Nucl. Phys. B* **191** (1981) 429.

[83] P. B. Arnold and L. D. McLerran, *The Sphaleron Strikes Back*, *Phys. Rev. D* **37** (1988) 1020.

[84] V. A. Rubakov and M. E. Shaposhnikov, *Electroweak baryon number nonconservation in the early universe and in high-energy collisions*, *Usp. Fiz. Nauk* **166** (1996) 493–537, [hep-ph/9603208].

[85] M. Nielsen and N. K. Nielsen, *Explicit construction of constrained instantons*, *Phys. Rev. D* **61** (2000) 105020, [hep-th/9912006].

[86] V. A. Kuzmin, V. A. Rubakov and M. E. Shaposhnikov, *On the Anomalous Electroweak Baryon Number Nonconservation in the Early Universe*, *Phys. Lett. B* **155** (1985) 36.

[87] G. D. Moore, *Measuring the broken phase sphaleron rate nonperturbatively*, *Phys. Rev. D* **59** (1999) 014503, [hep-ph/9805264].

[88] P. B. Arnold, D. Son and L. G. Yaffe, *The Hot baryon violation rate is O (alpha-w**5 T**4)*, *Phys. Rev. D* **55** (1997) 6264–6273, [hep-ph/9609481].

[89] D. Bodeker, *On the effective dynamics of soft nonAbelian gauge fields at finite temperature*, *Phys. Lett. B* **426** (1998) 351–360, [hep-ph/9801430].

[90] P. B. Arnold, D. T. Son and L. G. Yaffe, *Effective dynamics of hot, soft nonAbelian gauge fields. Color conductivity and log(1/alpha) effects*, *Phys. Rev. D* **59** (1999) 105020, [hep-ph/9810216].

[91] G. D. Moore, *The Sphaleron rate: Bodeker's leading log*, *Nucl. Phys. B* **568** (2000) 367–404, [hep-ph/9810313].

[92] G. D. Moore and K. Rummukainen, *Classical sphaleron rate on fine lattices*, *Phys. Rev. D* **61** (2000) 105008, [hep-ph/9906259].

[93] D. Bodeker, G. D. Moore and K. Rummukainen, *Chern-Simons number diffusion and hard thermal loops on the lattice*, *Phys. Rev. D* **61** (2000) 056003, [hep-ph/9907545].

[94] S. Y. Khlebnikov and M. E. Shaposhnikov, *The Statistical Theory of Anomalous Fermion Number Nonconservation*, *Nucl. Phys. B* **308** (1988) 885–912.

[95] D. Bodeker, L. D. McLerran and A. V. Smilga, *Really computing nonperturbative real time correlation functions*, *Phys. Rev. D* **52** (1995) 4675–4690, [hep-th/9504123].

[96] M. D'Onofrio, K. Rummukainen and A. Tranberg, *Sphaleron Rate in the Minimal Standard Model*, *Phys. Rev. Lett.* **113** (2014) 141602, [1404.3565].

[97] L. Canetti, M. Drewes and M. Shaposhnikov, *Matter and Antimatter in the Universe*, *New J. Phys.* **14** (2012) 095012, [1204.4186].

[98] Planck collaboration, N. Aghanim et al., *Planck 2018 results. VI. Cosmological parameters*, *Astron. Astrophys.* **641** (2020) A6, [1807.06209].

[99] B. D. Fields, K. A. Olive, T.-H. Yeh and C. Young, *Big-Bang Nucleosynthesis after Planck*, *JCAP* **03** (2020) 010, [1912.01132].

[100] H. Kurki-Suonio, *Cosmology I*, *https://www.mv.helsinki.fi/home/hkurkisu/cosmology/* (2024) .

[101] A. D. Sakharov, *Violation of CP Invariance, C asymmetry, and baryon asymmetry of the universe*, *Pisma Zh. Eksp. Teor. Fiz.* **5** (1967) 32–35.

[102] D. Bodeker and W. Buchmuller, *Baryogenesis from the weak scale to the grand unification scale*, *Rev. Mod. Phys.* **93** (2021) 035004, [2009.07294].

[103] M. B. Gavela, P. Hernandez, J. Orloff, O. Pene and C. Quimbay, *Standard model CP violation and baryon asymmetry. Part 2: Finite temperature*, *Nucl. Phys. B* **430** (1994) 382–426, [hep-ph/9406289].

[104] P. Huet and E. Sather, *Electroweak baryogenesis and standard model CP violation*, *Phys. Rev. D* **51** (1995) 379–394, [hep-ph/9404302].

[105] T. Brauner, O. Taanila, A. Tranberg and A. Vuorinen, *Computing the temperature dependence of effective CP violation in the standard model*, *JHEP* **11** (2012) 076, [1208.5609].

[106] Y. Burnier, M. Laine and M. Shaposhnikov, *Baryon and lepton number violation rates across the electroweak crossover*, *JCAP* **02** (2006) 007, [hep-ph/0511246].

[107] M. Laine and A. Vuorinen, *Basics of Thermal Field Theory*, vol. 925. Springer, 2016, 10.1007/978-3-319-31933-9.

[108] A. Linde, *Infrared problem in the thermodynamics of the yang-mills gas*, *Physics Letters B* **96** (1980) 289–292.

[109] D. J. Gross, R. D. Pisarski and L. G. Yaffe, *Qcd and instantons at finite temperature*, *Rev. Mod. Phys.* **53** (Jan, 1981) 43–80.

[110] A. Ekstedt, P. Schicho and T. V. I. Tenkanen, *DRalgo: A package for effective field theory approach for thermal phase transitions*, *Comput. Phys. Commun.* **288** (2023) 108725, [2205.08815].

[111] K. Farakos, K. Kajantie, K. Rummukainen and M. E. Shaposhnikov, *3-d physics and the electroweak phase transition: A Framework for lattice Monte Carlo analysis*, *Nucl. Phys. B* **442** (1995) 317–363, [hep-lat/9412091].

[112] K. Farakos, K. Kajantie, K. Rummukainen and M. E. Shaposhnikov, *3-D physics and the electroweak phase transition: Perturbation theory*, *Nucl. Phys. B* **425** (1994) 67–109, [hep-ph/9404201].

[113] K. Kajantie, M. Laine, K. Rummukainen and M. E. Shaposhnikov, *Generic rules for high temperature dimensional reduction and their application to the standard model*, *Nucl. Phys. B* **458** (1996) 90–136, [hep-ph/9508379].

[114] M. Laine, M. Meyer and G. Nardini, *Thermal phase transition with full 2-loop effective potential*, *Nucl. Phys. B* **920** (2017) 565–600, [1702.07479].

[115] D. Croon, O. Gould, P. Schicho, T. V. I. Tenkanen and G. White, *Theoretical uncertainties for cosmological first-order phase transitions*, *JHEP* **04** (2021) 055, [2009.10080].

[116] O. Gould, S. Güyer and K. Rummukainen, *First-order electroweak phase transitions: A nonperturbative update*, *Phys. Rev. D* **106** (2022) 114507, [2205.07238].

[117] K. Kajantie, K. Rummukainen and M. E. Shaposhnikov, *A Lattice Monte Carlo study of the hot electroweak phase transition*, *Nucl. Phys. B* **407** (1993) 356–372, [hep-ph/9305345].

[118] A. Jakovac, K. Kajantie and A. Patkos, *A Hierarchy of effective field theories of hot electroweak matter*, *Phys. Rev. D* **49** (1994) 6810–6821, [hep-ph/9312355].

[119] M. Laine, *The Renormalized gauge coupling and nonperturbative tests of dimensional reduction*, *JHEP* **06** (1999) 020, [hep-ph/9903513].

[120] F. Bernardo, P. Klose, P. Schicho and T. V. I. Tenkanen, *Higher-dimensional operators at finite-temperature affect gravitational-wave predictions*, 2503.18904.

[121] W.-H. Tang and J. Smit, *Chern-Simons diffusion rate near the electroweak phase transition for m(H) approximates m(W)*, *Nucl. Phys. B* **482** (1996) 265–285, [hep-lat/9605016].

[122] J. Ambjorn and A. Krasnitz, *Improved determination of the classical sphaleron transition rate*, *Nucl. Phys. B* **506** (1997) 387–403, [hep-ph/9705380].

[123] C. R. Hu and B. Muller, *Classical lattice gauge field with hard thermal loops*, *Phys. Lett. B* **409** (1997) 377–381, [hep-ph/9611292].

[124] G. D. Moore, C.-r. Hu and B. Muller, *Chern-Simons number diffusion with hard thermal loops*, *Phys. Rev. D* **58** (1998) 045001, [hep-ph/9710436].

[125] G. D. Moore, *Sphaleron rate in the symmetric electroweak phase*, *Phys. Rev. D* **62** (2000) 085011, [hep-ph/0001216].

[126] G. D. Moore and K. Rummukainen, *Electroweak bubble nucleation, nonperturbatively*, *Phys. Rev. D* **63** (2001) 045002, [hep-ph/0009132].

[127] D. Bodeker, *From hard thermal loops to Langevin dynamics*, *Nucl. Phys. B* **559** (1999) 502–538, [hep-ph/9905239].

[128] P. B. Arnold, D. T. Son and L. G. Yaffe, *Longitudinal subtleties in diffusive Langevin equations for nonAbelian plasmas*, *Phys. Rev. D* **60** (1999) 025007, [hep-ph/9901304].

[129] P. B. Arnold and L. G. Yaffe, *High temperature color conductivity at next-to-leading log order*, *Phys. Rev. D* **62** (2000) 125014, [hep-ph/9912306].

[130] K. G. Wilson, *Confinement of Quarks*, *Phys. Rev. D* **10** (1974) 2445–2459.

[131] K. Symanzik, *Continuum Limit and Improved Action in Lattice Theories. 1. Principles and φ^4 Theory*, *Nucl. Phys. B* **226** (1983) 187–204.

[132] H. J. Rothe, *Lattice Gauge Theories : An Introduction (Fourth Edition)*, vol. 43. World Scientific Publishing Company, 2012, 10.1142/8229.

[133] M. Laine and A. Rajantie, *Lattice continuum relations for 3-D SU(N) + Higgs theories*, *Nucl. Phys. B* **513** (1998) 471–489, [hep-lat/9705003].

[134] G. D. Moore, *Curing O(a) errors in 3-D lattice SU(2) x (1) Higgs theory*, *Nucl. Phys. B* **493** (1997) 439–474, [hep-lat/9610013].

[135] G. D. Moore, *O(a) errors in 3-D SU(N) Higgs theories*, *Nucl. Phys. B* **523** (1998) 569–593, [hep-lat/9709053].

[136] A. Kennedy and B. Pendleton, *Improved heatbath method for monte carlo calculations in lattice gauge theories*, *Physics Letters B* **156** (1985) 393–399.

[137] K. Kajantie, M. Laine, K. Rummukainen and M. E. Shaposhnikov, *The Electroweak phase transition: A Nonperturbative analysis*, *Nucl. Phys. B* **466** (1996) 189–258, [hep-lat/9510020].

[138] M. Laine and K. Rummukainen, *The MSSM electroweak phase transition on the lattice*, *Nucl. Phys. B* **535** (1998) 423–457, [hep-lat/9804019].

[139] J. Ambjorn and A. Krasnitz, *The Classical sphaleron transition rate exists and is equal to 1.1 (alpha(w) T)**4*, *Phys. Lett. B* **362** (1995) 97–104, [hep-ph/9508202].

[140] G. D. Moore and N. Turok, *Lattice Chern-Simons number without ultraviolet problems*, *Phys. Rev. D* **56** (1997) 6533–6546, [hep-ph/9703266].

[141] P. Weisz, *Continuum limit improved lattice action for pure yang-mills theory (i)*, *Nuclear Physics B* **212** (1983) 1–17.

[142] M. Luscher and P. Weisz, *On-shell improved lattice gauge theories*, *Commun. Math. Phys.* **98** (1985) 433.

[143] G. D. Moore, *Improved Hamiltonian for Minkowski Yang-Mills theory*, *Nucl. Phys. B* **480** (1996) 689–728, [hep-lat/9605001].

[144] P. B. Arnold and L. D. McLerran, *Sphalerons, Small Fluctuations and Baryon Number Violation in Electroweak Theory*, *Phys. Rev. D* **36** (1987) 581.

[145] M. D'Onofrio, K. Rummukainen and A. Tranberg, *The Sphaleron Rate through the Electroweak Cross-over*, *JHEP* **08** (2012) 123, [1207.0685].

[146] M. Lüscher, *Properties and uses of the Wilson flow in lattice QCD*, *JHEP* **08** (2010) 071, [1006.4518].

[147] B. A. Berg and T. Neuhaus, *Multicanonical algorithms for first order phase transitions*, *Physics Letters B* **267** (1991) 249–253.

[148] B. A. Berg, *Introduction to multicanonical Monte Carlo simulations*, *Fields Inst. Commun.* **26** (2000) 1, [cond-mat/9909236].

[149] D. Hilbert, *Die grundlagen der physik. (erste mitteilung)*, *Nachrichten von der Königlichen Gesellschaft der Wissenschaften zu Göttingen. Math.-phys.* **8** (11, 1916) 395–407.

[150] A. Einstein, *Einheitliche feldtheorie von gravitation und elektrizität*, *Verlag der Koeniglich-Preussichen Akademie der Wissenschaften* **22** (07, 1925) 414–419.

[151] M. Ferraris, M. Francaviglia and C. Reina, *Variational formulation of general relativity from 1915 to 1925 "Palatini's method" discovered by Einstein in 1925*, *General Relativity and Gravitation* **14** (Mar., 1982) 243–254.

[152] F. W. Hehl, P. Von Der Heyde, G. D. Kerlick and J. M. Nester, *General Relativity with Spin and Torsion: Foundations and Prospects*, *Rev. Mod. Phys.* **48** (1976) 393–416.

[153] A. Randono, *A Note on parity violation and the Immirzi parameter*, hep-th/0510001.

[154] L. Freidel, D. Minic and T. Takeuchi, *Quantum gravity, torsion, parity violation and all that*, *Phys. Rev.* **D72** (2005) 104002, [hep-th/0507253].

[155] A. Perez and C. Rovelli, *Physical effects of the Immirzi parameter*, *Phys. Rev.* **D73** (2006) 044013, [gr-qc/0505081].

[156] S. Mercuri, *Fermions in Ashtekar-Barbero connections formalism for arbitrary values of the Immirzi parameter*, *Phys. Rev.* **D73** (2006) 084016, [gr-qc/0601013].

[157] S. Mercuri, *Nieh-Yan Invariant and Fermions in Ashtekar-Barbero-Immirzi Formalism*, in *Recent developments in theoretical and experimental general relativity, gravitation and relativistic field theories. Proceedings, 11th Marcel Grossmann Meeting, MG11, Berlin, Germany, July 23-29, 2006. Pt. A-C*, pp. 2794–2796, 2006, gr-qc/0610026.

[158] M. Bojowald and R. Das, *Canonical gravity with fermions*, *Phys. Rev.* **D78** (2008) 064009, [0710.5722].

[159] M. Kazmierczak, *Einstein-Cartan gravity with Holst term and fermions*, *Phys. Rev.* **D79** (2009) 064029, [0812.1298].

[160] M. Shaposhnikov, A. Shkerin, I. Timiryasov and S. Zell, *Higgs inflation in Einstein-Cartan gravity*, *JCAP* **02** (2021) 008, [2007.14978].

[161] G. W. Gibbons and S. W. Hawking, *Action Integrals and Partition Functions in Quantum Gravity*, *Phys. Rev. D* **15** (1977) 2752–2756.

[162] J. W. York, Jr., *Role of conformal three geometry in the dynamics of gravitation*, *Phys. Rev. Lett.* **28** (1972) 1082–1085.

[163] T. P. Sotiriou and S. Liberati, *Metric-affine f(R) theories of gravity*, *Annals Phys.* **322** (2007) 935–966, [gr-qc/0604006].

[164] F. W. Hehl, P. Von Der Heyde, G. D. Kerlick and J. M. Nester, *General Relativity with Spin and Torsion: Foundations and Prospects*, *Rev. Mod. Phys.* **48** (1976) 393–416.

[165] S. Holst, *Barbero's Hamiltonian derived from a generalized Hilbert-Palatini action*, *Phys. Rev. D* **53** (1996) 5966–5969, [gr-qc/9511026].

[166] M. Långvik, J.-M. Ojanperä, S. Raatikainen and S. Rasanen, *Higgs inflation with the Holst and the Nieh–Yan term*, *Phys. Rev. D* **103** (2021) 083514, [2007.12595].

[167] V. Vitagliano, T. P. Sotiriou and S. Liberati, *The dynamics of metric-affine gravity*, *Annals Phys.* **326** (2011) 1259–1273, [1008.0171].

[168] F. W. Hehl and G. D. Kerlick, *Metric-affine variational principles in general relativity. I - Riemannian space-time*, *General Relativity and Gravitation* **9** (Aug., 1978) 691–710.

[169] N. Dadhich and J. M. Pons, *On the equivalence of the Einstein-Hilbert and the Einstein-Palatini formulations of general relativity for an arbitrary connection*, *Gen. Rel. Grav.* **44** (2012) 2337–2352, [1010.0869].

[170] K. Aoki and K. Shimada, *Scalar-metric-affine theories: Can we get ghost-free theories from symmetry?*, *Phys. Rev.* **D100** (2019) 044037, [1904.10175].

[171] J. Beltrán Jiménez and A. Delhom, *Ghosts in metric-affine higher order curvature gravity*, *Eur. Phys. J. C* **79** (2019) 656, [1901.08988].

[172] J. Beltrán Jiménez and A. Delhom, *Instabilities in metric-affine theories of gravity with higher order curvature terms*, *Eur. Phys. J. C* **80** (2020) 585, [2004.11357].

[173] S. Räsänen, *Higgs inflation in the Palatini formulation with kinetic terms for the metric*, *Open J. Astrophys.* **2** (2019) 1, [1811.09514].

[174] W. Barker and S. Zell, *Consistent particle physics in metric-affine gravity from extended projective symmetry*, 2402.14917.

[175] A. Belenchia, M. Letizia, S. Liberati and E. D. Casola, *Higher-order theories of gravity: diagnosis, extraction and reformulation via non-metric extra degrees of freedom—a review*, *Rept. Prog. Phys.* **81** (2018) 036001, [1612.07749].

[176] A. Golovnev and T. Koivisto, *Cosmological perturbations in modified teleparallel gravity models*, *JCAP* **11** (2018) 012, [1808.05565].

[177] M. C. Pookkillath, A. De Felice and A. A. Starobinsky, *Anisotropic instability in a higher order gravity theory*, *JCAP* **07** (2020) 041, [2004.03912].

[178] J. Beltrán Jiménez and A. Jiménez-Cano, *On the strong coupling of Einsteinian Cubic Gravity and its generalisations*, *JCAP* **01** (2021) 069, [2009.08197].

[179] A. Delhom, A. Jiménez-Cano and F. J. Maldonado Torralba, *Instabilities in Field Theory: A Primer with Applications in Modified Gravity*, SpringerBriefs in Physics, Springer, 7, 2022, 2207.13431, DOI.

[180] V. A. Rubakov, *The Null Energy Condition and its violation*, *Phys. Usp.* **57** (2014) 128–142, [1401.4024].

[181] A. Jiménez Cano, *Metric-affine Gauge theories of gravity. Foundations and new insights*, Ph.D. thesis, Granada U., Theor. Phys. Astrophys., 2021. 2201.12847.

[182] A. Salvio, *Quadratic Gravity*, *Front. in Phys.* **6** (2018) 77, [1804.09944].

[183] J. M. Cline, S. Jeon and G. D. Moore, *The Phantom menaced: Constraints on low-energy effective ghosts*, *Phys. Rev. D* **70** (2004) 043543, [hep-ph/0311312].

[184] A. R. Solomon and M. Trodden, *Higher-derivative operators and effective field theory for general scalar-tensor theories*, *JCAP* **02** (2018) 031, [1709.09695].

[185] A. Smilga, *Classical and quantum dynamics of higher-derivative systems*, *Int. J. Mod. Phys. A* **32** (2017) 1730025, [1710.11538].

[186] J. F. Donoghue and G. Menezes, *Unitarity, stability and loops of unstable ghosts*, *Phys. Rev. D* **100** (2019) 105006, [1908.02416].

[187] J. F. Donoghue and G. Menezes, *Arrow of Causality and Quantum Gravity*, *Phys. Rev. Lett.* **123** (2019) 171601, [1908.04170].

[188] J. F. Donoghue and G. Menezes, *Quantum causality and the arrows of time and thermodynamics*, *Prog. Part. Nucl. Phys.* **115** (2020) 103812, [2003.09047].

[189] J. F. Donoghue and G. Menezes, *Ostrogradsky instability can be overcome by quantum physics*, *Phys. Rev. D* **104** (2021) 045010, [2105.00898].

[190] V. Errasti Díez, J. Gaset Rifà and G. Staudt, *Foundations of ghost stability*, 2408.16832.

[191] W. Barker, C. Marzo and C. Rigouzzo, *PSALTer: Particle Spectrum for Any Tensor Lagrangian*, 2406.09500.

[192] W. Barker and C. Marzo, *Particle spectra of general Ricci-type Palatini or metric-affine theories*, *Phys. Rev. D* **109** (2024) 104017, [2402.07641].

[193] G. Magnano, M. Ferraris and M. Francaviglia, *Nonlinear gravitational Lagrangians*, *Gen. Rel. Grav.* **19** (1987) 465.

[194] M. Ferraris, M. Francaviglia and G. Magnano, *Do non-linear metric theories of gravitation really exist?*, *Class. Quant. Grav.* **5** (1988) L95.

[195] G. Magnano, M. Ferraris and M. Francaviglia, *Legendre transformation and dynamical structure of higher derivative gravity*, *Class. Quant. Grav.* **7** (1990) 557–570.

[196] J.-i. Koga and K.-i. Maeda, *Equivalence of black hole thermodynamics between a generalized theory of gravity and the Einstein theory*, *Phys. Rev. D* **58** (1998) 064020, [gr-qc/9803086].

[197] V. I. Afonso, C. Bejarano, J. Beltran Jimenez, G. J. Olmo and E. Orazi, *The trivial role of torsion in projective invariant theories of gravity with non-minimally coupled matter fields*, *Class. Quant. Grav.* **34** (2017) 235003, [1705.03806].

[198] Y. N. Obukhov, E. J. Vlachynsky, W. Esser and F. W. Hehl, *Effective einstein theory from metric-affine gravity models via irreducible decompositions*, *Phys. Rev. D* **56** (Dec, 1997) 7769–7778.

[199] P. van Nieuwenhuizen, *On ghost-free tensor lagrangians and linearized gravitation*, *Nuclear Physics B* **60** (1973) 478 – 492.

[200] A. Ashtekar and E. Bianchi, *A short review of loop quantum gravity*, *Rept. Prog. Phys.* **84** (2021) 042001, [2104.04394].

[201] K. Hayashi and T. Shirafuji, *Gravity From Poincare Gauge Theory of the Fundamental Particles. 4. Mass and Energy of Particle Spectrum*, *Prog. Theor. Phys.* **64** (1980) 2222.

[202] H.-J. Yo and J. M. Nester, *Hamiltonian analysis of Poincare gauge theory: Higher spin modes*, *Int. J. Mod. Phys. D* **11** (2002) 747–780, [gr-qc/0112030].

[203] T. B. Vasilev, J. A. R. Cembranos, J. G. Valcarcel and P. Martín-Moruno, *Stability in quadratic torsion theories*, *Eur. Phys. J. C* **77** (2017) 755, [1706.07080].

[204] W. Barker and S. Zell, *Einstein-Proca theory from the Einstein-Cartan formulation*, *Phys. Rev. D* **109** (2024) 024007, [2306.14953].

[205] A. A. Starobinsky, *Spectrum of relict gravitational radiation and the early state of the universe*, *JETP Lett.* **30** (1979) 682–685.

[206] A. A. Starobinsky, *A New Type of Isotropic Cosmological Models Without Singularity*, *Phys. Lett. B* **91** (1980) 99–102.

[207] D. Kazanas, *Dynamics of the Universe and Spontaneous Symmetry Breaking*, *Astrophys. J. Lett.* **241** (1980) L59–L63.

[208] A. H. Guth, *The Inflationary Universe: A Possible Solution to the Horizon and Flatness Problems*, *Phys. Rev. D* **23** (1981) 347–356.

[209] A. D. Linde, *A New Inflationary Universe Scenario: A Possible Solution of the Horizon, Flatness, Homogeneity, Isotropy and Primordial Monopole Problems*, *Phys. Lett. B* **108** (1982) 389–393.

[210] A. A. Starobinsky, *Dynamics of Phase Transition in the New Inflationary Universe Scenario and Generation of Perturbations*, *Phys. Lett. B* **117** (1982) 175–178.

[211] D. Baumann, *Inflation*, in *Theoretical Advanced Study Institute in Elementary Particle Physics: Physics of the Large and the Small*, pp. 523–686, 2011, 0907.5424, DOI.

[212] Planck collaboration, Y. Akrami et al., *Planck 2018 results. X. Constraints on inflation*, *Astron. Astrophys.* **641** (2020) A10, [1807.06211].

[213] C. W. Misner, K. S. Thorne and J. A. Wheeler, *Gravitation*. W. H. Freeman, San Francisco, 1973.

[214] D. H. Lyth and A. R. Liddle, *The primordial density perturbation: Cosmology, inflation and the origin of structure*. 2009.

[215] L. Kofman, A. D. Linde and A. A. Starobinsky, *Towards the theory of reheating after inflation*, *Phys. Rev. D* **56** (1997) 3258–3295, [hep-ph/9704452].

[216] R. Allahverdi, R. Brandenberger, F.-Y. Cyr-Racine and A. Mazumdar, *Reheating in Inflationary Cosmology: Theory and Applications*, *Ann. Rev. Nucl. Part. Sci.* **60** (2010) 27–51, [1001.2600].

[217] M. A. Amin, M. P. Hertzberg, D. I. Kaiser and J. Karouby, *Nonperturbative Dynamics Of Reheating After Inflation: A Review*, *Int. J. Mod. Phys. D* **24** (2014) 1530003, [1410.3808].

[218] A. R. Liddle and S. M. Leach, *How long before the end of inflation were observable perturbations produced?*, *Phys. Rev. D* **68** (2003) 103503, [astro-ph/0305263].

[219] T. Koivisto and H. Kurki-Suonio, *Cosmological perturbations in the palatini formulation of modified gravity*, *Class. Quant. Grav.* **23** (2006) 2355–2369, [astro-ph/0509422].

[220] M. Kubota, K.-Y. Oda, K. Shimada and M. Yamaguchi, *Cosmological Perturbations in Palatini Formalism*, *JCAP* **03** (2021) 006, [2010.07867].

[221] A. R. Liddle and D. H. Lyth, *Cosmological inflation and large scale structure*. 2000, 10.1017/CBO9781139175180.

[222] H. Kurki-Suonio, *Cosmological Perturbation Theory I & II*, *https://www.mv.helsinki.fi/home/hkurkisu/cpt/* (2024) .

[223] S. Weinberg, *Cosmology*. 2008.

[224] V. F. Mukhanov, *Gravitational Instability of the Universe Filled with a Scalar Field*, *JETP Lett.* **41** (1985) 493–496.

[225] M. Sasaki, *Large Scale Quantum Fluctuations in the Inflationary Universe*, *Prog. Theor. Phys.* **76** (1986) 1036.

[226] V. F. Mukhanov, *Quantum Theory of Gauge Invariant Cosmological Perturbations*, *Sov. Phys. JETP* **67** (1988) 1297–1302.

[227] V. F. Mukhanov, *Quantum Theory of Cosmological Perturbations in R(2) Gravity*, *Phys. Lett. B* **218** (1989) 17–20.

[228] V. Mukhanov, H. Feldman and R. Brandenberger, *Theory of cosmological perturbations*, *Physics Reports* **215** (1992) 203–333.

[229] J. M. Maldacena, *Non-Gaussian features of primordial fluctuations in single field inflationary models*, *JHEP* **05** (2003) 013, [astro-ph/0210603].

[230] T. S. Bunch and P. C. W. Davies, *Quantum Field Theory in de Sitter Space: Renormalization by Point Splitting*, *Proc. Roy. Soc. Lond. A* **360** (1978) 117–134.

[231] N. D. Birrell and P. C. W. Davies, *Quantum Fields in Curved Space*. Cambridge Monographs on Mathematical Physics. Cambridge Univ. Press, Cambridge, UK, 1984, 10.1017/CBO9780511622632.

[232] S. Weinberg, *Adiabatic modes in cosmology*, *Phys. Rev. D* **67** (2003) 123504, [astro-ph/0302326].

[233] D. H. Lyth, K. A. Malik and M. Sasaki, *A General proof of the conservation of the curvature perturbation*, *JCAP* **05** (2005) 004, [astro-ph/0411220].

[234] A. Albrecht, P. Ferreira, M. Joyce and T. Prokopec, *Inflation and squeezed quantum states*, *Phys. Rev. D* **50** (1994) 4807–4820, [astro-ph/9303001].

[235] E. D. Stewart and D. H. Lyth, *A More accurate analytic calculation of the spectrum of cosmological perturbations produced during inflation*, *Phys. Lett. B* **302** (1993) 171–175, [gr-qc/9302019].

[236] BICEP, Keck collaboration, P. A. R. Ade et al., *Improved Constraints on Primordial Gravitational Waves using Planck, WMAP, and BICEP/Keck Observations through the 2018 Observing Season*, *Phys. Rev. Lett.* **127** (2021) 151301, [2110.00483].

[237] V.-M. Enckell, K. Enqvist, S. Rasanen and L.-P. Wahlman, *Inflation with R^2 term in the Palatini formalism*, *JCAP* **02** (2019) 022, [1810.05536].

[238] J. Annala, *Higgs inflation and higher-order gravity in palatini formulation*, *Master's Thesis, University of Helsinki,* *http://urn.fi/URN:NBN:fi:hulib-202005292527* (May, 2020) , [2106.09438].

[239] H. B. Nezhad and S. Rasanen, *Scalar fields with derivative coupling to curvature in the Palatini and the metric formulation*, *JCAP* **02** (2024) 009, [2307.04618].

[240] M. Minamitsuji, *Disformal transformation of cosmological perturbations*, *Phys. Lett. B* **737** (2014) 139–150, [1409.1566].

[241] S. Tsujikawa, *Disformal invariance of cosmological perturbations in a generalized class of Horndeski theories*, *JCAP* **04** (2015) 043, [1412.6210].

[242] H. Motohashi and J. White, *Disformal invariance of curvature perturbation*, *JCAP* **02** (2016) 065, [1504.00846].

[243] Y. Watanabe, A. Naruko and M. Sasaki, *Multi-disformal invariance of non-linear primordial perturbations*, *EPL* **111** (2015) 39002, [1504.00672].

[244] G. Domènech, A. Naruko and M. Sasaki, *Cosmological disformal invariance*, *JCAP* **10** (2015) 067, [1505.00174].

[245] J. Fumagalli, S. Mooij and M. Postma, *Disformal transformations as a change of units*, 1610.08460.

[246] K. Takahashi, H. Motohashi, T. Suyama and T. Kobayashi, *General invertible transformation and physical degrees of freedom*, *Phys. Rev. D* **95** (2017) 084053, [1702.01849].

[247] T. Chiba, F. Chibana and M. Yamaguchi, *Disformal invariance of cosmological observables*, *JCAP* **06** (2020) 003, [2003.10633].

[248] P. Jiroušek, K. Shimada, A. Vikman and M. Yamaguchi, *New dynamical degrees of freedom from invertible transformations*, *JHEP* **07** (2023) 154, [2208.05951].